Title of the Doctoral Thesis

LOCAL CIRCUITS OF THE MOUSE GRANULAR RETROSPLENIAL CORTEX

Doctoral Thesis presented by

Rita Mariana Robles Picó

Thesis Director: **Salvador Martínez Pérez**

Thesis Co-Director: **Emilio Carlos Geijo Barrientos**

PhD Program in Neuroscience

Neurosciences Institute

University Miguel Hernández of Elche

- 2021 -

INSTITUTO DE NEUROCIENCIAS

1999 - 2019

INSTITUTO DE NEUROCIENCIAS

EXCELENCIA SEVERO OCHOA

This Doctoral Thesis, entitled ***Local circuits of the mouse granular retrosplenial cortex*** is presented as a compendium of the following publication belonging to the first quartil (Q1) in the databases proposed by the regulations:

- Robles, R. M., Domínguez-Sala, E., Martínez, S., & Geijo-Barrientos, E. (2020). Layer 2/3 Pyramidal Neurons of the Mouse Granular Retrosplenial Cortex and Their Innervation by Cortico-Cortical Axons. *Frontiers in Neural Circuits*, *3*(November), 1–15. https://doi.org/10.3389/fncir.2020.576504

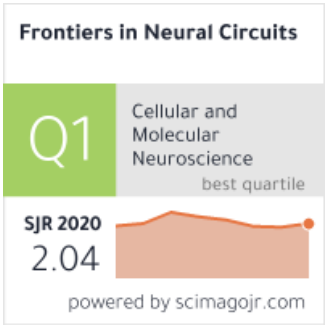

Sant Joan d'Alacant, 20 July 2021

Dr. *Salvador Martínez Pérez*, Director, and Dr. *"Emilio Carlos Geijo Barrientos"*, co-director of the doctoral thesis entitled ***Local circuits of the mouse granular retrosplenial cortex*.**

CERTIFIES:

That Mrs Rita Mariana Robles Picó has carried out under our supervision the work entitled ***Local circuits of the mouse granular retrosplenial cortex*** in accordance with the terms and conditions defined in his/her Research Plan and in accordance with the Code of Good Practice of the University Miguel Hernández of Elche, satisfactorily fulfilling the objectives foreseen for its public defence as a doctoral thesis.

We sign for appropriate purposes, at San Juan de Alicante, 20th of July of 2021

Thesis director

Dr. *Salvador Martinez Pérez*

Thesis co-director

Dr. *Emilio Carlos Geijo Barrientos*

CSIC UNIVERSITAS Miguel Hernández

INSTITUTO DE NEUROCIENCIAS

UNIVERSITAS Miguel Hernández

EXCELENCIA SEVERO OCHOA

Sant Joan d'Alacant, 20 July 2021

Ms. Elvira de la Peña García, Coordinator of the Neurosciences PhD programme at the Institute of Neurosciences in Alicante, a joint centre of the Miguel Hernández University (UMH) and the Spanish National Research Council (CSIC),

INFORMS:

That Mrs Rita Mariana Robles Picó has carried out under the supervision of our PhD Programme the work entitled *Local circuits of the mouse granular retrosplenial cortex* in accordance with the terms and conditions defined in its Research Plan and in accordance with the Code of Good Practice of the University Miguel Hernández de Elche, fulfilling the objectives satisfactorily for its public defence as a doctoral thesis.

Which I sign for the appropriate purposes, in Sant Joan d'Alacant, 20 July 2021

Dr Elvira de la Peña García

Coordinator of the PhD Programme in Neurosciences

E-mail: elvirap@umh.es
www.in.umh.es

Tel: +34 965 919533
Fax: +34 965 919549

Av Ramón y Cajal s/n
SANT JOAN CAMPUS
03550 SANT JOAN D'ALACANT- SPAIN

Funding/grants/scholarship with which the thesis was carried out:

- **Ministerio de Economía y Competitividad: Resolución de 12 de noviembre de 2015 de la Secretaría de Estado de Investigación, Desarrollo e Innovación, por la que se conceden ayudas para contratos predoctorales para la formación de doctores, convocatoria 2015.**
  Nº 198
  CIF: Q2818002D
  Referencia Centro I+D: BES-C-2015-0018
  Razón Social: AGENCIA ESTATAL CONSEJO SUPERIOR DE INVESTIGACIONES CIENTIFICAS (CSIC)
  Código proyecto: SEV-2013-0317-06
  Referencia: BES-2015-073419
  Duración ayuda: 48 meses

- **EMBO Short-Term Fellowship (for part of abroad stay)**
  Referencia: 7833
  Duración ayuda: 90 días

- **Contrato de trabajo para la realización de un proyecto de investigación denominado *Microcircuitos neuronales de la corteza cerebral retrosplenial: desarrollo, estructura, propiedades funcionales y sus alteraciones en modelos animales de displasia cortical*.**
  Razón social: Fondo Europeo de Desarrollo Regional (FEDER) *Una manera de hacer Europa* / Ministerio de Ciencia e Innovación- Agencia Estatal de Investigación SAF2017-83702-R
  Referencia de convocatoria: 03/20.
  Responsables: Dr. Salvador Martínez Pérez y el Dr. Emilio Carlos Geijo Barrientos.
  Código del proyecto: 2018/00050/001.
  Duración ayuda: 10 meses y 10 días.

UNIVERSITAS Miguel Hernández

CSIC UNIVERSITAS Miguel Hernández INSTITUTO DE NEUROCIENCIAS

EMBO excellence in life sciences

EXCELENCIA SEVERO OCHOA

AGRADECIMIENTOS

Los agradecimientos posiblemente sean la parte más difícil de redactar y la que más me ha costado ponerme manos a la obra. Una de las causas es el miedo a que se me olvide alguien, algún nombre en concreto que forme parte de este laborioso proyecto de vida. Por ello, quiero empezar dando las gracias a todas esas personas que no aparecen con su nombre propio pero que saben que forman parte de esta etapa tan diferencial de mi vida. Gracias.

Con el comienzo de nombres, deseo empezar con mi tutor de tesis, Emilio. A veces, cuando decides iniciar una carrera investigadora debes poner en una balanza tus intereses científicos a priorizar: un jefe que mantenga un gran laboratorio con un gran equipo produciendo mucho de manera automatizada, o un jefe con un laboratorio pequeño en el cual como estudiante de doctorado asimiles a que todo irá más despacio pero aprenderás a ser técnico de laboratorio, predoc, postdoc,…, me atrevería a decir que en ocasiones hasta IP (Investigador Principal) escribiendo y guiando tu propio proyecto. Como bien sabéis, elegí la segunda opción que aunque me haya llevado a alargar este periodo me ha permitido aprender todo tipo de técnicas y/o necesidades que puedan surgir en un laboratorio de Neurociencias. Emilio, te doy las gracias por formarme como lo has hecho, desde la base, sin saltarnos ningún paso, y por brindarme la oportunidad de convertirme en electrofisióloga con un profesional como tú, que además antepone la enseñanza, la humildad y la bondad ante los resultados científicos, puesto que para la primera fase de esta carrera pienso que es clave. Gracias por ser un compañero cuando lo he necesitado tanto en lo laboral como en lo personal. Somos la noche y el día: tú paciente y tranquilo; y yo

impaciente y un saco de nervios, pero juntos hemos sabido formar un equipo de dos que ha superado estos últimos años tan complicados y accidentados en España, no solo por la pandemia sino por la situación de investigación en ciencias de la salud de la última década. Gracias.

Otro científico imprescindible en esta etapa ha sido Salvador, mi director de tesis. Gracias por brindarme la oportunidad de formar parte de tu gran equipo científico, gracias por concederme la beca que tanto ayuda durante este proceso. Eres nuestro referente. Cuando llegué los compañeros me contaban que eran los años más complicados que se estaban viviendo en el laboratorio, sin embargo, lo has sabido levantar aun compartiendo tu tiempo dirigiendo un centro tan importante como es el INA. Me alegra poder ver los laboratorios llenos de gente de nuevo gracias a tu constancia y profesionalidad. Gracias por abrirnos las puertas de tu casa en Abengibre y prepararnos esas barbacoas tan ricas con sus posteriores bailes, o por llevarnos hasta Murcia para degustar su gastronomía. En otras palabras, gracias por hacer de un grupo de trabajo una eterna familia.

Gracias a Constantino Sotelo por compartir su sabiduría y experiencia mediante debates científicos durante los *retreats* y congresos.

Gracias a Edu y a Diego, por sus agradables sonrisas y su predisposición a ayudar a los alumnos/as. Diego, gracias por ser el cómplice de todos los estudiantes, por enseñarnos proyectos de vida como el de la Semana del Cerebro o Bielorrusia, eres un ejemplo de humanidad y sentido del humor, entre otros muchos valores que te caracterizan. Edu, gracias por tu simpatía, por la manera de tratarnos y por compartir tantas comidas entre risas en el comedor con los estudiantes.

Nuestras conversaciones sobre deporte mientras el resto nos miraban como unos frikis obsesionados también se agradecen para amenizar las horas en el laboratorio y recordarnos que se puede compaginar todo.

Gracias a Marusa, nuestra *lab manager*, porque sin ella el laboratorio no sería lo que es, no sé qué vamos a hacer sin ti. Has sido uno de los pilares centrales para todos/as. Gracias por ayudarnos en todo y por ser la vitalidad del laboratorio. Mucha suerte en tu nueva etapa, te deseo lo mejor.

Gracias a mi querida y amiga Paqui, una de las técnicos de laboratorio que todos desearían tener, un andamio fundamental del laboratorio. Sin tus millones de consejos y modificaciones del protocolo de Biocitina no tendría mis neuronitas tan chiquititas teñidas, a trabajadora no te gana nadie. Aunque de ti resaltaré tu personalidad, tu estilo y nuestra complicidad para todo, y los cafés con sus conversaciones. Se me queda corto el texto sin escribir todo lo que pienso de ti, sabes lo que te aprecio y lo que te voy a echar de menos.

Gracias a Alicia, el otro andamio que sustenta el laboratorio con su gran labor como técnico de laboratorio. Nadie me ha sonreído igual que tú al entrar en el laboratorio o por los pasillos, tu simpatía y tu forma de divertirse es contagiosa. Gracias por ayudarme siempre que te lo he pedido y contar conmigo para preciosos proyectos de divulgación en colegios con experimentos divertidos mostrando a la mujer en ciencia. Mucha suerte en tu nueva etapa, te deseo lo mejor.

En cuanto a los estudiantes de doctorado y postdocs, empiezo por los compañeros del laboratorio 239, los que me vieron salir del cascarón al aterrizar en el laboratorio. Gracias Edu

Junior por enseñarme a registrar, la técnica en la que se basa nuestro laboratorio y nuestras tesis doctorales. La forma en la que lo hiciste fue la mejor, el segundo día ya me enfrenté sola al *setup* sin miedo sabiendo que te tenía a pocos metros para llenarte de preguntas. Gracias por permitir que completara datos de tu proyecto y presentarlos en mi memoria de prácticas de empresa y en el congreso de la SENC. Esas figuras sin tu ayuda y sin tus datos previos no tendrían sentido. Gracias Alejandro "Chispi" por tus explicaciones y debates científicos con esquemas en la pizarra, por preocuparte para que aprendiera y no solo sacara datos, y por tu amistad en esos años compartidos. Llegué en vuestra etapa final, casi de escritura, y ahora os entiendo y sé que no es fácil de lidiar y menos con estudiantes por medio. Nunca olvidaré nuestras conversaciones de tres, nuestras risas, nuestra música, nuestras fiestas en la *Stereo* o entrenos en la terraza. Gracias a Víctor porque aunque no haya compartido espacio físico porque cuando yo llegué y tú defendías la tesis, fuiste el primer doctor que vi defender su Proyecto. Gracias por tus consejos y tu simpatía cada vez que has venido a visitarnos. También quiero agradecer a los alumnos de master a los que he podido ayudar pero que también me han enseñado como Noelia, Auxi, Guillermo o Roberto.

A Laura Almaraz, por ser la IP del laboratorio de al lado aunque nosotros te tenemos como miembro del 239, gracias por tus consejos y tu sabiduría, por ser un ejemplo de IP que adora la ciencia y quiere seguir experimentando en sus manos y trasteando en su laboratorio como el primer día.

Y qué decir de los compañeros de la primera planta de los laboratorios de anatomía 101, 102 y 138, con los que compartía almuerzos, comidas y meriendas a diario, ¡cuántas risas y cotilleos

compartidos! Ana y Raquel, gracias por solucionarme dudas y tratarme como lo habéis hecho, sois mi ejemplo a seguir por vuestra constancia, paciencia y dedicación. A mi "acho", gracias Jesús por ser como eres y por sacarnos carcajadas como lo haces. A Juan Antonio, por ser el cerebrito y el *xixonenc* del laboratorio, te mereces todo lo bueno que te está pasando científicamente. A Elena y Arancha por las comidas y décimos de lotería compartidos. A Mª Paz por ser una compañera todoterreno con la que también comparto la afición del deporte. A Mª Luisa por los buenos ratitos en el laboratorio cuando viene de Murcia. A Diego Pastor por los viajes a congresos compartiendo coche, por compartir nuestro querido deporte, los cafés en Elche y tu sonora risa y humor negro. A los murcianos Loli, Mónica, Carlos y Marta por las comidas y *Abengibres* vividos. Más tarde llegaron al laboratorio 138 nuevos estudiantes con los que he compartido mucho más que horas de trabajo. Gracias a Vero y Raquel por aparecer en el ecuador de mi etapa doctoral, por sacarme del estancamiento en ese momento y preocuparos día tras día de mantenerme con luz cuando solo veía oscuridad. Además, me habéis enseñado muchos valores que habéis aprendido a lo largo de vuestras vidas que me han enriquecido como persona. Nunca olvidaré nuestros consejos de sabias. Quiero destacar y agradecer a sus familias que me abrieron las puertas de su casa como una más: Álvaro, súper Pepa, Roc, Rosa, Tomás y mis peques Pere y Roc. A Iris, por compartir esta etapa doctoral casi a la par, por ser las únicas que nos ponemos leche en el café, y por enseñarnos su trabajo previo tan interesante como terapeuta ocupacional. A Abraham, por cuidarnos tan bien aunque nos cebara a donuts al principio a todas horas. Tenemos la celebración de tu boda con Onofre pendiente que el COVID-19 no nos arrebatará. A Pili, mi niña bonita, qué parecidas y

diferentes somos a la vez y qué bien nos entendemos, aunque no hayamos compartido laboratorio te tengo como una compi muy especial, sé que no se te olvidará poner solución con carbógeno si haces rodajas. A Tono y a Claudia a los que animo con sus tesis doctorales. A Mª Carmen por compartir muchas zamburiñas. A los alumnos/as de máster y estancias como Carla, Fran, Adri, Camila, Cris, Víctor, Sara, etc.

A los alumno/as de mi promoción del Máster de Neurociencias, con vosotros empezó todo y tenemos mil anécdotas en clase y en las cenas en el Pekín que nunca olvidaré. Es precioso seguir en contacto con mucho/as de vosotros/as compartiendo celebraciones y buenos ratitos.

A mucha gente del INA que me ha alegrado los días o compartido buenos momentos fuera del centro: mis queridos Álvaro, Óscar y Kike, Rafa, Kika, Irene, Belén, Mar, Edu, Álvaro, Aida, etc.

Al personal de Servicios comunes del INA que son clave para el funcionamiento de esta institución: Trini (lavados), Trini (PCR), Jesús, Maite, Virtudes, Elvira, Miguel, Rosa (cultivos), Ruth, etc.

Fuera del laboratorio, pero en el ámbito de la Universidad, quiero agradecer el continuo apoyo de mis amigas de Biología, mi querida *Crème*. A un profesor de Fisiología con el que sigo el contacto, Sergi, no solo por ser mi tutor de prácticas en empresa en mi actual laboratorio, contar conmigo para dar un seminario anual en la Universidad de Alicante y ser parte de mi tribunal de tesis, sino también por la afición que compartimos en el deporte, nuestra pasión por quemar las zapatillas en el asfalto corriendo kilómetro tras kilómetro. Gracias a todos los miembros del

tribunal de mi tesis, tanto los presentes como los suplentes, por aceptar este marrón y formar parte de esto.

Mis amigos/as que han permitido que desapareciera durante los cursos académicos pero están siempre ahí y me acogen de vuelta en verano, en las celebraciones puntuales o simplemente cunado nos necesitamos. En especial a *Las Renacidas*, gracias por quererme tal y como soy, con muchos más defectos que virtudes, es un privilegio crecer y madurar a vuestro lado.

A mi familia que también me ha visto poco en los momentos estresantes y de mucho estudio/trabajo. A mis hermanos Fernando y Cosme, y a mi cuñada Lydia. A Emma, mi primera y única sobrina que decidió nacer dos días después de irme de estancia a Noruega para marcar esa etapa tan importante del doctorado; nos das vida pequeña, te amo con locura. A mi tía María por ser mi segunda madre, te quiero tanto que no encuentro las palabras adecuadas que mereces.

Por último y no menos importante, a mis padres. Mis dos pilares fundamentales, los que me sostienen en pie, los que evitan que me caiga aunque se me quiebren los talones. Extraoficialmente no soy la única autora de este proyecto, ellos deberían aparecer en la portada en mayúsculas porque sin ellos hoy no estaría escribiendo esto ni estaría a punto de ser doctora. Sabéis como nadie lo que he vivido y lo que ha conllevado, siempre me habéis tendido la mano para ayudarme y me habéis motivado a seguir adelante a pesar de no ponerlo nada fácil por mi parte. Gracias por ser mis padres, mis psicólogos, mis jefes, mis compañeros, mis hermanos, mis amigos y mis ejemplos a seguir en todo. Mi gente cercana opina que mis padres son únicos y especiales, amigas los llaman padres, y este trato y admiración no ocurre con todos. Ellos son humildes y se

niegan en reconocer lo espectaculares y magníficos que son, pero yo quiero gritarle al mundo lo orgullosa que estoy de ser su hija. Gracias por existir y acompañarme durante toda mi vida, deberíais ser infinitos, GRACIAS por existir, saber ser y estar. Esto es de los tres y va dedicado a vosotros. Os amo.

GRACIAS.

A mis padres

Index

INDEX

List of abreviations

1. LIST OF ABREVIATIONS

ACSF = Artificial cerebrospinal fluid

CB1R = cannabinoid receptor type I

CGP 55845 = ((2S)-3-[[(1S)-1-(3,4-dichlorophenyl) ethyl] amino-2- hydroxypropyl] (phenylmethyl) phosphonic acid hydrochloride)

CGP 52432 = (3- [[(3,4-Dichlorophenyl)methyl]amino]propyl] diethoxymethyl) acid)

CNQX = AMPA/kainateRs competitive blocker = 6-Cyano-7-nitroquinoxaline-2,3-dione

CRACM = ChR2-assisted circuit mapping

DAB = 3,3-diaminobenzidine

E/I balance = excitatory/inhibitory balance

EPSCs = excitatory postsynaptic currents

EPSPs = excitatory postsynaptic potentials

Erev = equilibrium reversal potential

fMRI = functional magnetic resonance imaging

$GABA_A$Rs blocker = (-)-Bicuculline methiodide ([*R*-(*R**,*S**)]-5-(6,8-Dihydro-8-oxofuro[3,4-*e*]-1,3- benzodioxol-6-yl)-5,6,7,8-tetrahydro-6,6-dimethyl-1,3-dioxolo[4,5-*g*]isoquinolinium iodide)

GABA = γ-aminobutyric acid

$GABA_BR$ = $GABA_B$ receptor

GRSC = granular retrosplenial cortex

5-HT = 5-hydroxytryptamine; serotonin

IPSCs = inhibitory postsynaptic currents

IPSPs = inhibitory postsynaptic potential

Kir = inward-rectifier potassium

L(1, 2/3, 4, 5, 6) = layer(1, 2, 2/3, 4, 5, 6)

LS = late spiking

mACSF = modified ACSF

PBS = phosphate-buffered saline

PV-FS = parvalbumin-positive fast-spiking

RS = regular spiking

RSC = retrosplenial cortex

Rs = Series resistance

List of figures and tables

2. LIST OF FIGURES AND TABLES

All figures and the table of this thesis are numerated inside each section in order not to provoke confusion with figures of the publicated manuscript.

2.1. Introduction

2.2. Results

Figure 7.2. Examples of late-spiking (LS) and non-LS pyramidal neurons.

Figure 7.3. Electrophysiological parameters are measured in LS and non-LS neurons.

Figure 7.4. LS and non-LS pyramidal neurons respond differently to incoming epileptiform discharges.

Figure 7.5. Synaptic currents evoked by electrical stimulation in LS and non-LS pyramidal neurons.

Figure 7.6. Synaptic currents elicited by glutamate application in LS and non-LS pyramidal neurons.

Figure 7.7. Synaptic responses to ipsilateral stimulation of simultaneously recorded pairs of layer 2/3 pyramidal neurons.

Figure 7.8. Synaptic responses to contralateral stimulation of simultaneously recorded pairs of layer 2/3 pyramidal neurons.

Figure 7.9. E/I balance and latency of responses evoked by contralateral stimuli.

2.3. Annex of results

Figure 8.1. Firing pattern and morphology of pyramidal neurons recorded in L5 of the GRSC.

Figure 8.12. Membrane currents recorded in LS pyramidal neurons evoked by the direct application of GABA.

Table 8.1. Reversal potentials of the currents evoked by the application of GABA in LS and non-LS pyramidal neurons.

2.4. Discussion

Figure 9.3.1. Local neuronal circuit scheme of L2/3 GRSC.

Abstract

3. ABSTRACT/RESUMEN/RESUM

3.1. Abstract

The granular retrosplenial cortex (GRSC) of rodents is a cortical area implicated in functions such as memory and spatial learning. Most pyramidal neurons of the superficial layers of the GRSC show a late-spiking (LS) firing pattern due to the presence of A-type potassium currents. We have studied the local circuits involving this type of pyramidal neurons using intracellular recordings in LS and non-LS pyramidal neurons of L2/3 and in some cases in L5 of the GRSC in coronal brain slices from mice of 14-22 postnatal days. LS and non-LS neurons were identified by the firing pattern, the higher input membrane resistance, shorter action potential and shorter time to fire the first spike.

First, during the propagation of epileptiform discharges, almost all non-LS neurons fired large bursts of action potentials; in contrast, LS neurons showed bursts of excitatory postsynaptic potentials (EPSPs) whose amplitude never reached the threshold for spike firing.

Second, the stimulation of horizontal axonal collaterals with local application of glutamate evoked excitatory postsynaptic currents (EPSCs) in LS neurons only when the stimulus was close (100-200μm) to the recorded neuron; in contrast, non-LS neurons showed large EPSCs in response to the stimulation at longer distances (~1200μm).

Third, in response to electrical stimuli applied to the contralateral homotopic cortex and at 1200 μm ipsilaterally, we recorded pairs of pyramidal neurons recorded simultaneously formed by a LS and a non-LS neurons. In these L2/3 pairs, EPSCs evoked were significantly smaller and less frequently in LS than in non-LS neurons; also, the latency of the EPSC recorded in the LS neurons was longer than in non-LS neurons. Our data suggest that these neurons, in contrast to neighbour non-LS pyramidal neurons, are innervated by local axonal collaterals and show smaller synaptic currents in response to the stimulation of long-range axons. These results show differences in the local microcircuits involving LS and non-LS neurons in the GRSC and suggest that LS neurons are innervated mainly by short-range collateral axons.

Four, we also have studied and compared the feed-forward inhibitory responses and the excitatory/inhibitory balance (E/I balance) in LS and non-LS pyramidal neurons of L2/3 of the GRSC in order to discard that these differences are due to their E/I balance. In response to ipsilateral stimuli the peak amplitude of the EPSCs and the IPSCs were similar in both LS and non-LS neurons; this caused an E/I balance close to 1 that was not different in both neuron types. In contrast, in response to the stimulation of callosal contralateral axons, the EPSCs were smaller than the IPSCs in both types of neurons. These results suggest that both LS and non-LS neurons are more effectively activated by ipsilateral axons than by contralateral axons.

Five, we have researched if the small disynaptic responses recorded in LS neurons were due to inputs from upper L5b pyramidal neurons. The results from simultaneous

recordings from pyramidal neurons of L2/3 and pyramidal neurons from upper L5b did not answer this point. The recording of synaptic responses in upper layer 5b showed large excitatory and inhibitory synaptic currents in response to ipsi- and contralateral axons, similar to the responses recorded in layer 2/3 non-LS neurons. However, in layer 5 neurons the E/I balance in response to ipsilateral inputs was smaller than in layer 2/3 non-LS neurons.

Finally, the application of blockers of $GABA_B$ receptors ($GABA_BRs$) (CGP55845 or CGP52432) increased the size of the EPSPs in LS neurons, leading to firing in most of them. These results show the presence of differences in the local microcircuits involving LS and non-LS pyramidal neurons in the GRSC and suggest the presence of an inhibitory component dependent on the activation of $GABA_BRs$ in LS neurons.

3.2. Resumen

La corteza granular retrosplenial (GRSC) de los roedores es una área cortical implicada en funciones como la memoria y el aprendizaje espacial. La mayoría de las neuronas piramidales de las capas superficiales de la GRSC muestran un patrón de disparo tardío (LS) debido a la presencia de corrientes de potasio de tipo A. Hemos estudiado los circuitos locales que involucran a este tipo de neuronas piramidales mediante registros intracelulares en neuronas piramidales LS y no-LS de L2/3 y en algunos casos en L5 de la GRSC en cortes cerebrales coronales de ratones de 14-22 días posnatales. Las neuronas LS y no-LS se identificaron por el patrón de disparo, la mayor resistencia de entrada de membrana, el potencial de acción más corto y el tiempo más corto para disparar el primer potencial de acción.

En primer lugar, durante la propagación de descargas epileptiformes, casi todas las neuronas no-LS dispararon grandes ráfagas de potenciales de acción; por el contrario, las neuronas LS mostraron ráfagas de potenciales postsinápticos excitadores (EPSP) cuya amplitud nunca alcanzó el umbral de disparo de picos.

En segundo lugar, la estimulación de los axones colaterales horizontales con la aplicación local de glutamato provocó corrientes postsinápticas excitatorias (EPSC) en las neuronas LS solo cuando el estímulo estaba cerca (100-200 μm) de la neurona registrada; por el contrario, las neuronas no-LS mostraron grandes EPSC en respuesta a la estimulación a distancias más largas (~ 1200 μm).

En tercer lugar, en respuesta a los estímulos eléctricos aplicados a la corteza homotópica contralateral y a 1200 μm ipsilateralmente, registramos simultáneamente pares de neuronas piramidales formados por una neurona LS y una no-LS. En estos pares L2/3, los EPSCs evocados fueron significativamente más pequeños y menos frecuentes en las neuronas LS que en las no-LS; además, la latencia del EPSC registrado en las neuronas LS fue más larga que en las no-LS. Nuestros datos sugieren que estas neuronas, a diferencia de las neuronas piramidales vecinas no-LS, están inervadas por axones colaterales locales y muestran corrientes sinápticas más pequeñas en respuesta a la estimulación de los axones de largo alcance. Los resultados presentados hasta aquí muestran diferencias en los microcircuitos locales que implican a las neuronas LS y no-LS en la GRSC y sugieren que las neuronas LS están inervadas principalmente por axones colaterales de corto alcance.

En cuarto lugar, también hemos estudiado y comparado las respuestas inhibitorias feed-forward y el balance excitatorio/inhibitorio (balance E/I) en las neuronas piramidales LS y no-LS de L2/3 de la GRSC para descartar que estas diferencias se deban a su balance E/I. En respuesta a los estímulos ipsilaterales, la amplitud máxima de los EPSCs y de los IPSCs fue similar en las neuronas LS y no-LS; esto provocó un balance E/I cercano a 1 que no fue diferente en ambos tipos de neuronas. Por el contrario, en respuesta a la estimulación de los axones contralaterales callosos, los EPSCs fueron menores que los IPSCs en ambos tipos de neuronas. Estos resultados sugieren que tanto

las neuronas LS como las no-LS son más activadas por los axones ipsilaterales que por los axones contralaterales.

En quinto lugar, hemos investigado si las pequeñas respuestas disinápticas registradas en las neuronas LS se debían a las aferencias de neuronas piramidales de la capa superficial L5b. Los resultados de los registros simultáneos de las neuronas piramidales de L2/3 y neuronas piramidales de la parte superficial de L5b no contestaron este punto. Las respuestas sinápticas registradas en la parte superficial de la L5b mostraron corrientes sinápticas excitatorias e inhibidoras grandes en respuesta a axones ipsi- y contralaterales, similares a las respuestas registradas en las neuronas no-LS de L2/3. No obstante, en las neuronas de L5 el balance E/I en respuesta a aferencias ipsilaterales fue menor que en las neuronas no-LS de L2/3.

Por último, la aplicación de bloqueantes de los receptores $GABA_B$ ($GABA_BRs$) (CGP55845 o CGP52432) aumentó el tamaño de los EPSPs en las neuronas de L5b, provocando el disparo en la mayoría de ellas. Estos resultados muestran la presencia de diferencias en los microcircuitos locales que implican a las neuronas piramidales LS y no-LS en la GRSC y sugieren la presencia de un componente inhibitorio dependiente de la activación de los $GABA_BRs$ en las neuronas LS.

3.3. Resum

L'escorça retroesplenial granular (GRSC) dels rosegadors és una àrea cortical implicada en funcions com la memòria i l'aprenentatge espacial. La majoria de les neurones piramidals de les capes superficials de la GRSC mostren un patró de tret tardà (LS) a causa de la presència de corrents de potassi de tipus A. Hem estudiat els circuits locals que involucren a aquesta mena de neurones piramidals mitjançant registres intracel·lulars en neurones piramidals LS i no-LS de L2/3 i en alguns casos en L5 de la GRSC en talls cerebrals coronals de ratolins de 14-22 dies postnatals. Les neurones LS i no-LS es van identificar pel patró de tret, la major resistència d'entrada de membrana, el potencial d'acció més curt i el temps més curt per a disparar el primer potencial d'acció.

En primer lloc, durant la propagació de descàrregues epileptiformes, quasi totes les neurones no-LS van disparar grans ràfegues de potencials d'acció; per contra, les neurones LS van mostrar ràfegues de potencials postsinàptics excitadors (EPSP) l'amplitud dels quals mai va aconseguir el llindar de tret de pics.

En segon lloc, l'estimulació dels axons col·laterals horitzontals amb l'aplicació local de glutamat va provocar corrents postsinàptiques excitadores (EPSC) en les neurones LS només quan l'estímul era a prop (100-200 μm) de la neurona registrada; per contra, les neurones no-LS van mostrar grans EPSC en resposta a l'estimulació a distàncies més llargues (~ 1200 μm).

En tercer lloc, en resposta als estímuls elèctrics aplicats a l'escorça homotòpica contralateral i a 1200 μm ipsilateralment, registrarem parells de neurones piramidals simultàniament formats per una neurona LS i una no-LS. En aquests parells L2/3, les EPSCs evocades van ser significativament més xicotetes i menys freqüents en les neurones LS que en les no-LS; a més a més, la latència de la EPSC registrada en les neurones LS va ser més llarga que en les no-LS. Les nostres dades suggereixen que aquestes neurones, a diferència de les neurones piramidals veïnes no-LS, estan innervades per axons col·laterals locals i mostren corrents sinàptiques més xicotetes en resposta a l'estimulació dels axons de llarg abast. Aquests resultats mostren diferències en els microcircuits locals que impliquen les neurones LS i no-LS en la GRSC i suggereixen que les neurones LS estan innervades principalment per axons col·laterals de curt abast.

En quart lloc, també hem estudiat i comparat les respostes inhibitòries feed-forward i el balanç excitatori/inhibitori (balanç E/I) en les neurones piramidals LS i no-LS de L2/3 de la GRSC per a descartar que aquestes diferències es deguen al seu balanç E/I. En resposta als estímuls ipsilaterals, l'amplitud màxima de les EPSCs i de les IPSCs va ser similar en les neurones LS i no-LS; això va provocar un balanç E/I pròxim a 1 que no va ser diferent en tots dos tipus de neurones. Per contra, en resposta a l'estimulació dels axons contralaterales callosos, les EPSCs van ser menors que les IPSCs en tots dos tipus de neurones. Aquests resultats suggereixen que tant les neurones LS com les no-LS són més activades pels axons ipsilaterals que pels axons contralaterals.

En cinqué lloc, hem investigat si les xicotetes respostes disinàptiques registrades en les neurones LS es devien a les aferències de neurones piramidals de la capa superficial de L5b. Els resultats dels registres simultanis de les neurones piramidals de L2/3 i neurones piramidals de la part superficial de L5b no van contestar aquest punt. Les respostes sinàptiques registrades en la part superficial de la L5b van mostrar corrents sinàptiques excitatòries i inhibidores grans en resposta a axon ipsi- i contralaterals, similars a les respostes registrades en les neurones no-LS de L2/3. No obstant això, en les neurones de L5 el balanç E/I en resposta a aferències ipsilaterals va ser menor que en les neurones no-LS de L2/3.

Finalment, l'aplicació de bloquejants dels receptors $GABA_B$ ($GABA_BRs$) (CGP55845 o CGP52432) va augmentar la grandària de les EPSPs en les neurones de L5b, provocant el tret en la majoria d'elles. Aquests resultats mostren la presència de diferències en els microcircuits locals que impliquen les neurones piramidals LS i no-LS en la GRSC i suggereixen la presència d'un component inhibitori dependent de l'activació dels $GABA_BRs$ en les neurones LS.

Introduction

4. INTRODUCTION

Detailed General introductions of all topics included in the Thesis (including the paper and results not published: Sections 1 and 2 from the annex of results).

4.1. Neocortical circuits

Cortical structures in the forebrain are formed by networks of excitatory and inhibitory neurons which are born in distant locations. Knowing the integration of these two major classes of neurons into unique functional cell assemblies could shed light on the organization of cortical circuits (Bartolini et al., 2013).

Fluctuations in environment, learning and behaviour sculpt brain circuits through life. It is known that neuronal plasticity occurs on a variety of levels during learning from subcellular changes at individual synapsis to large-scale alterations of cortical regions in response to injury. In some brain regions, neural plasticity occurs at cellular level too with the addition and integration of neurons into preexisting circuits continuously, requiring the development of new repertoires of synapses in the adult brain completely (Pino & Marín, 2014).

It is thought that the complex microcircuitry of the cerebral cortex is a critical substrate from which arise the impressive capabilities of the mammalian brain (Jiang et

al., 2015). The electrical behavioural and synaptic interactions of the constituent neurons originate the activity patterns of microcircuit. In a microcircuit, each neuron translates massive convergent input from multiple presynaptic axons into a single output. The synaptic integration is not merely a summation of inputs since active properties of the receiving dendrites modified them. Neurons express a wide variety of channel subtypes composed of particular combinations of pore-forming and auxiliary subunits. As well as ion selectivity, the voltage sensitivity and gating kinetics (transitions between open and closed states) define the functional characteristics of the channels. In many neurons, persistent inward currents activated at membrane potentials more hyperpolarized than the spike thresholds aid repetitive firing. Apart from persistent inward currents, repetitive firing and, in fact, the waveform of the action potential depends on the K^+ channels expressed in specific cell types. K^+ channels present a principal role in determining the interspike interval and in that way in setting the firing frequency of neurons. Furthermore, they regulate the shape of action potentials too and thus determine Ca^{2+} influx at presynaptic terminals (Toledo-Rodríguez et al., 2005).

The isocortex develops from the dorsalmost area of the pallium, in the roof of the telencephalic vesicle (Puelles et al., 2013). In mammals, this region undergoes a great surface expansion, becoming the largest nervous center of the brain. The isocortex is characterized by three structural constancies common to all mammals: (1) in the horizontal dimension, neurons are arranged in layers and the layer identity of a given cell determines many of its morphological and physiological features (Sempere-Fernàndez,

2016): (2) regional discontinuities exist, reflecting the differential layer organization, size, density and distribution of neurons and (3) in the radial dimension, neurons are stereotypically interconnected forming what many have interpreted as unitary functional columns.

So that the diagram of cortical wiring, incorporating local columnar and layer microcircuits and their inputs and outputs, forms neocortical function and plasticity. It is thought that microcircuits are highly stereotyped and comparable across functionally different areas (Douglas & Martin, 2007; Pentreanu et al., 2007; Sempere-Fernàndez et al., 2019).

On the one hand, as I said before, an indicator of neocortical areas is its layer distribution with neurons from different layer showing distinct genetic, morphologic and functional features. Functional properties researched in sensory, motor and associative cortex in vivo through electrophysiological recordings and calcium images have revealed that pyramidal neurons in L2/3 implement a sparse firing code (Beloozerova et al., 2003a,b; Crochet et al., 2011; Crochet & Petersen, 2006; Sakata & Harris, 2009; Sawinski et al., 2009). The pyramidal neurons remain silent or are sharply-tuned, firing in response to specific configurations of the stimuli. Against, large pyramidal neurons in L5b with thick apical dendritic tufts are broadly-tuned and respond in a more unspecific manner. The distinct activity patterns shown by L2/3 and L5b pyramidal neurons are found both

in awake and anesthetized animals, indicating that this layer distinction is a general signature of cortical functions (Sempere-Ferràndez et al., 2019).

Other study said that L2/3 axons connect with neurons in L2/3, L5 and L6, but not in L4, in both ipsilateral and contralateral cortex. In both hemispheres the L2/3-to-L5 projection is stronger than the L2/3-to-L2/3 projection, suggesting that layer specificity may be identical for local and long-range cortical projections (Petreanu et al., 2007).

On the other hand, one of the principal fiber bundles of the brain of placental mammals is the corpus callosum. The axons forming the corpus callosum sustain interhemispheric connections between homotopic cortical areas along the entire rostrocaudal axis of the cortex having an important in role in sensorimotor integration and high-order cognitive functions, including self-perception (Sempere-Fernàndez et al., 2016).

In our laboratory, it has been studied recently in cortical slices throughout the columnar extension of the RSC how neurons integrate the contralateral input from callosal projecting neurons. They researched the arborization of callosal axons originated in superficial callosal projecting neurons of the dysgranular RSC. These results showed that pyramidal neurons in L2/3 and large thick-tufted pyramidal neurons in L5b presented larger excitatory callosal responses than L5a and L5b thin-tufted pyramidal neurons to the input, whereas L6 remained silent. Feed-forward inhibitory currents

generated by parvalbumin positive-fast spiking (PV-FS) GABAergic interneurons recruited by callosal axons mimicked the response size distribution of excitatory responses across pyramidal subtypes. The response size is larger in pyramidal neurons of superficial layers and in the in the L5b thick-tufted pyramidal cells. Generally, the combination of excitatory and inhibitory currents due to callosal input had a strong and opposed effect in different layers of the cortex; whereas L2/3 pyramidal neurons were powerfully inhibited, the thick-tufted pyramidal neurons in L5 were strongly recruited. An important point is that stronger PV-FS dependent feed-forward inhibition in the former was not a particular feature of the callosal projection, but a general property of the organization of retrosplenial local microcircuits (Sempere-Fernàndez et al., 2016). Moreover, while upper layers PV microcircuits are organized in a feed-forward manner, in deeper layers they follow a feed-back organization which was more permissive for integrating synaptic excitation (Sempere-Fernàndez et al., 2019). Our laboratory also observed that a crucial determinant of the large L5b excitability comparing to L2/3 pyramidal neurons had IPSCs of lower amplitude and the temporal delay between the excitatory and inhibitory synaptic components was also larger in these cells. Their data also proposed that this difference depends on the lower gain of the cortical response of L5 PV-FS comparing to L2/3. They suggested that whereas superficial L2/3 PV-FS GABAergic interneurons were well suited to provide a powerful feed-forward inhibitory control of pyramidal neuron excitability, L5 PV-FS interneurons are mainly engaged in a feedback inhibitory loop and only after a substantial recruitment of surrounding pyramidal neurons responding to an external input.

4.2. Neocortical pyramidal cells

Approximately, a 85% excitatory pyramidal neurons and a 15% inhibitory interneurons comprise the mammalian neocortex (Cajal, 1991; DeFelipe & Fariñas, 1992; Markham et al. 2007; Ramaswamy & Markram 2015; Spruston 2008).

The nervous system consists in an enormous variety of neurons that present distinct dendritic morphologies, local and long-distance axonal connections, neurotransmitter phenotypes and patterns of gene expression. The generation of these different characteristics uses a range of cellular and early regionalization of the neural tube acting in conjunction with intracellular signals, temporally regulated factors and cell-intrinsic cues to determinate the fates and identities of specific classes of neurons progressively.

Pyramidal neurons are formed and travel radially from the periventricular surface to their final destination, close to the pia (Rakic 1972). In the mammalian isocortex, this migration follows an inside-out pattern, in other words, those pyramidal neurons from deeper layer are formed and reach their destination before those in superficial layers, which will have to travel through the formers to get their final position (Rakic, 1972; Rakic, 2010).

In the mammalian cerebral cortex, pyramidal neurons could be classified into two principal classes: cortico-cortical projection neurons (upper layers) and subcortical projection neurons (deeper layers). On the one hand, in the ventricular zone, early progenitor cells form deep layer neurons which express transcription factors as Sox5, Fezf2, and Ctip2, playing important roles in the specification of subcortically projecting axons. On the other hand, progenitors in the subventricular zone, which express Satb2 required for the formation of axonal projections that connect the two cerebral hemispheres, produce upper layer neurons. During development, the Fezf2/Ctip2 and Satb2 pathways appear to be mutually repressive in order to ensure that individual neurons adopt a subcortical or callosal projection neuron identity at early times. In addition, it is known that Satb2 regulates gene expression with molecular mechanism involving long-term epigenetic changes in chromatin configuration that could enable cell fate decisions in order to be maintained during development (Leone et al., 2008).

The cerebral cortex is organized in layers that are limited by the densities and morphologies of their neurons since Cajal appreciated it for the first time. Thanks to retrograde tracing techniques and intracellular dye injections it is generally known neurons in the upper L2/3 tend to form cortico-cortical connections, including projections to the contralateral hemisphere across the corpus callosum, while neurons in L5/6, and the subplate are the source of subcortical projections to targets that include the spinal cord, pons midbrain and thalamus. Neurons in L1 and L4 extend axons locally within the cortex. Although it is revealed that cortical interneurons arise from the same

progenitor population as those that generate projection neurons Furthermore, the bulk of these neurons derive from the ganglionic eminence, which serves as the progenitor pool for the striatum and basal ganglia.

As it is said above, progenitor cells that line the dorsal aspect of the lateral ventricles in the forebrain derive the cortical projection neurons. So that neurons of different layers are generated in a stereotypic temporal sequence during development. First, in the ventricular zone, immediately adjacent to the ventricles, mitotically active cells are found. Second, in the subventricular zone at later stages, which forms between the ventricular zone and the overlying intermediate zone. With more detail, the first neurons to specify and migrate out of the ventricular zone until the preplate. The preplate is split into two zones subsequently due to the arrival of neurons that form the cortical plate. On the one hand, the upper preplate (marginal zone) is occupied by Cajal-Retzius neurons, of which the vast majority are derived from a region known as the cortical hem and then migrate tangentially to populate the neocortex; and, on the other hand, the deeper domain of the preplate becomes the subplate being a largely transient zone of neurons which are involved in axon targeting during development. In order to make experiments, it is important to differentiate that neurons o the deepest layers (L5 and L6) are generated earlier than neurons of L4, L3 and L2 (MuhChyi et al., 2013; Leone et al., 2008; Tyler et al., 2015).

Regarding morphology, pyramidal neurons (or principal cells) present: a triangular soma; 2 different dendritic domains with high density of spines emanating from the base (basal dendrites) around the soma, and the apex of the soma (apical dendrites) which extend towards the Pia forming multiple oblique dendrites in route and terminating in a distinct tuft that is associated with high branching density; and an axon which usually forms several local collaterals before leaving the neocortex to project to distant brain regions. Functionally, apical dendrites characterized pyramidal cells with unique properties that are essential for integrating top-down, from association areas) and bottom-up streams of input (from primary sensory and motor areas) to the neocortex to shape the output firing pattern of pyramidal cells. Apical dendrites also form the basis for the generation of active dendritic and synaptic events: back-propagating action potentials, calcium transients in dendrites, integration of synaptic inputs from different cortical layers, and spike-timing dependent plasticity.

Until this moment, there is no a consensus on the number of morphologically different types of pyramidal cells in the neocortex. Even most neurons that are visually distinguishable, there is no an official morphological description to define them. This is the case of LS pyramidal neurons compared to regular spiking (RS or in our thesis named as non-LS) pyramidal neurons,

Types of pyramidal cells are objectively defined by their unique functional properties which are thought to be associated with morphology, as specific firing patterns

(Deitcher et al., 2017) and distinct synaptic subnetworks formed within and across layers (Kampa et al., 2006; Kanari et al., 2019; Yoshimura et al., 2005). Therefore, morphological cell types are separated using the branding properties of the apical trees (Jiang et al., 2015; Kanari et al., 2019). Nevertheless, it is nonconsensual and ambiguous classifications due to the subjective visual inspection despite the researcher experience (DeFelipe et al., 2013; Kanari et al., 2019; Ledergerber & Lakum 2010; Markram et al., 2015; Marx & Feldemeyer 2013). Apical branching structure was analyzed topologically in pyramidal cells by Markram's laboratory (Kanari et al., 2019) revealing 16 subtypes of neurons in all cortical layers, and also one more subtype was objectively identified in L6. They justified the presence of 3 subtypes in L2, 2 subtypes in L3, 3 subtypes in L4, 3 subtypes in L5 and 6 subtypes in L6. However, no pyramidal cells were found in L1. They described that apical dendrites of pyramidal cells in supragranular L2/3 reach L1 and the pia. The apical dendrites of pyramidal neurons in L4 and L6 often reach the supragranular layers, but not L1. Principal pyramidal cells subtypes in L5 have the longest apical dendrites, which reach L1 and the pia, and minor pyramidal cell subtypes in L5 tend to extend to the supragranular layers, bit not L1 (Figure 4.1). Moreover, they said that there is the existence of 2 subtypes that are not justified by the topological analysis: a subtype of tufted pyramidal cells in L5, and a horizontally oriented cell type in L6 (Kanari et al., 2019). This study validates the appearance of a common type of pyramidal cells across L2-L6 tufted pyramidal neuron and the existence of several types that are unique to specific layers (spiny stellate cells in L4 and the bitufted pyramidal neurons in L6). An interesting point is that the diversity of apical dendrites shapes is bigger with the distance from the pia,

stipulating that the large morphological variability that is present in deeper layers support its higher functional complexity (Kanari et al., 2019; Reimann et al., 2017). In fact, long-range axonal projection of pyramidal cells is a crucial property to classificate them because it enables different computational functions (Boudewijns et al., 2011; Brown & Hestrin 2009; Hattox & Nelson, 2007; Kanari et al., 2019; Larssen & Callway 2005). Hopefully, these observations could help to get a systematic characterization of whole-cell reconstructions in order to quantify their long-range axonal projection features and associate them to their local dendritic characteristics.

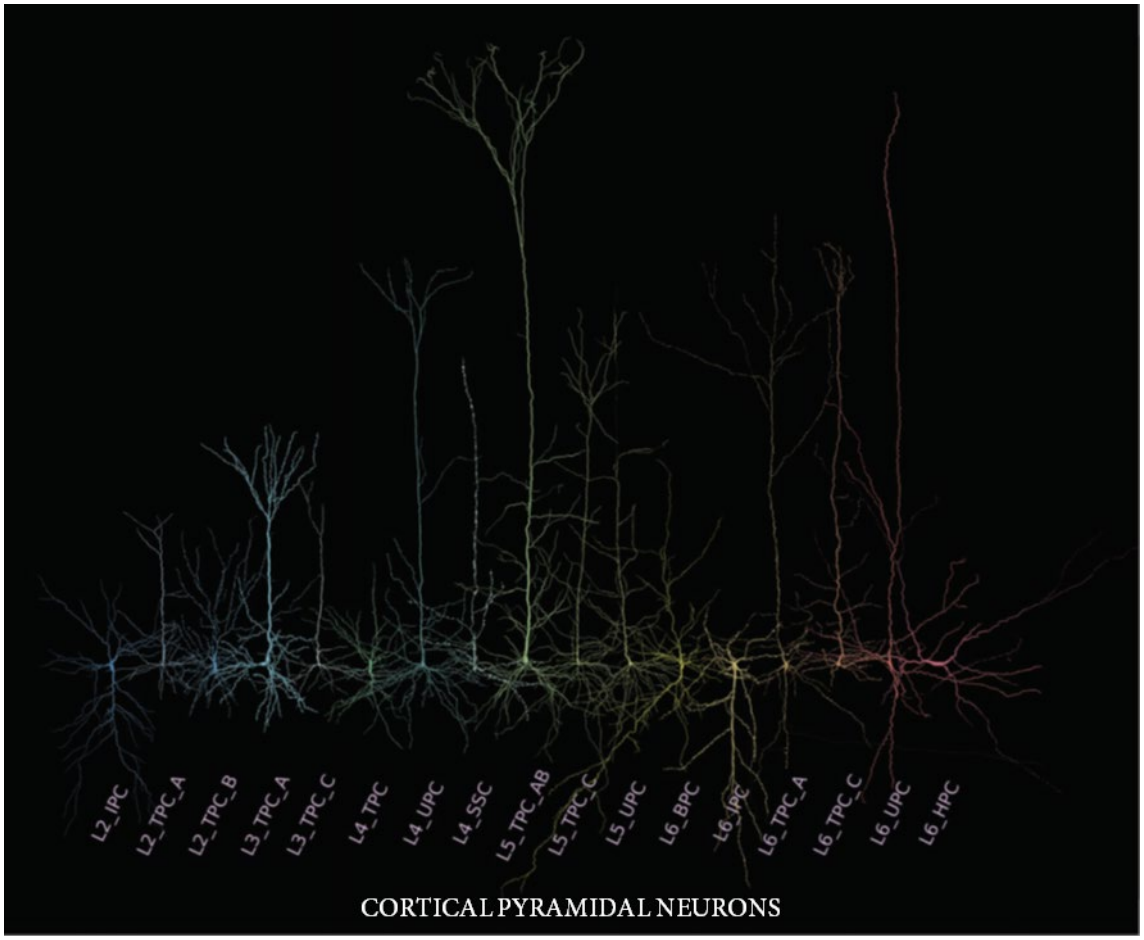

Figure 4.1. Cortical pyramidal cell types. Representations of somata and cell of all types/subtypes. On the one hand, deeper layers express a larger diversity of pyramidal cell types as the complexity of branching types increases from L2 to L6. The dendritic diameters have been scaled x2 to improve resolution of the dendritic morphologies. (IPC=inverted pyramidal cells); TPC= tufted pyramidal cells; UPC= untufted pyramidal cells; SSC= spiny stellate cells; BPC= bitufted pyramidal cells; HPC= horizontal pyramidal cells). Figure modified from Kanari et al., 2019.

4.3. Rodent retrosplenial cortex

Within rodent cerebral cortex, the RSC belongs to the isocortex. It is the most caudal part of the cingulate cortex (Czajkowski et al., 2014). However, there are no posterior cingulate areas 23 and 31 as in primates (Czajkowski et al., 2014; Van Groen & Wyss, 2003; Vann et al., 2009; Vogt & Paxinos, 2014).

For RSC research, location is everything. The term 'retrosplenial' defines the position immediately behind the splenium, the most caudal part of the corpus callosum (Vann et al., 2009). A striking feature of the rat RSC is its size that extends over half the length of the entire cerebrum, making it one of the largest cortical regions in this species (Vann et al., 2009). As in the primate, it is further divided into areas A29a–c (granular cortex) and area A30 (dysgranular cortex) (Figure 4.1) (Czajkowski et al., 2014; Shibata, 2000; Sigwald et al., 2016; Van Groen & Wyss, 2003). This nomenclature refers to the existence in the ventral region of smaller pyramidal neurons of high density of a L2/3 that disappear moving dorsally. These morphological differences are accompanied by differences in the electrophysiology of these neurons. The pyramidal neurons of the ventral region respond to depolarize current pulses with a firing pattern of LS, while in the dorsal region they show the pattern of RS classic pyramidal accommodation (Kurotani et al., 2013). We are going to refer to the regions and subregions as described by Van Groen and Wyss that is dysgranular, granular a and granular b regions (Figure 4.1) (Czajkowski et al., 2014; Van Groen & Wyss, 2003).

In 1994 was described in rat the cytoarchitecture of area 29, posterior cingulate cortex or posterior parietal cortex and its intrinsic and extrinsic connections (Hedberg & Stanton 1995), permitting interpretation of their results on the basis of a known population of posterior cingulate cortex neurons and their connectivities. Response to subiculo-cingulate tract and Corpus Callosum stimulation is best understood in light of the structural elements of posterior cingulate cortex (area 29): (1) a molecular L1 contained primarily of dendritic ramifications of L5 pyramidal neurons, the apical dendritic tufts of small and fusiform pyramidal cells and afferent axonal plexus; (2) a granular tightly packed L2/3 consisting of the somata of small and fusiform pyramids that are found only in this cortical region, dendritic tufts of large L5 and medium L6 pyramidal neurons and some non-orienting (extraverted) large pyramidal neurons; (3) an agranular L4 which comprises a spatially dispersed representation of the pyramidal neuron types occurring in L2/3; (4) a deep magnocellular L5 involving large pyramidal neurons which receive dense innervation from transcallosal and thalamic fibers and whose vertically oriented apical dendrites undergo extensive arborization in L1 and L2/3; (5) a deep L6 containing small and very large pyramids with efferent axons coursing to contralateral and anterior cingulate cortex as well as to anterior thalamic nuclei. Throughout all submolecular layer, a huge number of polymorphic and intrinsically projecting local circuit interneurons are homogeneously distributed. These interneurons are largely GABAergic and probably mediate both feedforward and feedback inhibition of excitatory afferent inputs.

In summary, the findings of the last study indicate that: (1) posterior cingulate cortex is 'tuned' to respond maximally to θ-frequency input from subiculum; (2) within the 3-8 Hz tuning window, subiculo-cingulate tract-driven EPSP and first action potential latencies in neurons of superficial and deep layers reach maximal synchrony and are thus configured to synaptically relay subiculo-cingulate tract input in a 1:1 correspondence to both intracingulate and upstream sites; (3) θ -frequency input can likewise 'prime' normally quiescent synapses for long term synaptic plasticity induction permitting the recruitment of additional intra and extracingulate circuitries or subroutines; (4) tetanization of corpus callosum or subiculo-cingulate tract inputs elicited the expected homosynaptic LTP of the deep layer pyramidal response, but failed to induce long-term plasticity in polysynaptically driven superficial layer pyramidal neurons; (5) θ -burst tetanization of corpus callosum inputs coupled with the interleaving of out-of-phase subiculo-cingulate tract stimulation at 5 Hz yielded associative LTD, however heterosynaptic LTD of equivalent magnitude could also be elicited in this pathway in the absence of 5 Hz stimulation; (6) low frequency (1-5 Hz) stimulation of either corpus callosum or subiculo-cingulate tract produced homosynaptic LTD in each pathway and finally; (7) these findings are in accordance with a model of the organization of posterior cingulate cortex microcircuitry reported previously (Hedberg & Stanton 1995).

Collision and latency studies have suggested that most superficial layers (L2/3-L4) pyramidal neurons driven by subiculo-cingulate tract stimulation are activated polysynaptically, via the ascending axonal collaterals of deep layer pyramidal neurons

evoking a mixture of longer latency pure EPSPs and recurrent inhibitory postsynaptic potentials (IPSPs). Superficial layers intracellular recordings thus show complex, mixed-sign postsynaptic potentials. Posterior cingulate cortex, as a synaptic target of hippocampal output and thalamic sensory information, is the site of generation of characteristic neuronal population potentials by a predictable sequence of both intra- and interlayer processing of that synaptic input. The induction of long-term changes in the strength of critical synaptic pathways could thus play a significant role in: (1) the processing and storage of amplitude and frequency modulated input; (2) the gating of hippocampal output; and (3) selective response sensitivity to particular input firing frequencies. Since the only spiny apical dendrite branchings in L2/3 arise from medium and large pyramidal neurons with somata confined to L5 and L6 (deep pyramidal neurons) and these same neurons send axonal collaterals back up into superficial layer where they innervate both superficial pyramidal neurons and interneurons. Posterior cingulate cortex microcircuitry reviewed in detail, may be sufficient to sustain a bilayer back-propagation loop. Accordingly, elucidation of specific patterns of activity that induce long-term plasticity in each layer is a crucial step in determining the information processing capabilities of posterior cingulate cortex in relation to hippocampal input and its integration with thalamic and other extracingulate input. The importance of such determinations arises from the possibility that the subiculo-cingulate tract / posterior cingulate cortex system may serve as a comparator or 'gate' to motor areas for environmentally relevant information encoded in the corticopetal output of neural comparisons computed at synapses on CA3 pyramidal neurons. Variations in both the

period and coherence (synchronicity) of the rhythmic discharges carried from hippocampus have been repeatedly linked with learned perception of novel stimuli in a number of behavioural paradigms (Hedberg & Stanton 1995).

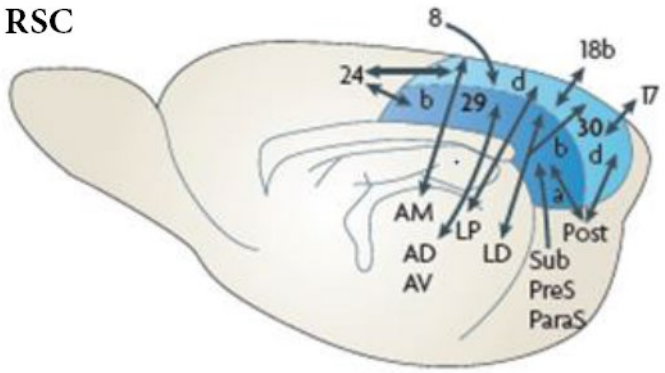

Figure 4.2. Location and principal connections of the rat RSC. d indicates the dysgranular cortex (area 30); a and b respectively indicate divisions granular a region and granular b region within the granular cortex (area 29). The arrowheads in area 29 do not distinguish between granular a region and granular b region. Figure modified from Vann et al., 2009.

Compatible with this cytoarchitecture, on the one side, the GRSC is connected with limbic regions preferentially (anterior thalamus and the hippocampus that is

essential for many kinds of memory) having a greater involvement in internally directed navigation that contains "head-direction" cells (Shibata, 2000).

On the other side, the dysgranular RSC presents a greater connectivity with early visual regions, the parietal cortex and the parahippocampal region, more closely connected with neocortical regions and playing an important role linking limbic memory areas with spatial and behavioural processing and navigation (Harland et al., 2014; Knight & Hayman, 2014; Miller et al., 2014; Oda et al., 2014; Palomero-Gallagher et al., 2009; Vogt & Paxinos, 2014). The "head-direction" cells in these different regions have different discharge properties. In the RSC, the directional firing of some head-direction cells is modulated by the animal's movements. However, the relationship of the head-direction cells between RSC, laterodorsal and anterodorsal nucleus remains unclear. Understanding the circuitry that conveys the head-direction signals between the RSC and laterodorsal nucleus; and RSC and anterior nuclei is indispensable for elucidating the neural mechanisms of the sense of directional movement (Shibata, 2000).

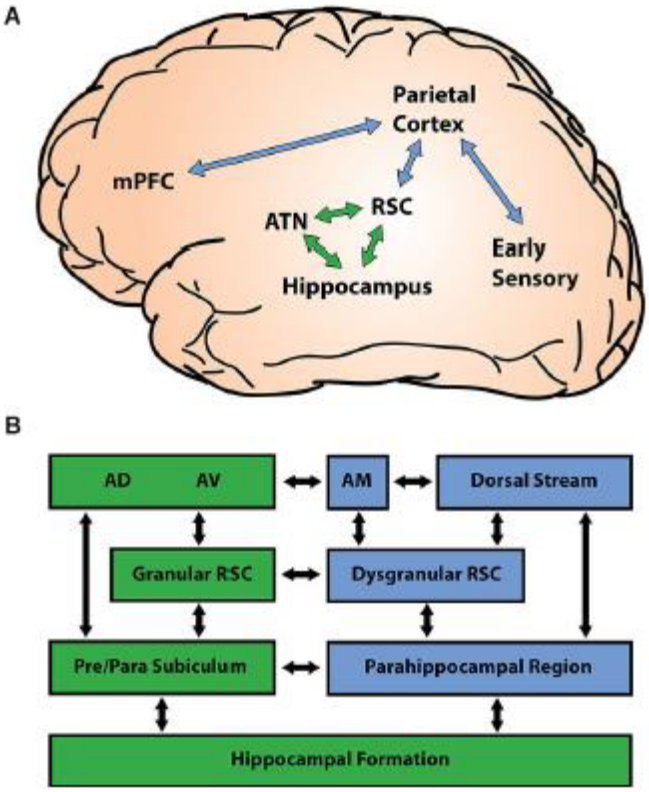

Figure 4.3. RSC connectivity. (A) RSC is centrally positioned between cortical sensory regions (blue) and limbic memory regions (green). (B) RSC presents regional differences in connectivity with limbic (green) and cortical (blue) regions. GRSC (areas 29a-c) manifests greater connectivity with limbic regions such us the subicular cortex and the anterodorsal and anteroventral nuclei of the anterior thalamic nuclei, while the dysgranular RSC (area 30) presents greater connectivity with cortical regions involving the parahippocampal region, the posterior parietal cortex and early visual areas. The connections of the anterior thalamic nuclei also differ by region, with the anterodorsal and anteroventral nuclei exhibiting greater connectivity with limbic areas and the anteromedial nucleus presenting greater connectivity with neocortical regions. Figure taken from Miller et al., 2014.

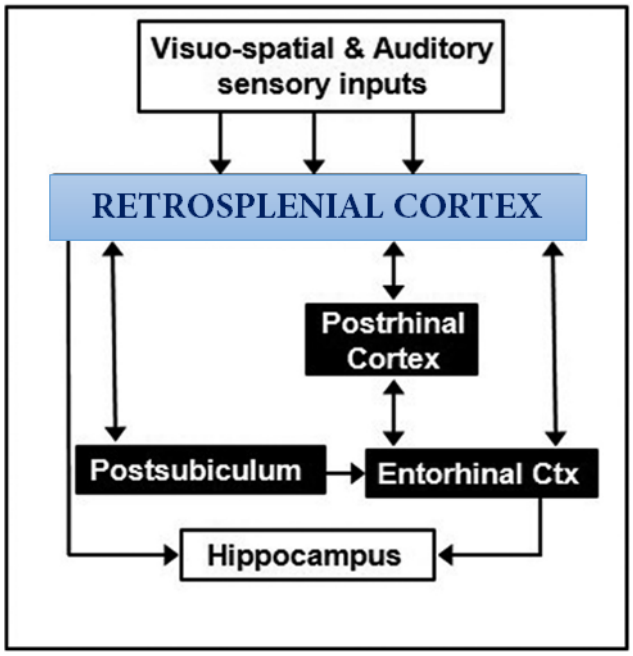

Figure 4.4. Schematic diagram of corticoretrosplenial circuitry involved in processing contextual information.

Simplified illustrating only the densest connections. Figure modified from Robinson et al., 2014.

Humans differ also in abilities of individual navigation. These differences individually may exist because successful navigation relies on several disparate abilities in part, which rely on different brain structures. One such navigational capability is path integration, the updating of position and orientation, in which navigators track distances, directions and locations in space during movement. Stern's laboratory suggested that

these three aspects of path integration are largely independent (Chrastil et al., 2017). The RSC is positioned and interconnected between limbic areas which are important for memory formation (hippocampus and the anterior thalamus, limbic regions and cortical regions along the dorsal stream) (Figure 4.2) known to contribute importantly to long-term spatial and contextual representation (posterior parietal/visual cortex). The specific deficits seen in tests of human and rodent navigation suggest that RSC supports allocentric representation by processing the stable features of the environment and the spatial relationship among them (Sulpizio et al., 2015). Specifically, RSC is central to translating egocentric spatial information into allocentric reference frames (Lin et al., 2015). A study from 2017 showed that recordings made from RSC while rats navigated through a complex environment has revealed populations of cells that encode route-segments as well as the relative position of these segments within an allocentric framework (Clark, 2017). A more specific study was done in 2015 where it is said that other sites may be able to compensate for the loss of the RSC because there are good reasons to suppose that the RSC has a very different role in spatial memory from that of the hippocampus and anterior thalamic nuclei (Nelson et al., 2015). They demonstrated through RSC lesions that RSC use both allocentric and directional information, exacerbated by an impaired ability to switch between different cue types (Nelson et al., 2015). Nevertheless, the subset of thalamocortical projections to RSC has unique molecular basis in the glutamatergic transmission system (Oda et al., 2014). In addition to spatial cognition, it is compiled in a recent review (Chrastil, 2018) that RSC plays a key role in contextual and episodic memory. In this way, RSC plays a dual role as part of the

feedforward network providing sensory and mnemonic input to the hippocampus and as a target of the hippocampal-dependent systems consolidation of long-term memory. The findings of Shan's laboratory indicate two possible networks regarding RSC: a sensory-cognitive network that has a hub in the RSC and that processes sensory information, episodic memory and spatial learning; and other network that is involved in the regulation of visceral functions and arousal. Furthermore, between the bilateral RSC was observed functional asymmetry (Wang et al., 2016).

And the results of Stark's laboratory placed clear handicaps on the experimental methods to aim to research the representations contexts and items during performance of associative memory tasks (Huffman & Stark, 2017). Moreover, their results provoke interesting theoretical questions related to the disambiguation of memory-related representations from processing-related representations. Furthermore, it was revealed an early post-training involvement of anterior RSC in the processing of a long-lasting aversive memory (Katche & Medina, 2017). In addition, the posterior cingulate cortex in humans, which is RSC in rodent, has a key role in integrating the neural representations of self-location and body ownership (Guterstam et al., 2015). Moreover, it was suggested in humans that a greater waking connectivity between the RSC/hippocampus and various nodes of the Default Mode Network was associated with lower sleep efficiency, lower amounts of rapid eye movement sleep and greater sleep-onset latency, in other words, insomnia (Regen et al., 2016). Also in humans, it was associated the subjective cognitive impairment which is a clinical state characterize by subjective cognitive deficits without

cognitive impairment. It was implied that reduced functional connectivity in cortical midline structures comes up with overestimation of the experience of forgetfulness (Yasuno et al., 2015). The RSC complex is a region implicated in spatial navigation (Burles et al., 2017; Miller et al., 2014). Moreover, it was demonstrated in 2014 that RSC has a role in processing temporal information and in turn extend the role of the RSC beyond the physical context to now include the temporal context (Todd et al., 2015). RSC has a critical role in the retrieval acquired auditory fear memories, and it was suggested that this is related to the quality of the memory, with less precise memories being RSC dependent (Todd et al., 2016). All the areas of the RSC provide sparse projections, mainly ipsilateral, to the anterodorsal nucleus, with a crude topographic pattern such that the rostrocaudal axis of the RSC corresponds to the caudorostral axis of the anterodorsal nucleus. The data of Shibata indicates that each area of the RSC has a different projection field within the anterior thalamic nuclei suggesting that each of these projections transmits distinct information which is important for complex memory and learning functions, e.g. spatial memory and discriminative avoidance learning. The interaction between the RSC and the anterior thalamic nuclei is especially interesting for such behavioural learning and spatial memory like contextual fear conditioning (Shibata, 1998; Todd et al., 2017).

Additionally, it was demonstrated that blocking protein synthesis in the RSC before, but not after acquisition impairs rats memory for trace neutral conditional

stimulus and context fear without affecting memory for the neutral conditional stimulus in standard delay fear conditioning (Kwapis et al., 2015). The last research also showed that NMDA receptor blockade in the RSC transiently impairs memory retrieval for trace, but not delay memory. So that, the RSC therefore appears to critically contribute to formation of trace and context fear memory in addition to its previously recognized role in context memory retrieval.

Neurons within cortical L4-L5 of A29 (GRSC) are critically required for efficient retrieval of contextual fear memory (Sigwald et al., 2016). To elucidate the involvement of RSC areas 29c and 30 in spatial memory, an experiment was done with c-Fos expression in rats during several days (Malinowska et al., 2016). What they obtained was that areas 29c and 30 seem to be activated during spatial memory processing on the first day of training, while area 30 appear suppressed during long-term memory functioning on the third day when rats effectively avoid.

It was delighted a positive point to functional connectivity between subgenual anterior cingulate cortex and bilateral parietal regions such as RSC potentially underlining this connection as being important in the modulation of the non-prospective, hastiness-related aspects of impulsivity (Golchert et a., 2016). This proposes that poor perseveration and premeditation may be linked to dysfunctions in how the rostral zone of the anterior cingulate cortex interacts with the multiple demand network that allows cognition to proceed in a controlled way.

A positive urgency was elated to functional connectivity between subgenual anterior cingulate cortex and bilateral parietal regions such as RSC potentially highlighting this connection as being important in the modulation of the non-prospective, hastiness-related aspects of impulsivity (Golchert et al., 2016). This suggests that poor perseveration and premeditation might be linked to dysfunctions in how the rostral zone of the anterior cingulate cortex interacts with the multiple demand network that allows cognition to proceed in a controlled way.

In addition, in 2017, it was suggested the selective vulnerability of the primary sensorimotor cortices and associations between cortical thinning in the prefrontal and parietal cortices and cognitive impairment in HIV-infected patients (Shin et al., 2017). Furthermore, for the first time, Yoon's laboratory proposed retrosplenial cortical thinning as a possible major contributor to HIV-associated cognitive impairment.

Other study in humans confirmed that using functional magnetic resonance imaging (fMRI) it was suggested that: according to the rodent bibliography, the human thalamus might integrate visual and body-based orientation cues; global reference be used to integrated head direction across separate individual locals; and immersive training procedures providing full body-based cues might help to clarify the neural mechanisms supporting spatial navigation (Shine et al., 2016).

Furthermore, it was revealed an implication of RSC in temporal order memory and that rat RSC involves one of a group of closely interlinked regions that enable recency memory, including the hippocampal formation, medial diencephalon and medial frontal cortex (Powel et al., 2017). Considering the well-established importance of the RSC for spatial learning, the findings support the notion that, with its frontal and hippocampal connections, RSC has a key role for both what/when and where/when information. Dynamic processes recruit RSC, hippocampus and parahippocampal cortex too in support of path integration, involving a homing vector system that tracks movement relative to home (Chrastil et al., 2015).

RSC is reciprocally connected with several areas in the parahippocampal region (Agster & Burwell, 2009; Kononenko & Witter, 2016) and share some functional properties with spatially and directionally modulated neurons in presubiculum, parasubiculum and medial entorhinal cortex (Alexander & Nitz, 2015; Olsen et al., 2017). Consequently, the RSC is positioned at the interface between the medial temporal lobe memory system and sensory regions. In fact, there are studies indicating that RSC might serve as a sensory integration center (Bos et al., 2017; Olsen et al., 2017). RSC present projections to medial entorhinal cortex and this might be an inefficient route to the hippocampal-projecting neurons of medial entorhinal cortex. First, posterior parietal cortex preferentially projects to rostral RSC, whereas it is the caudal RSC that originates the biggest input to medial entorhinal cortex. Second, RSC projections mostly terminates in L5 of medial entorhinal cortex where the receiving neurons relay to superficial layers.

Therefore, although RSC projects directly to medial entorhinal cortex, some relays within RSC and medial entorhinal cortex are necessary for information from posterior parietal cortex to reach superficial layers of medial entorhinal cortex. On the other side, the whole rostrocaudal axis of RSC strongly projects to presubiculum adding importance to this area as a relay since it distributes, similar to postrhinal, projections to superficial layers of medial entorhinal cortex, likely targeting hippocampal-projecting neurons even though synaptic contacts are made onto L5 neurons. To sum up, presubiculum remains as the parahippocampal area that provides the most efficient route for posterior parietal cortex projections to lead superficial layers of medial entorhinal cortex and ultimately the hippocampal formation (Olsen et al., 2017).

Posterior parietal cortex is implicated in spatial functions as navigation. Hippocampal and parahippocampal region and RSC are critically implicated in navigational processes and connections between the parahippocampal/retrosplenial domain and the posterior parietal cortex. Considering the close association of the presubiculum with RSC, Witter's laboratory incorporates the latter in their analysis in rat. They indicated that posterior parietal cortex is moderately connected with RSC, concretely with rostral area 30. The insufficiency of the connectivity with the parahippocampal and retrosplenial domains proposes that posterior parietal cortex is only a modest actor in the formation of spatial representations underlying spatial memory and navigation in parahippocampal and RSC (Olsen et al., 2017; Zgraggen et al., 2012) The relative sparseness of the connectivity with the parahippocampal and retrosplenial

domains suggests that posterior parietal cortex is only a modest actor in forming spatial representations underlying navigation and spatial memory in parahippocampal and RSC described (Olsen et al., 2017; Zgraggen et al., 2012). However, an integrated account of the organization of these connections is lacking.

Human being vary substantially in orientation and navigation ability within the environment. However, it is difficult determine specific causes of these individual differences. For building a mental representation of an environment, stable landmarks are crucial. Poor navigators, in contrast to good, have been shown to have difficulty identifying permanent landmarks with a concomitant reduction in fMRI activity in the RSC (Auger et al., 2017).

Furthermore, hippocampus is a key structure for coding an animal's detailed location in time and space; and for linking noticeable behavioural events to this spatiotemporal framework (Bos et al., 2017; Robinson et al., 2014). Memory and spatial navigation depend on the neural coding of an organism's location. It is suggested that fine-grained coding of location depends on the hippocampus. Equally, animals benefit from knowledge parsing their environment into larger spatial segments, which are important to task performance (Bos et al., 2017).

Moreover, hippocampus is essential for retrieving spatial and contextual memories. It is supposed that it mediates representations of the environment that were

created during learning. In addition, dorsal hippocampus can modulate fear responding independent of the ventral hippocampus (Tanaka et al., 2014). In contrast, it is checked that learning does not require the hippocampus because Urba's group tested the involvement of the RSC in this process and they stipulated that RSC might participate to episodic memory formation by linking essential sensory stimuli during learning (Cowansage et al., 2014; Robinson et al., 2014). Furthermore, Perirhinal cortex mediates discrimination and learning of complex configurations in the environment which might incorporate multiple items and environmental context. Its firing patterns are maintained across large spatial segments of the task environment. This is opposed to transient firing in sensory neocortex and hippocampus (Bos et al., 2017). These results from different laboratories might have noticeable implications for our understanding of the genesis of contextual and spatial coding in the hierarchy from sensory cortices to the hippocampal system. The data of Urban's laboratory stipulate that RSC has a crucial role in forming association between multiple sensory stimuli in the absence of reinforcement, a principal component of episodic memory (Robinson et al., 2014).

Regarding anatomy, RSC receives inputs from dorsal hippocampal networks and in turn projects to medial neocortical areas, also a particular prominent projection extends rostrally to the posterior secondary motor cortex, proposing a functional cortico-cortical link from the RSC to secondary motor cortex and therefore bridge between hippocampal and neocortical networks involucrated in sensorimotor and mnemonic aspects of navigation (Yamawaki et al., 2016). The findings of Shepherd's laboratory

established an excitatory RSC to secondary motor cortex cortico-cortical circuit that engages diverse types of excitatory projection neurons in the downstream areas, stipulating a basis for direct communication from dorsal hippocampal networks included in spatial memory and navigation to neocortical networks involucrated in diverse aspects of motor control and sensorimotor integration.

4.3.1. Retrosplenial cortex lamination

RSC is contemplated as an intermediate cortex because this cortical area displays a transitional cortical pattern of lamination compared with the 6-layered neocortex and 3-layered archicortex (Zgraggen et al., 2012). Comparable to neocortex, the medial limbic region develops in an "inside-out" fashion; infragranular deep cells are generated earlier than supragranular superficial cells as it is explained above (Leone et al., 2008). Whereas neurons in medial regions are generated later than those in more lateral subdivision in the neocortex, in the limbic cortex is not a continuation of the adjacent somatic neocortex, at least in terms of ontogenic pattern (Zgraggen et al., 2012). The studies of Kiss's laboratory showed a notable pool of postmitotic cortical glutamatergic precursors localized in the dorsomedial corner of the ventricular zone/subventricular zone underlying the medial limbic cortex. In their data it was demonstrated that theses cells exit the subventricular zone and migrate radially toward L2 during the first postnatal week, forming the last-formed pyramidal subpopulation of the medial limbic cortex. In

the GRSC, the vast majority of these cells give rise to well-described dendritic bundling cells (Zgraggen et al., 2012). At 7 postnatal day age, almost all cells (98%) were accumulated in L2 because it takes place between 5-7 postnatal days. Thus, pyramidal precursors, which migrate out of the ventricular zone/subventricular zone postnatally, are already postmitotic at 0 postnatal day. Less than 5% of the postnatally migrating neurons in L2 displayed GABAergic phenotype. The fact that the large majority of migrating cells and neurons settled in L2 express Satb2 is consistent with the notion that these cells are transcallosal-projecting neurons.

Memory depends on lasting adaptations of neuronal properties elicited by stimulus-driven plastic changes. The strengthening and weakening of synapses results in the establishment of functional ensembles. It is presumed that such ensembles, or engrams, are activated during memory acquisition and re-activated upon memory retrieval. RSC has appeared as a key brain area supporting memory in humans and spatial memory in rodents. Regarding dysgranular RSC, it is densely connected with dorsal stream visual areas and contains place-like and head-directions cells, making it a prime candidate for integrating navigational information as we said before (Milczarek et al., 2018). The studies of Milczarek in mouse dysgranular RSC directly provide confirmation for the interdependence of spatial memory consolidation and RSC engram formation. It is denoted the participation of RSC in spatial memory storage at the level of neuronal

ensembles. So that, gradual emergence of a context-specific pattern of neuronal activity, which is retained over long periods of time, accompanies spatial learning. Moreover, a relationship with the degree of forgetting is displayed by the stability of the reactivated engram, giving for the first time direct demonstration for the interdependence of spatial memory consolidation and RSC engram formation. Related to that, Maguire's laboratory concludes that a decreased ability to process landmark permanence might be a participative factor to sub-optimal navigation and could be associated to the level of RSC engagement (Augeret et al., 2017). To sum up, in spite of the consensus that environmental representation are built upon permanent, stable landmarks, variability in the processing of permanent landmarks as a potential source of individual differences in navigation has been almost ignored. More investigations of this with contribution of RSC could help to understanding how spatial representations are built, varied and are amenable to change. In addition, in many cases, long-term representations consolidated in cortical regions can then support spatial navigation independent to hippocampus (Bicanski & Burgess 2016; Fink & Meyer 2002; Hedberg & Stanton 1994; Mayford et al., 1996; Miller et al., 2014; Yasuda & Mayford 2006;).

Furthermore, naturally occurring conditions that compromise the default network, including Alzheimer's disease and normal ageing, are well known to impair episodic memory and other cognitive deficits from the earliest stages of this disease

(Aggleton & Nelson, 2014; Ash et al., 2016;Harland et al., 2014; Oda et al., 2014; Bos et al., 2017; Vann et al., 2009).

In addition, transient memories are formed as we go about our daily life at home or work. They generally occur against the background of relevant prior knowledge. Many of these "everyday" memories, being of little consequence, are forgotten rapidly as Ebbinghaus first reported with experiments on memory training for nonsense syllables (Ebbinghaus, 1885, as cited in Ebbinghaus, 2004). However, a subset of everyday memories may be retained overnight or for longer (Wixted, 2004). More recent studies suggests a new observation consisting in a stronger gene-activation in hippocampus and RSC following spaced than massed training (Nonaka et al., 2017). Distinctive features of their protocol include its potential validity as a model of memory encoding used routinely by human subjects every day, and the possibility of multiple within-subject comparisons to speed up assays of novel compounds.

According to its function, it was suggested for the first time in 2015 using contextual fear conditioning in rats that the cannabinoid system of the RSC also modulated emotional memory improving long-term memory consolidation with agonists of the cannabinoid receptor type I (CB1R) (Sachser et al., 2015). For contextual fear conditioning, memory relies upon the RSC without regard to how long ago conditioning occurred, while areas connected to the RSC (anterior cingulate cortex and dorsal hippocampus) appear to play roles which are time-limited. Accordingly, the degree of

coherence between brain areas and the RSC might contribute and predict to context memory retrieval and retrieval-related phenomena like fear extinction. Notably, even though theta coherence in this circuit rises during memory encoding retrieval of recent memory, failure to decrease RSC-dorsal hippocampus theta coherence may be linked to retrieval deficit in the long term and perhaps contribute to aberrant memory processing characteristic neuropsychiatric disorders (Corcoran et al., 2017). Moreover, RSC is involved in the spreading of epileptic activity like perirhinal cortex (Salaj et al., 2015).

Other finding from our laboratory provided knowledge about the propagation of synchronic electrical activity in the cerebral cortex, including its modulation by serotonin, and suggest the presence of deep differences between the anterior cingulate cortex and RSC in the structure of the local cortical microcircuits underlying the propagation of synchronous discharges (Rovira & Geijo-Barrientos, 2016). In a research it was revealed the importance of the RSC for processing various classes of visuospatial information and highlight a broader role in the incidental learning of the features of a spatial array, consistent with the translation of scene information (Nelson et al., 2015).

4.3.2. Rodent granular retrosplenial cortex

More concretely, we have studied the GRSC. The modular organization was first discovered in rat (Wyss et al., 1990). Structures associated with the small-scale module are called "minicolumn" and it can be observed frequently in the cerebral cortex. Distinguished features of the L1 GRSC modular organization in rat (Figure 4.3) comprise: (1) the aggregation or segregation of apical dendrites (receiver) of types of pyramidal cells, the same or different, respectively, and (2) the fact that certain types of terminals (inputs) either match or interdigitate with a specific type of dendritic aggregation (Ichinohe, 2012). It was found that the well-filled dendrites of callosally projecting L2 pyramidal neurons group together in discrete bundles meanwhile they ascend toward the pial surface (Figure 4.3) (Ichinohe, 2012; Van Groen & Wyss, 2003). Moreover, several other recent investigations provide evidence that disrupting the dense reciprocal connections between the GRSC and anterior thalamic nucleus results in a striking loss of synaptic plasticity in the superficial layers of the GRSC (Kurotani et al., 2013).

Okamura's laboratory recopilated that many anterograde and retrograde tracing studies of the RSC have reported that GRSC has reciprocal connections with the anterior cingulate cortex, the area 18b (visual) cortex, the subiculum, and the anterior ventral and lateral dorsal thalamic nuclei. The GRSC also receives projections from the precentral agranular cortex, the claustrum, and the horizontal limb of the diagonal band of Broca. There is a layer organization of the efferent neurons in the GRSC. A point-to-point

projection originates in the neurons of the superficial layers L2, L3, and L5, and a somewhat more widespread projection originates from the neurons in L3 and L5. The intrinsic projections from the GRSC arise from projects predominantly to L2, whereas the postsubiculum projects to L1 and L3-L5. Axons from the contralateral GRSC formed a dense terminal plexus in L4 and L5. Thus, the IL-18R-ir neurons in L5 of the GRSC exchange and associate limbic regions and visual information with the cingulate, the subicular and the area 18b (visual) cortices. Many parvalbumin-, calretinin- and calbindin-containing neurons are found in the GRSC. Parvalbumin-containing neurons co-localize with γ-Aminobutyric acid (GABA). These parvalbumin-, calretinin- and calbindin- containing neurons are small and distributed throughout the GRSC, but not confined to L5. Considering their cell sizes, the location and the distribution pattern of their dendrite, these calcium-binding protein-containing neurons were thought to be interneurons in the RSC (Hayakawa et al., 2016).

GRSC has dense connections between the anterior thalamic nuclei and hippocampal formation. These three areas have been assumed to operate conjointly to support spatial learning and memory, default mode network and emotional evaluation of behavioural contexts. Connections between the GRSC and anterior thalamic nuclei strongly affect association learning. Moreover, the hippocampal-retrosplenial network is responsible for spatial representation (Honda et al., 2011). Studies of Kurotani's laboratory researched employing fast voltage-sensitive dye imaging in slices of rat brain. On the one hand, using coronal slices, L1 stimulation, which activates thalamic fibers

presumably, evoked propagation of excitatory synaptic signals from L2-L4 to L5-L6 in a perpendicular direction to the layer axis, followed by transverse signal propagation within each layer. Using ionotropic glutamate receptor antagonist, direct activation interneurons in L1 induced inhibitory responses in superficial layers. On the other hand, using horizontal slices, excitatory signals in deep layers propagated transversely via superficial layers mainly from posterior to anterior. Moreover, cortical inhibitory responses upon L1 were weaker in horizontal slices than in coronal slices. Differences were found between coronal and horizontal plane proposing anisotropy of the intracortical circuitry. In conclusion, both in horizontal and coronal planes of the GRSC, anterior thalamic nuclei inputs are processed differently and conveyed to other cortical areas. Furthermore, superficial layers of GRSC in both planes play a crucial role in signal propagation suggesting the importance of the superficial neuronal cascade in the integration of multiple information sources (Nixima et al., 2017). Nevertheless, there is a limited knowledge of the functional connectivity on GRSC. Then, in order to understand the GRSC function, it should be elucidated how anterior thalamic nuclei inputs are processed in the GRSC microcircuitry by these peculiar superficial neurons particularly. Also in Kurotani's laboratory (Nixima et al., 2017), using optical recordings of neuronal activity through fast voltage-sensitive dye in brain slices of rat GRSC, it was evidenced that thalamic inputs first activate superficial GRSC layers and then deeper GRSC layers. Apart from that hippocampal formation inputs project to GRSC deeper layers directly, superficial neuronal cascades temporally modulate anterior thalamic nuclei and hippocampal formation and might trigger synaptic plasticity in deeper layers. It was

demonstrated too that superficial layers are essential for transverse propagation of excitation along the cortical layers to other cortical regions, proposing a possible role as an information hub of GRSC.

A recent study of 2019 specify one step more investigating the potential circuit suggested by projections to GRSC L1 from GABAergic CA1 neurons and anterior thalamic nuclei. They found that CA1 project GRSC projections stem from GABAergic neurons with a distinct morphology, electrophysiology and molecular profile. Their long-range axons inhibit L5 pyramidal neurons in GRSC via potent synapses onto apical tuft dendrites in L1. These inhibitory inputs intercept L1-targeting thalamocortical excitatory inputs from anterior thalamic nuclei to co-regulate GRSC activity. Subicular axons, in contrast, excite proximal dendrites in deeper layers. However, short-term plasticity differs at each connection and CA1 to GRSC or anterior thalamic nuclei to GRSC connections oppositely affects the encoding of contextual memory (Yamawaki et al., 2019). They established retrosplenial-projecting CA1 neurons as a distinct class of long-range dendrite-targeting GABAergic neuron, and delineate an unusual cortical circuit specialized for integrating long-range inhibition and thalamocortical excitation. In addition, it was suggested that plasticity in the GRSC could be involved in the positive modulatory effects of post-training intracranial self-stimulation on TWAA (two way active avoidance conditioning) memory consolidation (Kádár et al., 2016).

The underlying substrates of GRSC function are complex, and are likely to incorporate both intrinsic cellular specializations as well as network properties. Theta rhythmic activity has been postulated to coordinate activity in distributed systems, including the GRSC, during mnemonic processes. Detailed information for the GRSC, however, is largely limited to anatomical characterization of individual neuronal types, and identification of the major inputs and outputs (Kurotani et al., 2013).

A distinctive feature of the rodent GRSC is an accentuated L2, consisting mainly of closely packed, callosally projecting small pyramidal neurons (Ichinohe, 2012, Nixima et al., 2017; Van Groen & Wyss, 2003). In the rat, the apical dendrites of these neurons form prominent bundles, which co-localize with parvalbumin-positive dendrites and with patches of thalamic terminations. The majority of pyramidal neurons in L2, and some in underlying L3, have a distinctive LS firing pattern, where an initial rapid rise in membrane potential is followed by a slowly ramping depolarization that leads to an action potential firing near the end of a just-threshold current step. It is worth mentioning that this LS property is unusual for pyramidal neurons, but has been previously reported for pyramidal neurons of rat perirhinal cortex and several cell types like medium spiny stellate neurons of the basal ganglia, neurons in the intermediate layers of the superior colliculus, and cortical neuroglia form cells (Chu et al., 2003; Kurotani et al., 2013). The most remarkable feature of L2/3 neurons is that their LS firing, which presumably facilitates comparison or integration of different timed synaptic inputs, consistent with the proposed role of the GRSC in memory-related processes (Nixima et al., 2017).

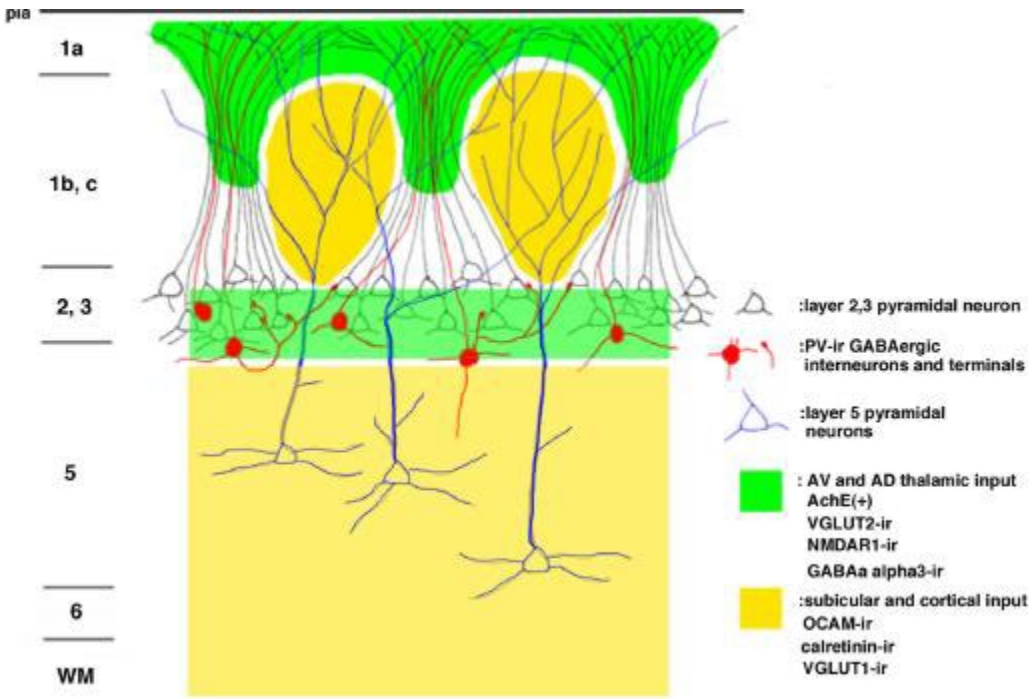

Figure 4.5. Schematic drawing of the modular organization of the L1 GRSC. Figure taken from Ichinohe, 2012.

Moreover, it is revealed that LS property is due to of delayed rectifier and A-type potassium channels, which are identified as Kv1.1, Kv1.4 and Kv4.3 (Kurotani et al., 2013). And it is known that Kv4.2, Kv4.3. and Kv1.4, which are encoded by A-type potassium channels differentially regulate intrinsic excitability of cortical pyramidal neurons (Carrasquillo et al., 2012). Our group researched about the current I_A, this I_A is a fast-activating and inactivating outward K^+ subthreshold voltage activated current that

activates at Vm=-50mV approximately and works against depolarization. It generates a change in membrane voltage enough to delay the action potential firing and generates the LS firing pattern. Moreover, the I_A is known to be a regulator of the repetitive action potential firing and membrane excitability in other neuron types and their cortical regions, but only the pyramidal neurons in the GRSC and perirhinal cortex show LS firing pattern that we know of.

Little is known about spatio-temporal dynamics of signal transduction in the GRSC. It is established that LS neuron network relaying thalamic inputs to deep layers, and anisotropic distribution of inhibition between coronal and horizontal planes in rat. Since deep layers of the GRSC receive inputs from the subiculum, GRSC circuits may work as an integrator of multiple sources such as sensory and memory information (Nixima et al., 2017). For that, LS property may facilitate comparison or integration of synaptic inputs during an interval delay according to the suggested role of GRSC in memory-related processes. But, what about local circuits involving LS neurons?

4.4. Gabaergic system

Normal brain function depends on precisely balanced excitatory and inhibitory neurotransmission. Then, a reduced inhibitory system has been associated with a wide variety of neurological disorders (Benke, 2013). Cortical structures consist of networks of excitatory and inhibitory neurons which are born in distant locations. Excitatory glutamatergic pyramidal neurons and inhibitory GABAergic interneurons comprise the principal cellular elements of each of the individual microcircuits or modules of the cerebral cortex. Pyramidal cells represent about 80% of the neurons in the cortex and their role is transmit information between different cortical areas of the brain. GABAergic interneurons, on the other hand, control and orchestrate the activity of pyramidal cells (Bartolini et al., 2013).

GABAergic signaling also regulate other processes in brain development, including neurogenesis, neuronal migration and synapse maturation (Del Pino & Marín, 2014). According to a large-scale, comprehensive profiling of L5 cortical neurons differentiated 15 principal types of interneurons, additionally to two layer-defined types of L2, L3 and L5 pyramidal neurons. Cortical interneurons present two types in L1 (eNGC-neurogliaform cells- and SBC-like-single-bouquet cell), seven in L2/3 (Martinotti cell, NGC, BTC-bitufted cell, double-bouquet cell, basket cell and chandelier cell), and six in L5 (Martinotti cell, NGC, basket cell, SC-shrub cell, HEC-horizontally elongated cell, and deep-projecting cell). The different types has stereotypical electrophysiological and

morphological properties and can be distinguished from all others by cell type-specific axonal geometry and axonal projection patterns. Notably, each type of cell has its own specific input-output connectivity profile and these connect with other constituent neuronal type with varying degrees of specificity in layer location, postsynaptic targets and synaptic features. Regarding characteristic patterns of connection for each neuron type, it was revealed that a small number of simple connectivity motifs are repeated across layers and neuron types defining a canonical cortical microcircuit (Jiang et al., 2015).

4.4.1. γ -Aminobutyryc acid (GABA)

GABA is a major inhibitory neurotransmitter in the mammalian central nervous system. GABAergic neurons are characterized by their release of GABA as a neurotransmitter and these neurons are widely distributed in the central nervous system. Essentially all neurons in the brain respond to GABA and perhaps 20% use it as their primary transmitter. It is compiled in a review (Möhler, 2012) that GABA has been implicated in many neurological and psychiatric disorders, including epilepsy, anxiety, depression, panic, schizophrenia, autism, bipolar disorder, impair memory, obsessive compulsive disorder, contextual hyperactivity, hyperalgesia, hypothermia, neuropathic pain, cerebral ischemia, spasticity, dystonia, locomotion and other cognitive impairments. Moreover, an agonist of $GABA_BR$, baclofen, has been involved with anti-

addictive effects (Agabio & Colombo, 2015). Furthermore, GABA transmitter system has an important role in modulating synaptic formation and activity during development. Specially, GABA commands cell proliferation and migration, raises protein synthesis, stimulates neuronal differentiation and controls neurite outgrowth and synapse formation during development. GABAergic signaling participates in neuronal localization and synaptic pruning too. Additionally, sensory processing, attention, learning and various other forms of behaviour are controlled by coordinated oscillatory activity (Bolton et al., 2015; Fujita et al., 2011; López-Bendito et al., 2003; Sebe et al., 2014b; Xiao et al., 2012).

GABA exercise its effects via two classes of receptors: $GABA_ARs$, that are multimeric ligand-gated Cl^- channels, and $GABA_BRs$ G protein coupled receptors that control $Ca2^+$ and K^+ channels via second messenger systems ($GABA_BR$ are coupled to adenylyl cyclase via G-protein; activation of $GABA_BRs$ inhibits adenylyl cyclase activity to reduce cAMP levels and decrease protein kinase A activity, increases potassium conductance and decreases calcium conductance) (Figure 4.5) (Agabio & Colombo, 2015; Benke et al., 2015; Bolton et al., 2015; Chalifoux & Carter, 2011; Kerr & Ong, 2003; Kumar et al., 2013; Raveh et al., 2015). $GABA_BRs$ produce slow and prolonged inhibitory signals and modulate the release of neurotransmitters (Li et al., 2003). Unlike ionotropic $GABA_ARs$, metabotropic $GABA_BR$ can be activated directly by GABA binding, and facilitate postsynaptic action potential (Figure 4.5) (Bolton et al., 2015; Chalifoux &

Carter, 2011; Kerr & Ong, 2003; Kim & Seo, 2014; Kumar et al., 2013; Möhler, 2012; Parker et al., 2004; Raveh et al., 2015; Sebe et al., 2014b).

4.4.2. $GABA_B$ Receptor

$GABA_B$Rs were discovered at the end of the 1970s by the Bowery's research team and were cloned in 1997 (Benke et al., 2015; Bowery et al., 1983; Kumar et al., 2013). $GABA_B$Rs regulate the excitability of neurons via activation of different downstream effector systems in pre- and postsynaptic cells and control all principal brain functions such as synaptic plasticity, neuronal development and neuronal network activity (Benke et al., 2015; Fábera & Mareš, 2014; Kim & Seo, 2014). They are directly present at presynaptic and extrasynaptic sites instead of the active zone or postsynaptic density of synapses. This location of $GABA_B$Rs entails that activation either needs spillover of GABA from glia cells or neuronal dendrites. At the level of single synapses, recent measurements suggested that even basal neuronal activity can locally generate sufficient ambient GABA concentrations for low-level tonic activation of presynaptic $GABA_B$Rs (Benke et al., 2015). $GABA_B$Rs are commonly divided into auto- and heteroreceptors (Fig. 4) depending on whether they control the release of GABA itself or other neurotransmitters such as glutamatergic, noradrenergic and cholinergic transmission. Specifically release of GABA from presynaptic site is controlled by $GABA_B$ autoreceptors and release of Glutamate or

others from presynaptic site is controlled by $GABA_B$ heteroreceptors. On the other hand, post-synaptic $GABA_B$ heteroreceptors dampen excitability by releasing Gβγ subunits to activate inward-rectifier potassium (Kir) channels, resulting in the development of IPSP and thereby controlling the neuronal excitability (Kumar et al., 2013).

Furthermore, $GABA_BRs$ is also associated with auxiliary K^+ channel tetramerization domain subunits which exert little allosteric influence on agonist affinity (Raveh et al., 2015). Action of GABA on postsynaptic $GABA_BRs$ results in generation of IPSPs activating Kir channels; this hyperpolarization lasts longer and has higher amplitude than IPSPs elicited by $GABA_ARs$. Also, $GABA_BR$ inhibits postsynaptic voltage-gate Ca^{2+} channels in dendrites and spines which prevents Ca^{2+} spikes and therefore diminish neuronal excitability. However, there are two targets recently described: two-pore K^+ channels (TREK 1/2) and NMDA receptors (Benke et al., 2015). Presynaptic $GABA_BRs$ decrease release of transmitter from the presynaptic ending inhibiting postsynaptic voltage-gated Ca^{2+} channels and activating presynaptic Kir channels (Benke et al., 2015; Bolton et al., 2015; Chalifoux & Carter, 2011; Fábera & Mareš, 2014; Kerr & Ong, 2003; Kim & Seo, 2014; Kumar et al., 2013; Möhler, 2012; Parker et al., 2004; Raveh et al., 2015; Sebe et al., 2014b).

This localization is a reason for ambiguous effects of $GABA_BR$ agonists like baclofen on epileptic seizures–anticonvulsant, proconvulsant and direct convulsant effects were described in various animal models (Fábera & Mareš, 2014).

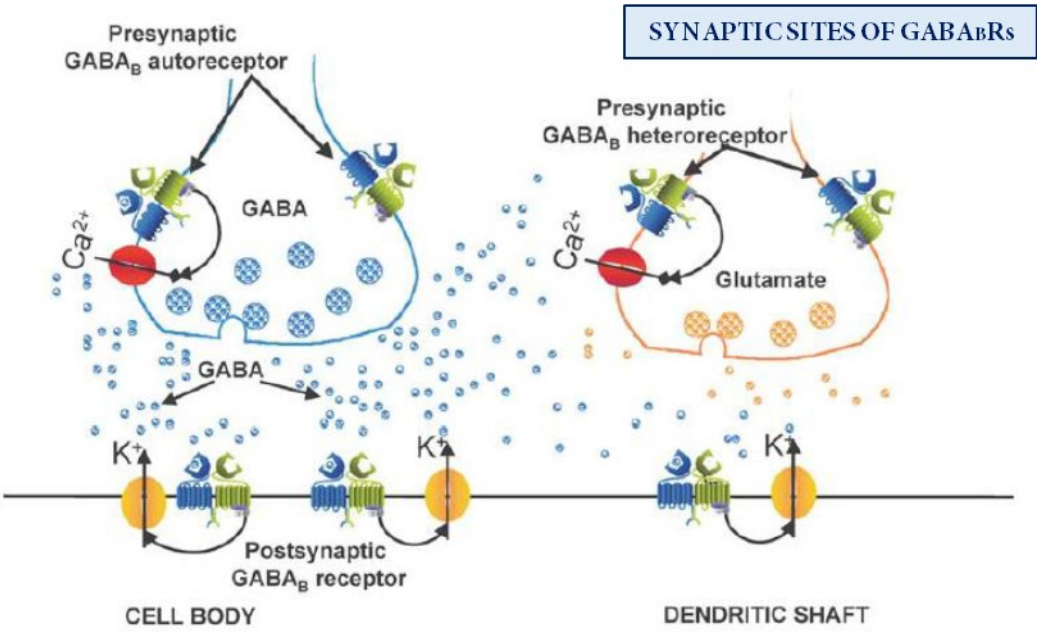

Figure 4.6. Localization of GABA$_B$Rs to synaptic sites. Figure modified from Filip & Frankowska, 2008.

As shown in Fig. 5, GABA$_B$R has two subunits GABA$_{BR1}$ and GABA$_{BR2}$, having molecular weight of 130 and 110 kDa respectively forming heterodimers (Charles et al., 2001; Filip & Frankowska, 2008; Kasten & Boehm, 2015; Vigot et al., 2006). Both subunits have a long extracellular N-terminal, seven transmembrane domains and a short intracellular carboxy-terminal forming a loop responsible for linking the two subunits (Filip & Frankowska, 2008). The same gene derives these subunits by alternative promoter

usage and solely differ in their N-terminal ectodomains. $GABA_{BR1a}$ presents N-terminal two sushi domains (SDs) which are lacking in $GABA_{BR2}$. Recently, it has been demonstrated that the $GABA_{BR1}$ subunit exists in two isoforms $GABA_{BR1a}$ and $GABA_{BR1b}$ (Pinard et al., 2010). On one hand, the presynaptic $GABA_BRs$ are composed of the $GABA_{BR1a}$ and $GABA_{B2}$ subunits, whereas the postsynaptic proteins are composed of $GABA_{BR1b}$ and $GABA_{BR2}$ subunits (Kumar et al., 2013; Vigot et al., 2006).

Recent studies demonstrate that $GABA_{B1}R$ is the ligand binding subunit and $GABA_{B2}R$ is a G-protein coupled subunit. The localization of $GABA_{B1}R$ and $GABA_{B2}R$ mRNAs correlates well with the distribution of GABAergic neurons (Benke, 2013; Bolton et al., 2015; Kerr & Ong, 2003; Li et al., 2003; Parker et al., 2004). Both subunits have different roles, B1a is related to maintenance and hyperactivity, while B1b is implicated in impaired memory formation and susceptibility to depression-like phenotypes (Kasten & Boehm, 2015).

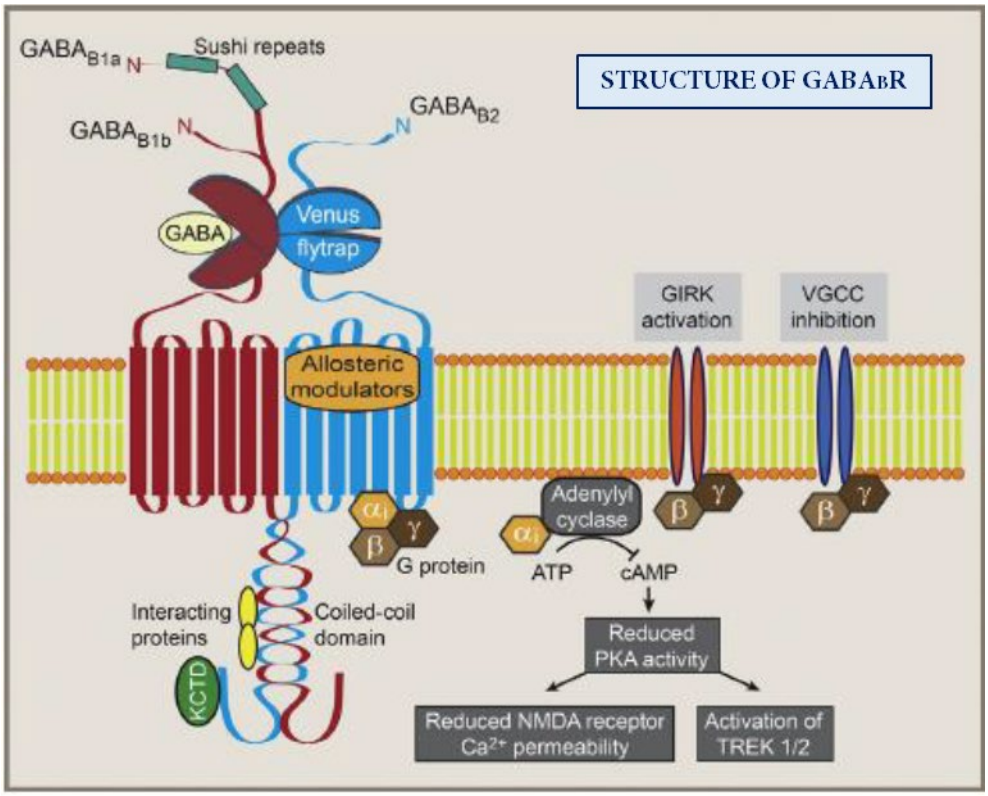

Figure 4.7. Structure of the $GABA_B$ receptor and its intracellular signal effectors. Figure modified from Benke et al., 2015.

These domains preferentially target $GABA_{B1a}$ to the presynaptic terminals of excitatory synapses, where it modulates glutamate release. On the postsynaptic side, both isoforms are found in dendrites but only $GABA_{B1b}$ is located in spines (Li et al., 2003; Raveh et al., 2015; Vigot et al., 2006). On the other hand, neuronal $GABA_B$Rs are thought to consist of four distinct subtypes on the basis of ligand binding studies. (Li et al., 2003). So that, $GABA_{B1a}$ and $GABA_{B1b}$ are differentially compartmentalized and fulfill distinct functions (Vigor et al., 2006).

In most neurons of L2/3 forward inputs elicited EPSPs that were followed by fast $GABA_A$- and slow $GABA_B$-mediated hyperpolarizing IPSPs. Thus, when forward and feedback inputs are simultaneously active, feedback inputs may provide late polysynaptic excitation that can offset slow IPSPs evoked by forward inputs and in turn may promote recurrent excitation through local intracolumnar circuits (Shao & Burkhalter, 1999).

It is known from developmental studies in rat somatosensory cortex that polysynaptic excitation is regulated by slow inhibition. This suggests that $GABA_BR$ mediated IPSPs play a role in the modulation of signal amplification (Shao & Burkhalter, 1999).

As a consequence of a partial or complete blockage of inhibition, is generated a synchronous epileptiform activity in the cortex. Epileptic seizures occur as a result of episodic abnormal synchronous discharges in cerebral neuronal networks. Although a variety of nonconventional mechanisms may play a role in epileptic synchronization. As is the case throughout the central nervous system, fast synaptic excitation within and between brain regions relevant to epilepsy is mediated predominantly by AMPA receptors. NMDA receptors may also contribute to epileptiform activity, but NMDA receptor blockade is not sufficient to eliminate epileptiform discharges (Rogawski, 2013). Moreover, $GABA_BR$ function does affect behaviour, agreeing that proper functioning of $GABA_BRs$ is crucial for numerous learning and memory tasks and that targeting this

system via pharmaceuticals may benefit several clinical populations (Heaney & Kinney, 2016).

Independent and different mechanisms regulate phenomena initiation, propagation and termination of cortical epileptiform activity in slices uninhibited. First, initiation depends on both excitation and synaptic inhibition and this is a slow and variable process. In contrast, the propagation of velocity and amplitude depends on the excitatory synaptic but no inhibition above the threshold level. In the case of L2/3 in the RSC, spread is a rapid process and is mediated by excitatory axonal collaterals between spiking regular (RS) pyramidal cells. Termination is modulated by excitation and synaptic inhibition and is characterized by blocking the depolarization. This activity is similar to that detected in seizures and it is due to coordinated firing of a group of neurons that generates a change in the local field potential (Pinto et al., 2005).

Hypothesis and objectives

5. HYPOTHESIS AND OBJECTIVES

The electrophysiological properties and responses of the cortical neurons, as well as the way in which they are interconnected by synapses (local microcircuits) establishes the core of the function of the cerebral cortex. Therefore, the study of the function of a particular cortical areas, as it is the RSC, requires to obtain a deep knowledge of, at least, the following: (1) the types of neurons making that particular cortical area; (2) the intrinsic electrophysiological properties of each one of these neuronal types; (3) the properties of the synapses connecting these neurons and (4) the organization and properties of the local circuits forms by these neurons. From this point of view, in this work we plan to study the functional properties and synaptic responses of a particular subset of pyramidal neurons (the LS pyramidal neurons), which are present in the GRSC as an initial step to understand the functional mechanisms of the cerebral cortex. From this point of view and considering the previous knowledge available in the literature about the RSC in rodents, we propose the following hypothesis: The LS pyramidal neurons of the GRSC play a specific role in the working of this cortical area due to their specific electrophysiological properties and to the way in which they are interconnected to the rest of cortical neurons.

To prove this hypothesis we proposed the following objectives for this work:

1. To study the intrinsic electrophysiological properties of LS neurons.

2. To study the activity of LS neurons during responses that are generated by the local cortical networks, such as the propagation of epileptiform discharges.

3. To study the synaptic connectivity of the pyramidal neurons of the L2/3 RSC.

4. To analyze the role on inhibitory GABA receptors (GABA Rs) in the function of LS neurons.

Material and methods

6. MATERIAL AND METHODS

Most of the methods used in this work are described in the paper "Robles et al., 2020"; however, in this section we give a more detailed description of this methodology, and we described some methods used for the experiments shown in Sections 1 and 2 from annex of results not included in the paper.

6.1. Animals and ethical approval

The vast majority of the experiments, except the recordings during epileptiform discharges, were done in GAD67:GFP mice. These animals are of the C57BL6 strain and express GFP under the GAD67 promoter; they are usually referred as GAD67:GFP (Tamamaki et al., 2003). The experiments of recording epileptiform discharges were done in C57BL6 mice from 14 to 22 postnatal days. We used males the vast majority of the time in order to diminish fluctuations do to hormones. However, we used some females to test if they have different response but we did not find any variability. Depends on the experiment, we got different number of animals. From each animal, we obtained three slices containing RSC and from each slice we could record until fourteen cells in some cases approximately. Nevertheless, in pharmacological experiments, using drugs which did not wash out we had to change the slice when we recorded only one neuron per slice.

So that, we used from seven or eight mice per experiment or until thirty animals per experiment. The Ethical Committee for the Experimental Research of the Universidad Miguel Hernández approved the experimental protocols (code: 2018/VSC/PEA/0035). Protocols were according with national and international laws and policies (Spanish Directive "Real Decreto 1201/2005"; European Union Directive 2010/63/UE).

6.2 Slice preparation

Slices of brain neocortex were obtained from 277 male mice of postnatal 14-22 days as we said above. Cervical dislocation was used for animals and their brains were quickly excised and submerged in ice-cold low Ca^{2+} / high Mg^{2+} cutting solution (composition in mM: NaCl 124, KCl 2.5, $NaHCO_3$ 26, $CaCl_2$ 0.5, $MgCl_2$ 2, NaH_2PO_4 1.25, glucose 10; pH 7.4 when saturated with 95% O_2 + 5% CO_2). In the cutting solution, the Calcium is further reduced and Magnesium is increased to diminish the neurotransmitter release to prevent cytotoxic neurotransmitter release like Glutamate (Igelström et al., 2011). Coronal slices were cut at 350 μm of thick using vibratome (Leica VT-1000; Germany) and transferred to a glass beaker in which the tissue was submerged in artificial cerebrospinal fluid (ACSF; composition in mM: NaCl 124, KCl 2.5, $NaHCO_3$ 26, $CaCl_2$ 2, $MgCl_2$ 1, NaH_2PO_4 1.25, glucose 10; pH 7.4 when saturated with 95% O_2 + 5% CO_2) during 30 min at 34ºC. Then, the slices were stored at least one hour at room temperature

submerged in ACSF before recordings were made. One slice at a time was transferred to a submersion-type recording chamber during the recording period kept at 32-34ºC. The ACSF used to bath the recording slices was fed into the recording chamber at a rate of 2-3 ml.min^{-1} and was bubbled with a gas mixture of 95% O_2 + 5% CO_2 continuously.

6.3. Intracellular recordings

We made somatic whole-cell recordings from neurons whose soma was located in the dorsal part of L2/3 or upper L5 of the GRSC. Recording location was in the transition between GRSC and dysgranular RSC. Several neurons were recorded sequentially from the same slice but others needed to change the slice for the drugs properties. In other words, if the slices were not washed out completely due to the type of drug applied we changed the slice in order to record another neuron. Pyramidal cells were identified by their specific shape, revealed by intracellular staining with Alexa Fluor 594 at 10 μM and, when slices from GAD67:GFP mice were used, by the absence of GFP expression. These neuronal cells presented a particular soma and a dominant apical spiny dendrite oriented to L1, whereas basal dendritic arbors were tangentially oriented.

Using an upright microscope (Olympus, BX50WI) equipped with Nomarski optics and 40X water immersion lens, recordings were made under visual control. Current-

clamp and/or voltage-clamp mode were used for recordings with a patch-clamp amplifier (Multiclamp 700B, Molecular Devices, USA). The pipette junction potential was estimated to be about -10mV using the junction potential calculator in the pClamp software, so that no correction was made.

Signals of current or voltage were filtered at 4 kHz and digitalized at 20 kHz with a 16-bit resolution analog to digital converter (Digidata 1440A, Molecular Devices, USA). The stimuli generation stimuli and signal acquisition and the analysis were configured by Clampex 10.3 software (part of the pClamp package; Molecular Devices, USA).

Patch pipettes made from borosilicate glass (1.5 mm outer diameter, 0.86 mm inner diameter, with inner filament) were used for recording; their resistance was between 4-7 MΩ filling them with intracellular solution (composition in mM): 130 K-gluconate, 5 KCl, 5 NaCl, 5 EGTA, 10 HEPES, 2 Mg-ATP, 0.2 Na-GTP, 0.01 Alexa Fluor 594; pH 7.2 adjusted with KOH; 285-295 mOsm). For this K-based internal solution, the theoretic Nernst equilibrium potentials were E_K=-105.7, E_{Na}=89.3 and E_{Cl^-}=-68.5).

More details are shown in results of the thesis or in material and methods of the publication attached in this thesis manuscript. Generally, on the one hand, current clump recordings were carried out at -70 mV and at the spontaneous resting membrane potential of the neurons. It is worth mentioning that neurons were selected once recorded based on three criteria: resting potential (< -50mV), overshoot (action potential has to pass 0mV)

and the amplitude of action potential (> 50mV). For analysis of records, Clampfit10.1 (Axon Instruments, USA) was used. For Series resistance (R_S), it was measured and balanced on-line by the Bridge Balance tool of the Clampex software under visual inspection. So that R_S was monitored at the beginning and at the end of each protocol, and re-balanced if needed.

On the other hand, for experiments of voltage clamp, EPSCs and IPSCs were recorded at holding potentials of -70 mV and 0 mV respectively, being these potentials close to the reversal potential for the inhibitory and excitatory postsynaptic currents respectively in order to identify them. Clampfit 10.3. perform quantification of intrinsic membrane properties and synaptic responses.

6.4 Electrical stimulation

For electrical stimuli, it was used a concentric bipolar electrode (CBAFC57 outer diameter 125 μm, Frederick Haer & Co, USA) placed as indicated in Results section. It was assessed the integrity of the callosal projection by extracellular recording prior to intracellular experiments for contralateral stimulation (Sempere-Fernàndez et al., 2018). Single square current pulses, 100-500 μA and 0.1 ms, were applied at a frequency of 0.2 Hz to evoke synaptic responses in the recorded neurons. The smallest stimulus strength

applied, 100μA, was close to the threshold to evoke postsynaptic responses and the largest stimulus intensities between the threshold and those evoking maximum responses was similar in different slices. In a typical experiment, recording of extracellular local field potential was used to confirm the efficacy of the stimulus protocol and to set the stimulus intensity (twice the threshold value) previously to go in whole-cell.

6.5. Glutamate application

Direct application of Glutamate (1 mM Glutamate dissolved in ACSF) using patch pipettes evoked synaptic currents. In this case, we stimulated neurons with Glutamate evoking firings from neighbour neurons in order to promote them to fire and evoke the synaptic currents that we wanted to record them in our recording neurons. We was accurate to avoid Glutamate currents directly on the soma of the recording neuron. The tip of the pipette was located at several distances from the soma of the recording pyramidal cell and Glutamate was released by pressure pulses of 5-10 psi during 20 ms applied through Picospritzer (General Valve Corp. USA). Pressure pulses were applied at intervals of 20 s.

6.6. Intracellular staining with biocytin

Some recorded neurons were labelled with biocytin using the method described by several laboratories (Jiang et al., 2015; Marx et al., 2013; Petreanu et al., 2007; Schnepel et al., 2015; Sempere-Fernàndez et al., 2019). Shortly, biocytin was added to the intracellular solution at a final concentration of 5mg/ml. Slices containing stained neurons were fixed overnight at 4°C in 100 mM phosphate-buffered saline (PBS, pH 7.4) with 4% paraformaldehyde. Then, slices were rinsed several times in PBS containing 1% Triton X-100 and the endogenous peroxidase was blocked by incubating in 30% H_2O_2. Then, slices were transferred to a complex of 1% avidin-biotinylated HRP that contained 0.5% Triton X-100 (ABC Peroxidase Standard PK-400 Vectastain; Vector Labs, Burlingame, CA, USA) and were sacked for 1 hour in a fentle manner. Slices were reacted using 3,3-diaminobenzidine (DAB;Sigma) and the reaction was stopped by adding 30% H_2O_2. Glass slides were used to mount the slices embedded in Glycerol jelly and then coverslipped. Once slices are prepared like that, biocytin-stained neurons were visualized and photographed using Leica DM4000B microscope (Leica Biosystems, Germany) and Leica DFC350FX camera (Leica Biosystems, Germany). In order to draw biocytin-stained neurons, Neurolucida software (MBF Bioscience, Vermont USA) was used. Laminar landmarks were visualized under bright-field illumination (Led stimulation pattern covering the visible part of the slice especially the borders of L2/3, L4, L5a, and L5b) at a low magnification (10x objective, NA 0.06, PlanN, Leica DM4000B, Leica Biosystems, Germany) and these cytoarchitectonic features were used to define laminar borders.

Sometime we also observed the stained cells under fluorescence with the same microscope (Leica DM4000B, Leica Biosystems, Germany).

6.7. Evoking and recording epileptiform discharges

For a group of experiments that we simulated epileptiform activity, we used modified ACSF (mACSF) (composition in mM: NaCl 124, KCL5, $NaHCO_3$ 26, $CaCl_2$ 1.2, $MgCl_2$ 1, NaH_2PO_4 1.25, glucose 10; pH 7.4 when saturated with 95% O_2 + 5% CO_2) at 34°C for 30 min to store the slices and then to record neurons. The ACSF was modified increasing excitability of the slice since we increased K^+ concentration and diminished calcium concentration.

In mACSF and in the presence of 10 μm Bicuculine (a $GABA_A$ receptor blocker) the stimulation of L1 evokes large oscillatory discharges that were recorded extracellularly (Martin et al., 2009; Rovira & Geijo-Barrientos, 2016). A concentric tungsten bipolar electrode stimulus (Frederik Haer and Co., USA) positioned in L1 was employed.

6.8. Blockers of synaptic receptors

We used several drugs to block neurotransmitter receptors (Martin et al., 2009). The $GABA_BRs$ blockers CGP 55845 ((2S)-3-[[(1S)-1-(3,4-dichlorophenyl) ethyl] amino-2- hydroxypropyl] (phenylmethyl) phosphonic acid hydrochloride) and CGP 52432 (3-[[(3,4-Dichlorophenyl)methyl]amino]propyl] diethoxymethyl) acid), the $GABA_ARs$ blocker (-)-Bicuculline methiodide ([*R*-(*R**,*S**)]-5-(6,8-Dihydro-8-oxofuro[3,4-*e*]-1,3-benzodioxol-6-yl)-5,6,7,8-tetrahydro-6,6-dimethyl-1,3-dioxolo[4,5-*g*]isoquinolinium iodide) to elicit epileptiform activity (Albertson et al., 2013; Igelström et al., 2011; Torres-Escalante et al., 2004; Walker et al., 2012), and the AMPA/kainite Rs competitive blocker CNQX (6-Cyano-7-nitroquinoxaline-2,3-dione) to increase GABA-mediated synaptic transmission (Brickley et al., 2001) were obtained from TOCRIS Bioscience (USA) and Sigma-Aldrich (USA). The $GABA_A$ blocker, Bicuculline, was applied at 10 and 20 μM dissolved in mACSF. In most experiments, we also applied CNQX at 10μM. Bicuculline, CNQX and CGP 52432 were prepared at 10 mM from stocks in H_2O and dissolved in ACSF for the final concentration to apply them. Nevertheless, Bicuculline was applied at 20 μM in some experiments. In addition, CGP 55845 was used at 5 μM from stock in DMSO and dissolved in ACSF to apply it at the final concentration; and CGP 52432 was used from 10μM stock in DMSO and dissolved in ACSF to apply it at the final concentration too (Martin et al., 2009).

6.9. Local application of GABA

Currents were evoked by the direct application of GABA to the recorded neuron using patch pipettes filled with 1 mM GABA dissolved in mACSF. The GABA was released by pressure pulses 5-10 psi applied with a Picospritzer (General Valve Corp. USA). Moreover, we prove the effect of GABA local application with 100μM and 10 mM of GABA to see the responses at different concentrations. The pipette used to apply GABA was placed at 200 μm of the recording electrode (Figure 8.12). First, we did some recordings using pipettes filled with mACSF in order to prove that there was no mechanical effect of the direct application pressure solution. Next, we added to the mACSF 10 μM CNQX (a competitive AMPA/kainate receptor antagonist) in order to block possible response due to glutamate receptors and isolate the currents carried by GABA Rs ($GABA_A$Rs and $GABA_B$Rs). Then, we recorded currents evoked by GABA in different conditions as it is explained in results section. To sum up, we tested the currents evoked in several conditions: (1) mACSF + 10 μM CNQX (Figure 8.12A) blocking the effect of Glutamate; (2) mACSF + 10 μM CNQX + 10 μM CGP52432 blocking $GABA_B$Rs and isolating $GABA_A$ currents; and (3) mACSF + 10 μM CNQX + 20 μM Bicuculline blocking $GABA_A$ receptors and isolating $GABA_B$ currents.

6.10. Statistics

Data are presented as values from individual cells and/or giving the mean ± standard deviation (s.d.) if it is not indicated other statistical parameter. On the one hand, comparisons between two samples were made with parametric test (t-test) or non-parametric tests (two-tailed Mann-Whitney rank sum test for independent samples and two-tailed Wilcoxon signed rank test for paired samples). On the other hand, comparisons among more than two samples (data on latencies shown in Figure 7.9) were made with the non-parametric Kruskal-Wallis one-way ANOVA on ranks (which is independent of the distribution samples); moreover, if the ANOVA gave significant differences among groups (p-value<0.05), a post-hoc Dunn's multiple comparison test was used to compare across all pairs of samples. These statistical analyses were performed on *OriginPro8* (Origin Lab Corporation) or *SigmaStat 3.11* (Systat Software Inc). The degree of statistical significance is given in each figure and a p-value < 0.05 was considered significant.

Results

7. RESULTS

7.1. Layer 2/3 pyramidal neurons of the mouse retrosplenial granular cortex and their innervation by cortico-cortical axons.

The work of this Doctoral Thesis was a continuation of the research lines followed in the laboratory of Dr. Salvador Martínez and Dr. Emilio Geijo. A large part of the results of my Doctoral Thesis was published last year:

- Robles, R. M., Domínguez-Sala, E., Martínez, S., & Geijo-Barrientos, E. (2020). Layer 2/3 pyramidal neurons of the mouse granular retrosplenial cortex and their innervation by cortico-cortical axons. *Frontiers in Neural Circuits*, *3*(November), 1–15. https://doi.org/10.3389/fncir.2020.576504

I am the first author and, in addition to the Director and Co-Director of the Thesis (S. Martínez and E. Geijo), there is also as an author Dr Dominguez-Sala, a former graduate student of the lab who participated in some of the experiments shown in the Figure 4 of the paper. They all agree to use it in my thesis. I performed all the experiments of the article under the supervision of Emilio Geijo and Salvador Martínez.

frontiers in Neural Circuits

ORIGINAL RESEARCH
published: 03 November 2020
doi: 10.3389/fncir.2020.576504

Layer 2/3 Pyramidal Neurons of the Mouse Granular Retrosplenial Cortex and Their Innervation by Cortico-Cortical Axons

Rita M. Robles[1], *Eduardo Domínguez-Sala*[1], *Salvador Martínez*[1,2] *and Emilio Geijo-Barrientos*[1]*

[1]*Instituto de Neurociencias, Universidad Miguel Hernández—CSIC, Campus de San Juan, Alicante, Spain,* [2]*CIBERSAM (Centro de Investigación Biomédica En Red en Salud Mental), Madrid, Spain*

OPEN ACCESS

Edited by:
Manuel S. Malmierca, University of Salamanca, Spain

Reviewed by:
Ede Rancz, Francis Crick Institute, United Kingdom
Toshio Miyashita, Teikyo University, Japan
Tohru Kurotani, National Center of Neurology and Psychiatry (Japan), Japan

***Correspondence:**
Emilio Geijo-Barrientos
emilio.geijo@umh.es

Received: *26 June 2020*
Accepted: *18 September 2020*
Published: *03 November 2020*

Citation:
Robles RM, Domínguez-Sala E, Martínez S and Geijo-Barrientos E (2020) Layer 2/3 Pyramidal Neurons of the Mouse Granular Retrosplenial Cortex and Their Innervation by Cortico-Cortical Axons. Front. Neural Circuits 14:576504. doi: 10.3389/fncir.2020.576504

The retrosplenial cortex forms part of the cingulate cortex and is involved in memory and navigation. It is ventral region, the granular retrosplenial cortex, or GRSC is characterized by the presence, of small pyramidal neurons with a distinctive late-spiking (LS) firing pattern in layer 2/3. Using *in vitro* brain slices of the mouse GRSC we have studied the electrophysiological properties and synaptic responses of these LS neurons, comparing them with neighboring non-LS pyramidal neurons. LS and non-LS neurons showed different responses during cortical propagation of epileptiform discharges. All non-LS neurons generated large supra-threshold excitatory responses that generated bursts of action potentials. Contrastingly, the LS neurons showed small, and invariably subthreshold excitatory synaptic potentials. Although both types of pyramidal neurons were readily intermingled in the GRSC, we observed differences in their innervation by cortico-cortical axons. The application of glutamate to activate cortical neurons evoked synaptic responses in LS neurons only when applied at less than 250 μm, while in non-LS neurons we found synaptic responses when glutamate was applied at larger distances. Analysis of the synaptic responses evoked by long-range cortico-cortical axons (with the origin at 1200 μm from the recorded neurons or in the contralateral hemisphere) confirmed that non-LS neurons were strongly innervated by these axons, while they evoked only small responses or no response at all in the LS neurons (contralateral stimulation, non-LS: 194.0 ± 196.63 pA, n = 22; LS: 51.91 ± 35.26 pA, n = 10; p = 0.004). The excitatory/inhibitory balance was similar in both types of pyramidal neurons, but the latency of the EPSCs evoked by long-range cortico-cortical axons was longer in LS neurons (contralateral stimulation non-LS: 8.13 ± 1.23 ms, n = 17; LS: 10.76 ± 1.58 ms, n = 7; p = 0.004) suggesting

a disynaptic mechanism. Our findings highlight the differential cortico-cortical axonal innervation of LS and non-LS pyramidal neurons, and that the two types of neurons are incorporated in different cortico-cortical neuronal circuits. This strongly suggests that the functional organization of the dorsal part of the GRSC is based on independent cortico-cortical circuits (among other elements).

Keywords: late-spiking neurons, callosal axons, cortico-cortical axons, excitatory/inhibitory balance, neocortex, cortical circuits, synaptic mechanisms, retrosplenial cortex (RSC)

INTRODUCTION

The retrosplenial cortex (RSC) is the most caudal part of the cingulate cortex. The RSC is interconnected with areas of the brain (the hippocampal formation or anterior thalamic nucleus) that are important for memory formation, and a network of dorsal-medial cortical areas involved in spatial memory (Vann et al., 2009). In humans, the RSC plays a role in several cognitive functions, such as memory (Aggleton, 2014), spatial navigation (Epstein, 2008), orientation (Vann et al., 2009), and planning (Miller et al., 2014). In rodents, it comprises the entire posterior cingulate cortex (Vogt and Peters, 1982) and lesion studies have shown it is involved in spatial memory tasks (Sutherland et al., 1988), allocentric working memory tasks (Vann and Aggleton, 2002, 2004), and navigation (Cooper and Mizumori, 1999; Whishaw et al., 2001). The rodent RSC includes several cytoarchitectonic areas; according to Vogt et al. (2004) and Vogt (2014), these are 29a-c and 30. Areas 29a-c are located ventrally and correspond to the granular RSC (GRSC), while area 30 (or area 29d according to Vogt and Peters, 1982; see Sugar et al., 2011 for a review of the nomenclature of RSC cytoarchitectonic areas) is dorsal and corresponds to the dysgranular (or agranular) RSC.

Although we lack a detailed understanding of the contributions of each RSC sub-area, some authors have proposed that area 30 (dysgranular RSC) is important for the processing of visual information involved in allocentric spatial working memory (Vann and Aggleton, 2005), and area 29c (part of the GRSC) alone may contribute to spatial working memory processing (van Groen et al., 2004). These functional differences between dysgranular RSC and GRSC are presumably related to different connections with other cortical and subcortical areas such as the frontal, anterior cingulate, visual, and retro-hippocampal cortices, and the anterior thalamic nucleus (van Groen and Wyss, 1990, 1992, 2003; Shibata, 1998, 2000; Van Groen et al., 1993; Shibata and Naito, 2008). In addition to these extrinsic connections, distinct areas within the RSC also have complex interconnections (van Groen and Wyss, 1992; Van Groen et al., 1993; Jones et al., 2005; Shibata et al., 2009).

A distinctive feature of the rodent GRSC is the presence of an accentuated superficial layer 2/3, which is mainly formed by small pyramidal neurons with densely packed somata (Sripanidkulchai and Wyss, 1987; Ichinohe et al., 2008). These are callosal projection neurons, and in rats, their apical dendrites form noticeable bundles within layer 1 that are co-localized with patchy terminations of thalamocortical axons, mostly originated in the anterior thalamic nucleus, and with dendrites of parvalbumin-expressing interneurons (Sripanidkulchai and Wyss, 1986; van Groen and Wyss, 1990, 2003; reviewed in Ichinohe, 2012). A particularly remarkable feature of these neurons, described in the rat GRSC, is their late-spiking firing pattern, which is due to the presence of delayed rectifier and A-type potassium channels such as Kv1.1, Kv1.4, and Kv4.3 (Kurotani et al., 2013). This firing pattern could permit the integration of synaptic inputs with different timing, which is consistent with the GRSC's suspected role in memory-related functions (Kurotani et al., 2013). Interestingly, the presence of late-spiking pyramidal neurons has been described in other brain areas related to the RSC such as the presubiculum (Abbasi and Kumar, 2013), the entorhinal cortex (Alonso and Klink, 1993), and the perirhinal cortex (Faulkner and Brown, 1999).

However, despite a large amount of information on the GRSC's connectivity, very little is known about the role of GRSC late-spiking pyramidal neurons in the function of local and long-range cortical circuits. We have studied the electrophysiology and synaptic responses of mouse GRSC late-spiking pyramidal neurons and compared the results to those obtained in the neighboring, regular spiking pyramidal neurons, which are similar to those found in the dysgranular RSC layer 2/3 (Sempere-Ferràndez et al., 2018). Our results show that cortico-cortical axons originated in relatively distant areas (the contralateral homotopic cortex and ipsilateral dysgranular RSC) do not make direct excitatory contacts with late-spiking neurons, which only receive weak disynaptic responses of local origin ($<$250 μm from the soma). However, nearby pyramidal neurons that did not present a late spiking-firing received large synaptic contacts from both local and long-range cortico-cortical axons.

MATERIALS AND METHODS

Animals and Ethical Approval

All experiments, except those recording epileptiform discharges, were done in GAD67:GFP mice; these animals are of the C57BL6 strain, present heterozygous GFP expression under the GAD67 promoter, and are usually referred to as GAD67:GFP (Tamamaki et al., 2003). By contrast, epileptiform discharges were recorded in C57BL6 mice. Mice were maintained, handled, and sacrificed following national and international laws and policies (Spanish Directive "Real Decreto 1201/2005"; European Community Council Directive 86/609/EEC). The experimental protocols were approved by the Experimental Research Ethics Committee of the Universidad Miguel Hernández.

Slice Preparation

Brain slices of neocortex were prepared from male mice with postnatal age of 14–22 days. Animals were killed by cervical dislocation and their brains were quickly excised and submerged in ice-cold low Ca^{2+} / high Mg^{2+} cutting solution (composition in mM: NaCl 124, KCl 2.5, $NaHCO_3$ 26, $CaCl_2$ 0.5, $MgCl_2$ 2, NaH_2PO_4 1.25, glucose 10; pH 7.4 when saturated with 95% O_2 + 5% CO_2). Coronal slices (350 μm thick) were cut using a vibratome (Leica VT-1000; Germany), transferred to a glass beaker and submerged in artificial cerebrospinal fluid (ACSF; composition in mM: NaCl 124, KCl 2.5, $NaHCO_3$ 26, $CaCl_2$ 2, $MgCl_2$ 1, NaH_2PO_4 1.25, glucose 10; pH 7.4 when saturated with 95% O_2 + 5% CO_2) at 34°C for 30 min. The slices were stored submerged in ACSF for at least 1 h at room temperature before recordings were made. Slices were individually transferred to a submersion-type recording chamber and kept at 32–34°C during the recording period. The ACSF used to bath the slices was fed into the recording chamber at a rate of 2–3 ml·min^{-1} and was continuously bubbled with a gas mixture of 95% O_2 + 5% CO_2.

Intracellular Recordings

We performed somatic whole-cell recordings from neurons whose somata were located in the dorsal part of layer 2/3 of the GRSC (−2.30 to −1.70 from Bregma). Pyramidal neurons were identified by their shape and confirmed by intracellular staining with Alexa Fluor 594 and the absence of GFP expression (in slices from GAD67:GFP mice). These neurons showed a characteristic pyramidal soma and a dominant apical spiny dendrite oriented to layer 1, while basal dendritic arbors were tangentially oriented.

Recordings were made under visual control using an upright microscope (Olympus BX50WI) equipped with Nomarski optics and a 40x water immersion lens. Measurements were obtained in current-clamp and/or voltage-clamp mode with a patch-clamp amplifier (Multiclamp 700B, Molecular Devices, San Jose, CA, USA). No correction was made for the pipette junction potential (which was estimated to be about −10 mV using the junction potential calculator included with the pClamp software). Voltage and current signals were filtered at 4 kHz and digitized at 20 kHz with a 16-bit resolution analog to digital converter (Digidata 1440A, Molecular Devices, San Jose, CA, USA). Clampex 10.3 software (part of the pClamp package; Molecular Devices, San Jose, CA, USA) was used to control stimulus generation and signal acquisition and analysis.

Patch pipettes made from borosilicate glass (1.5 mm o.d., 0.86 mm i.d., with inner filament) were used for intracellular recording; they had a resistance of 4–7 MΩ when filled with intracellular solution (composition in mM: K-gluconate 130, KCl 5, NaCl 5, EGTA 5, HEPES 10, Mg-ATP 2, Na-GTP 0.2, Alexa Fluor 594 0.01; pH 7.2 adjusted with KOH; 285–295 mOsm). The theoretical Nernst equilibrium potentials (in mV) for this K-based internal solution were: E_K = −105.7, E_{Na} = 89.3, E_{Cl} = −68.5.

Current clamp recordings were performed at −70 mV and the neurons' spontaneous resting membrane potential. Series resistance (R_s) was measured and balanced on-line under visual inspection assisted by the Clampex software bridge balance tool. R_s was monitored at the beginning and end of each protocol and re-balanced if needed. Cells in which R_s was >40 MΩ were discarded (R_s was typically <25 MΩ). For voltage-clamp experiments, EPSCs (excitatory synaptic currents) and IPSCs (inhibitory synaptic currents) were recorded at holding potentials of −70 and 0 mV, respectively, values which are close to their respective reversal potentials. To hold the membrane at a specific membrane potential, the error in the membrane potential (V_e) measurement was estimated from $V_e = I_{hold} * R_s$, where I_{hold} is the holding current needed to set the holding potential. The holding potential was then corrected by adding the calculated V_e and holding the membrane to the desired V_{hold} (holding potential) while taking into account the error due to R_s. Intrinsic membrane properties and synaptic responses were quantified using Clampfit 10.3.

Electrical Stimulation

Electrical stimuli were applied using a concentric bipolar electrode (CBAFC75 outer diameter 125 μm, Frederick Haer and Co., Bowdoin, ME, USA) placed as indicated in the "Results" section. Concerning contralateral stimulation, we assessed the integrity of the callosal projection through extracellular recordings before the intracellular experiments (Sempere-Ferràndez et al., 2018). We used Single square current pulses of 0.1 ms and supra-maximal stimulus intensities applied at 0.2 Hz to evoke synaptic responses in the recorded neurons. To determine the supra-maximal strength, we first detected the stimulus strength evoking the maximal response by progressively increasing the stimulus; this strength was increased by 10% to establish the supra-maximal value. The range was 100–500 μA, but in most slices, it was 400–500 mA.

Glutamate Application

Synaptic currents were evoked by the direct application of glutamate (1 mM glutamate dissolved in ACSF) using patch pipettes. The tip of the pipette was placed at several different distances from the soma of the recorded pyramidal neuron and glutamate was released by 20 ms pressure pulses of 5–10 psi applied with a Picospritzer (General Valve Corp. Fairfield, NJ, USA). Pressure pulses were applied at 20 s intervals.

Intracellular Staining With Biocytin

Some neurons were labeled with biocytin using the method described by Marx et al. (2012). Briefly, biocytin was added to the intracellular solution to give a final concentration of 5 mg/ml. Slices containing stained neurons were fixed overnight at 4°C in 100 mM phosphate-buffered saline (PBS; pH 7.4) with 4% paraformaldehyde. They were rinsed several times in PBS containing 1% Triton X-100 and the endogenous peroxidase was blocked by incubation in 30% H_2O_2. The slices were then transferred to a complex of 1% avidin–biotinylated HRP with 0.5% Triton X-100 (ABC Peroxidase Standard PK-400 Vectastain; Vector Labs, Burlingame, CA, USA) and left for 1 h with gentle shaking. They were reacted using

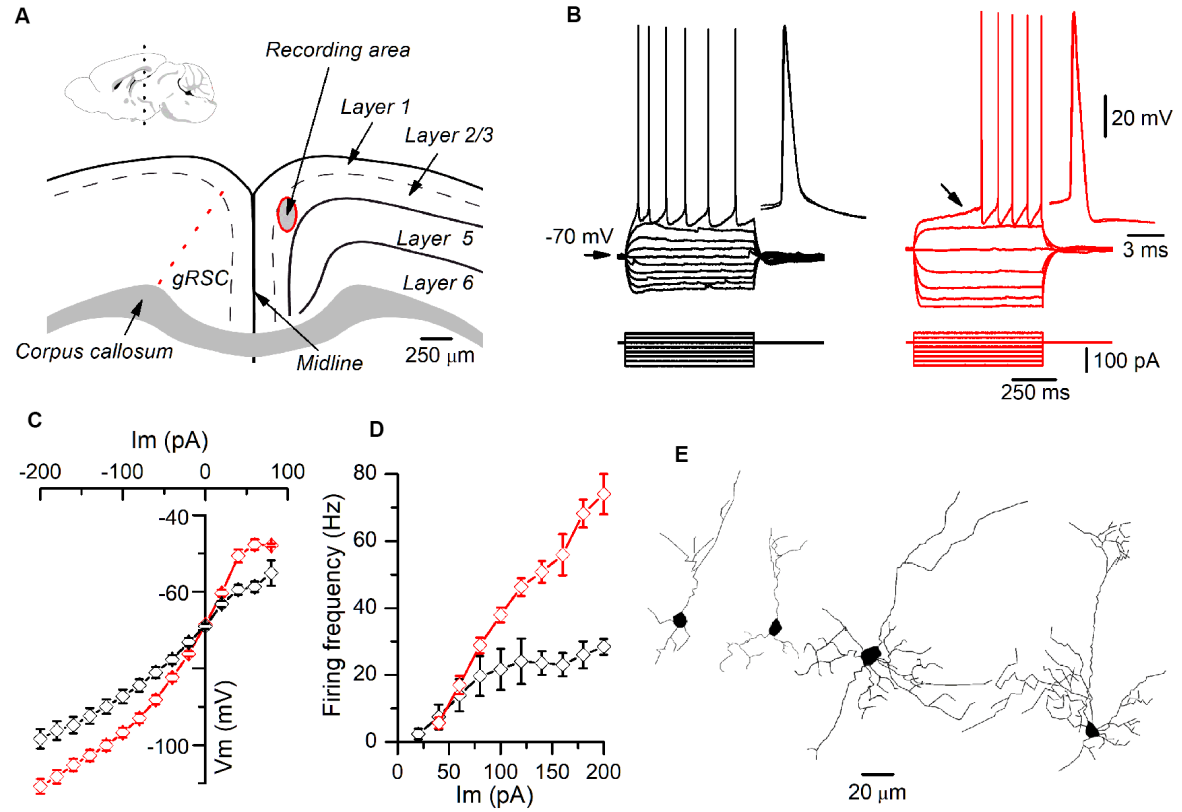

FIGURE 1 | Different firing patterns of layer 2/3 pyramidal neurons recorded in the granular retrosplenial cortex (GRSC). **(A)** Coronal view of the mouse GRSC highlighting the recording area. The dotted red line shows the approximate limit between the GRSC and the dysgranular RSC; this limit has been set according to Vogt and Paxinos (2014). The inset shows the mid-sagittal mouse brain with the approximate level of the coronal slices used for recordings (black dotted line; drawing taken from https://portal.brain-map.org/, reference atlas version 1, 2008; available online at: http://connectivity.brain-map.org/; 2014 Allen Institute for Brain Science). **(B)** Responses to hyperpolarizing and depolarizing current pulses of two pyramidal neurons recorded in layer 2/3 of the GRSC. The left panel (black traces) shows the regular spiking firing found in some neurons; the right panel (red traces) shows the late spiking firing pattern. Insets: two superimposed action potentials shown on larger time scales. The black arrow in the right panel shows the slow subthreshold depolarization that characterized the late-spiking (LS) firing pattern. Scale bars on the right also apply to the left panel. **(C)** I/V relationship of non-LS (black symbols; n = 5–16) and LS pyramidal neurons (red symbols; n = 9–20). **(D)** firing frequency vs. injected current measured in non-LS (black symbols; n = 5–16) and LS pyramidal neurons (red symbols; n = 5–16). The firing was evoked by square depolarizing current pulses as shown in panel B; the firing frequency was averaged throughout the firing in both LS and non-LS neurons. **(E)** Neurolucida drawings of two LS (left) and two non-LS neurons (right).

3,3-diaminobenzidine (DAB; Sigma) and the reaction stopped by adding 30% H_2O_2. Finally, the slices were mounted on glass slides, embedded in glycerol jelly, and coverslipped. Biocytin-stained neurons were drawn using Neurolucida software (MBF Bioscience, Williston, VT, USA).

Evoking and Recording Epileptiform Discharges

The slices were bathed in a modified ACSF (composition in mM: NaCl 124, KCl 5, PO_4H_2Na 1.25, $MgCl_2$ 1, $CaCl_2$ 1.2, $NaCO_3H$ 26, glucose 10; pH 7.4 when saturated with 95% O_2 and 5% CO_2). In modified ACSF and in the presence of 10 µM bicuculline (a $GABA_A$ receptor antagonist) the stimulation of layer 1 evokes large oscillatory discharges, which were recorded extracellularly with patch pipettes filled with modified ACSF (Rovira and Geijo-Barrientos, 2016). Modified ACSF and bicuculline were used only in the experiments of propagation of epileptiform activity reported in **Figure 4**. In all other experiments, standard ACSF described above in the paragraph "slice preparation" was used.

Statistics

Data are shown as values from individual neurons and/or giving the mean ± standard deviation (s.d.). Comparisons between two samples were made with non-parametric tests: the two-tailed Mann–Whitney rank-sum test for independent samples and the two-tailed Wilcoxon signed-rank test for paired samples. Comparisons of more than two samples (data on latencies shown in **Figure 9**) were made with the non-parametric Kruskal-Wallis one-way ANOVA on ranks which is independent of the samples' distribution). If the ANOVA gave significant differences among groups (p-value < 0.05), a *post hoc* Dunn's multiple comparison test was used to compare across all pairs of samples. Statistical analyses were performed using OriginPro8 (Origin Lab Corporation) or Sigma Stat 3.11 (Systat Software Inc). The degree

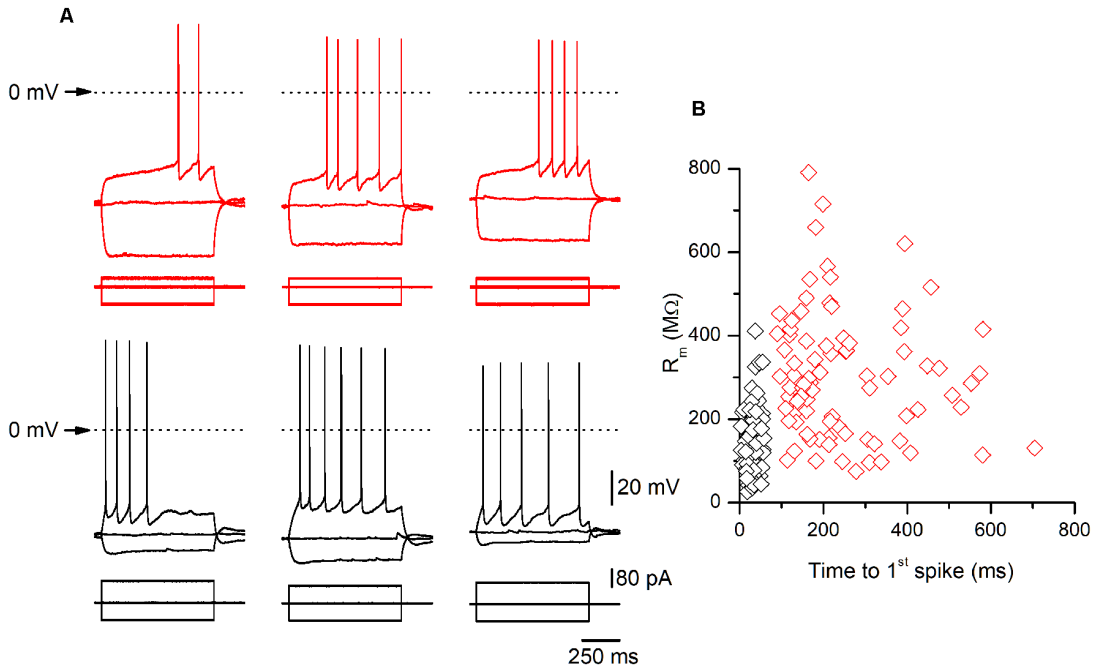

FIGURE 2 | Examples of late-spiking (LS) and non-LS pyramidal neurons. **(A)** Examples of the responses to hyperpolarizing and depolarizing current pulses of three LS (upper panels, red traces) and three non-LS pyramidal neurons (lower panels, black traces). Note the clear subthreshold slow depolarization in LS neurons, which is absent in the non-LS neurons. The hyperpolarizing pulse was of the same magnitude in all neurons (−80 pA) to illustrate the difference in input resistance (IR) between both types of neurons. The depolarizing current pulse was +40 pA in LS neurons (threshold pulse strength) and +80 / +100 pA in the non-LS neurons (minimum pulse strength necessary to evoke tonic discharge). The dotted line marks the 0 mV level. The scale bars apply to all panels. **(B)** The relationship between the input membrane resistance and time to 1st spike in LS (red symbols) and non-LS neurons (black symbols). The input resistance (R_m) was measured from the responses to small hyperpolarizing current pulses, and the time to 1st spike was measured between the onset of the depolarizing current pulse and the peak of the first spike fired by a depolarizing current pulse of strength corresponding to the rheobase.

of statistical significance is given in each figure and significance was set as $p < 0.05$.

RESULTS

Presence of Pyramidal Neurons With a Late-Spiking Firing Pattern in the Layer 2/3 of the Mouse GRSC

All data were obtained from somatic whole-cell recordings made in pyramidal neurons whose somata were located in the most dorsal part of layer 2/3 of the GRSC (**Figure 1A**). We found that this cortical region had two types of pyramidal neurons, each with different electrophysiological properties and easily discernible from their responses to hyperpolarizing and depolarizing current pulses (**Figure 1B**). To characterize the electrophysiological properties of these neurons we made an initial set of experiments using protocols with different series of hyper- and depolarizing current pulses. Some pyramidal neurons (**Figure 1B**, left panel) showed a regular spiking pattern, similar to that described for layer 2/3 pyramidal neurons of the dysgranular RSC (Sempere-Ferràndez et al., 2018). However, other pyramidal neurons showed, in response to long depolarizing current pulses, a pronounced slow depolarizing ramp that led to the threshold and delayed spike firing (**Figure 1B**, right panel); this firing pattern was similar to the late spiking firing (LS) pattern described in the GRSC of the rat (Kurotani et al., 2013). This slow depolarization ramp causing the late spiking was quantified measuring the time from the start of the depolarizing current pulse to the peak of the first spike in response to a current pulse of a strength corresponding to the rheobase (time to 1st spike). In pyramidal neurons showing this depolarization ramp the time to 1st spike was always longer than 90 ms, and were classified as Late Spiking pyramidal neurons (LS neurons). The remaining neurons were classified as non-LS pyramidal neurons, and their time to 1st spike was always shorter than 60 ms. According to our sample of pyramidal neurons, approximately 60% in the dorsal area of layer 2/3 of the GRSC were LS and 40% were non-LS, with the two types of neurons found to be readily intermingled. The LS neurons had a steeper I/V relationship (**Figure 1C**) than the non-LS neurons and fired at higher frequencies, revealing a non-saturating firing frequency vs. injected current relationship (**Figure 1D**). In response to suprathreshold current pulses, LS and non-LS neurons showed tonic firing, but with different degree of frequency adaptation. Frequency adaptation was measured as the quotient between the first and the last inter-spike interval in a current pulse of rheobase +40 pA; in LS neurons this quotient was close to 1 (no frequency adaptation), while in non-LS neurons was less than 1 (LS: 0.91 ± 0.26, $n = 21$; non-LS: 0.42 ± 0.18, $n = 14$; $p < 0.001$).

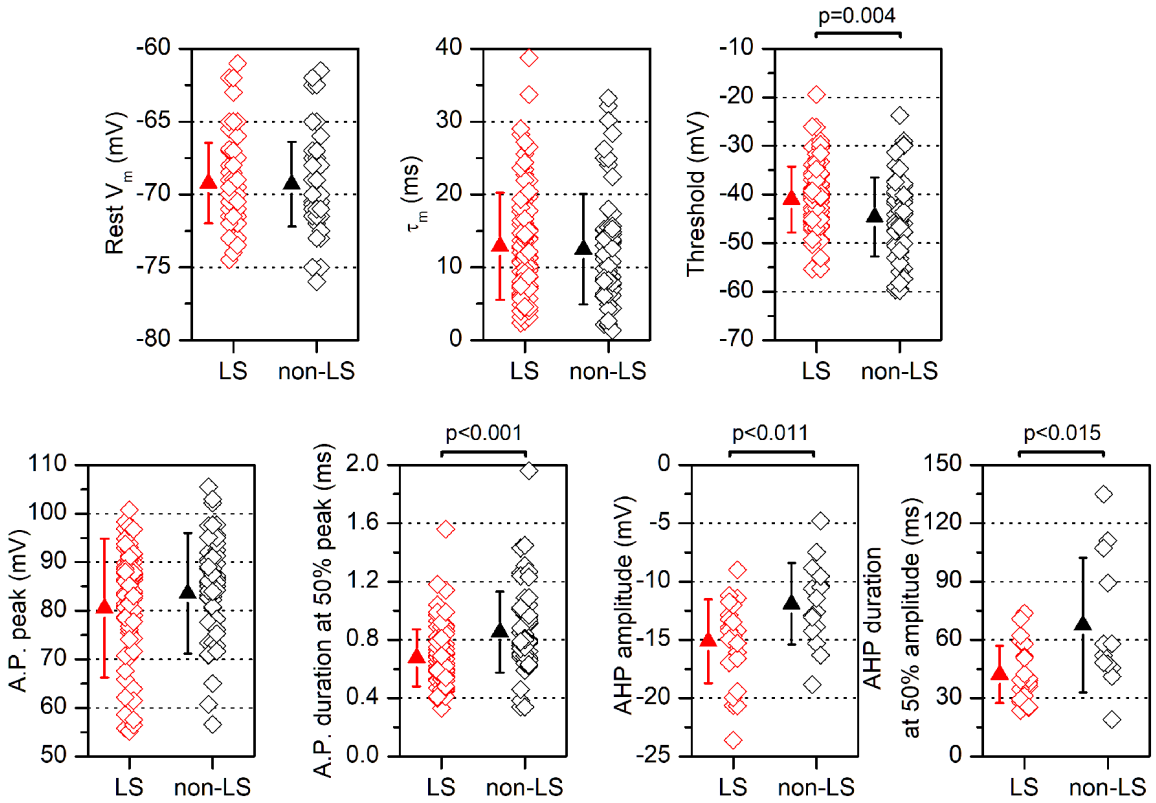

FIGURE 3 | Electrophysiological parameters are measured in LS and non-LS neurons. Each panel shows the values obtained from individual neurons (diamonds) and the mean ± s.d. (triangles) of several parameters measured in LS neurons and non-LS neurons. The resting membrane potential (V_m) was measured immediately after entering into the whole-cell mode; the threshold was measured at the 1st action potential in a just-threshold response; the action potential duration was measured at half amplitude; the peak amplitude of the action potential after-hyperpolarization (AHP) was measured from the threshold level, and the AHP duration was measured from the peak to 50% of the peak amplitude.

In response to hyperpolarizing current pulses, non-LS neurons showed a clear voltage sag, which was smaller in LS neurons; this voltage sag was measured as the voltage difference between the initial hyperpolarization and the steady-state value at the end of a current pulse of −40 pA (LS neurons: 0.92 ± 0.80 mV, n = 21; non-LS neurons 4.16 ± 3.49 mV, n = 13; p = 0.002). LS neurons also had smaller somata when viewed in living slices under DIC optics (LS: 173 ± 56.59 μm^2 n = 12, non-LS: 474.02 ± 119.86 μm^2, n = 12; $p < 0.001$). A sample of neurons was stained intracellularly with biocytin (**Figure 1E**). **Figure 2A** shows several examples of LS and non-LS neurons to illustrate the firing pattern of LS and non-LS neurons. In addition to a shorter time to 1st spike, LS neurons had a higher membrane input resistance (**Figure 2B**. Time to 1st spike: LS 252.22 ± 139.84 ms, n = 90, non-LS: 32.36 ± 14.94 ms n = 61; $p < 0.001$; membrane input resistance: LS 310.72 ± 157.20 MΩ n = 90, non-LS 148.58 ± 81.39 MΩ n = 61, $p < 0.001$). **Figure 2B** also shows that values of the time to 1st spike in LS and non-LS neurons did not overlap. The electrophysiological properties of these two types of pyramidal neurons are given in **Figure 3**. Several of these electrophysiological parameters were similar in both types of neurons (resting membrane potential: LS −69.22 ± 2.76 mV, n = 90, non-LS −69.29 ± 2.89 mV, n = 61; membrane time constant: LS 12.91 ± 7.33 ms n = 90, non-LS 12.48 ± 7.56 ms n = 61; action potential peak amplitude: LS 80.52 ± 14.30 mV n = 90, non-LS 83.56 ± 12.40 n = 61), but others showed differences between LS and non-LS neurons (threshold for spike firing: LS −41.02 ± 6.77 mV n = 90, non-LS −44.62 ± 8.10 mV n = 61, p = 0.004; action potential duration: LS 0.68 ± 0.20 ms n = 90, non-LS 0.85 ± 0.28 ms n = 61, $p < 0.001$; AHP amplitude: LS −15.12 ± 3.59 mV n = 24, non-LS −11.92 ± 3.49 mV n = 16, $p < 0.011$; AHP duration: LS 42.28 ± 14.69 ms n = 22, non-LS 67.66 ± 34.64 ms n = 12, $p < 0.015$). Not all parameters could be measured reliably in each neuron. The higher input resistance of LS neurons together with a similar membrane time constant suggests that the LS neurons had a lower membrane capacitance, which is consistent with a smaller size.

LS and Non-LS Pyramidal Neurons Behave Differently During the Propagation of Epileptiform Discharges

LS and non-LS pyramidal neurons were readily intermingled in the dorsal part of the GRSC; however, despite their proximity, they responded very differently during the propagation of epileptiform discharges along with the RSC (**Figure 4**).

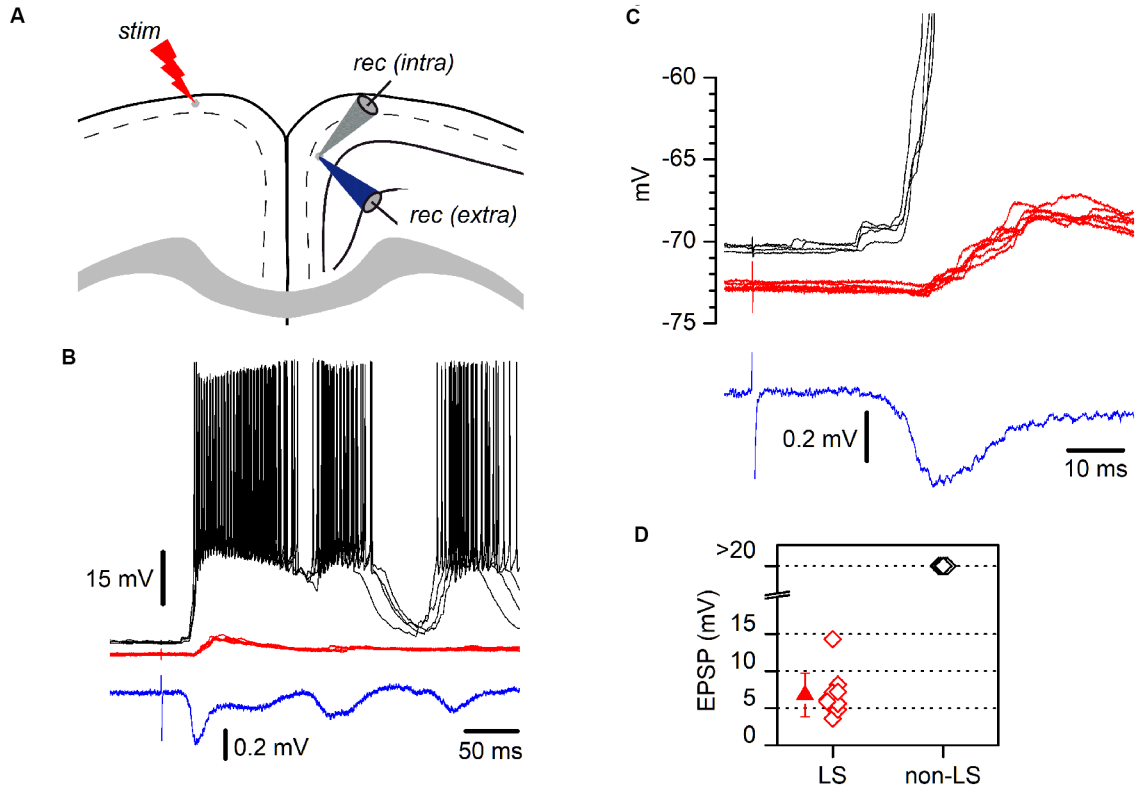

FIGURE 4 | LS and non-LS pyramidal neurons respond differently to incoming epileptiform discharges. **(A)** The diagram of a coronal GRSC slice showing the positions of recording and stimulating electrodes. The extracellular recording electrode (blue electrode) was kept in the same position while successive neurons were recorded intracellularly (gray electrode); electrical stimuli were applied to the contralateral side ("stim"). **(B)** Responses of a non-LS (black traces) and an LS pyramidal neuron (red traces) during the propagation of epileptiform discharges (blue trace: extracellular recordings) evoked by contralateral stimulation. Both neurons were recorded sequentially and their somata were placed close together. Each panel features five consecutive superimposed traces. The extracellular recording was the average of five consecutive responses. **(C)** The initial section of the responses shown in panel B presented on larger time and voltage scales; note the delayed onset and smaller amplitude of the response recorded in the LS neuron (red traces). **(D)** The peak amplitude of the EPSPs recorded during the propagation of epileptiform discharges: LS neurons, red symbols; non-LS neurons, black symbols. When the response was supra-threshold, we assigned an amplitude of >20 mV.

Epileptiform discharges were evoked by stimulation of layer 1 in the presence of a $GABA_A$ blocker (bicuculline 10 μM) and a modified ACSF (see "Materials and Methods" section). Under these conditions, large epileptiform discharges are known to propagate from the stimulation point to the ipsilateral layer 2/3 and, through the corpus callosum, to the contralateral cortex (Rovira and Geijo-Barrientos, 2016). All non-LS neurons recorded during the propagation of epileptiform discharges showed large depolarizations which always reached the threshold and provoked action potential burst firing (**Figures 4B,C**); in fact, the discharges recorded extracellularly were caused by the firing of non-LS neurons. Contrastingly, all recorded LS neurons presented only small, and always subthreshold, polysynaptic EPSPs (peak amplitude: 6.8 ± 2.94 mV, n = 10; **Figure 4D**). These synaptic responses often appeared delayed concerning the responses in non-LS neurons (**Figures 4B,C**). We do not know the circuit mechanisms responsible for the generation of the synaptic responses recorded during the propagation of epileptiform discharges, but the different responsiveness during this type of activity suggests that LS and non-LS pyramidal neurons form part of different neuronal circuits within layer 2/3, although they are located in very close to each other within the dorsal part of layer 2/3. These data suggest that propagating epileptiform seizures were only supported by non-LS neurons and that LS neurons were not involved in this kind of activity.

Long-Range Cortico-Cortical Axons Mostly Innervate Non-LS Pyramidal Neurons

One explanation of the different responses from LS and non-LS neurons during the propagation of epileptiform discharges is that they receive different afferent innervation. To test this possibility, we studied the synaptic currents evoked by stimulating long-range cortico-cortical axons. These axons were stimulated by applying electrical stimuli to two different sites: the ipsilateral layer 2/3 at 1.2 mm from the recording area and the homotopic contralateral layer 2/3 (**Figure 5**); the ipsilateral stimulation site was located in the dysgranular RSC. In response to ipsilateral layer 2/3 supra-maximal stimulation (**Figures 5B,C**), non-LS neurons generated large EPSCs, while LS neurons did not respond or generated only small EPSCs

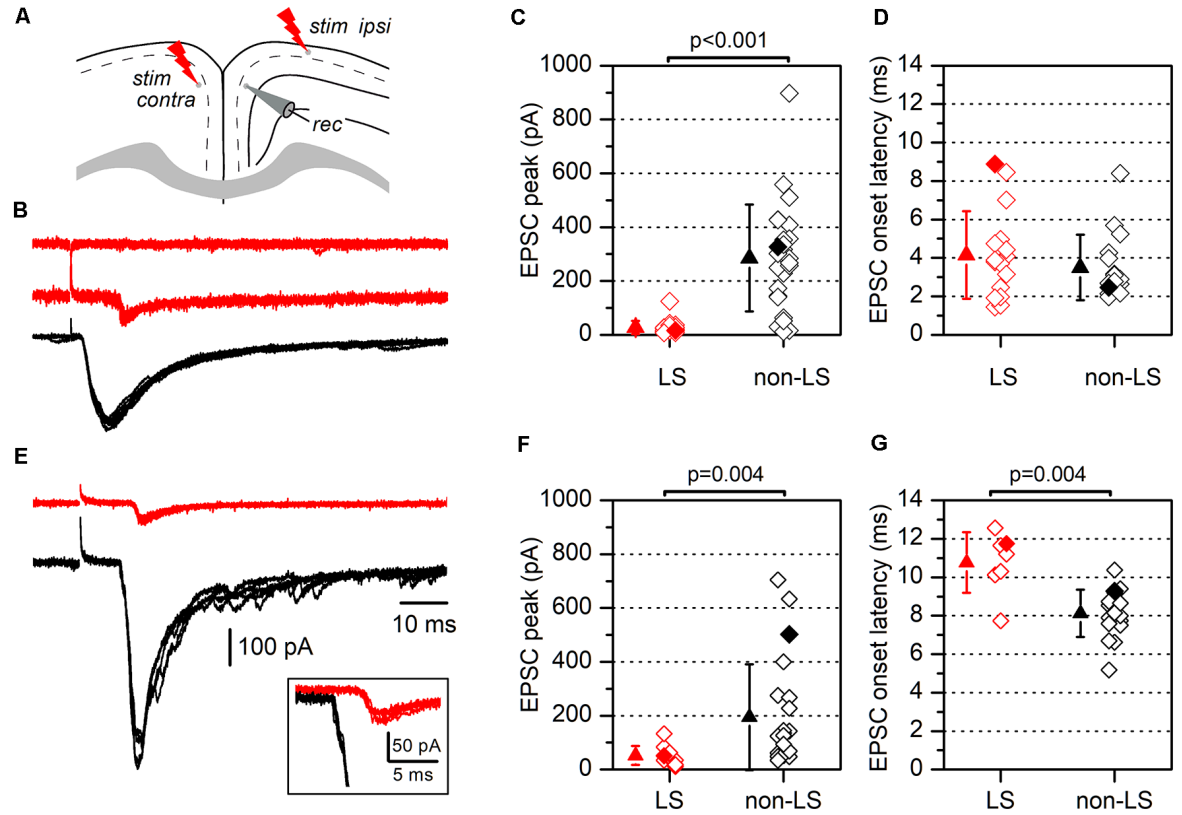

FIGURE 5 | Synaptic currents evoked by electrical stimulation in LS and non-LS pyramidal neurons. **(A)** The diagram of a coronal slice from the GRSC showing the positions of recording and stimulation electrodes for ipsilateral and contralateral stimulation ("*stim ipsi*" and "*stim contra*", respectively). **(B)** Examples of EPSCs recorded in response to ipsilateral electrical stimuli applied at 1.2 mm from the recorded neuron in one non-LS neuron (black traces) and two LS neurons (red traces). Each panel comprises four consecutive superimposed sweeps. **(C)** The peak amplitude, and **(D)** the latency of the EPSCs recorded in LS (red symbols; $n = 20$) and non-LS pyramidal neurons (black symbols; $n = 25$). **(E)** The examples of EPSCs recorded in response to contralateral stimulation in one non-LS (black traces) and one LS neuron (red traces). Each panel contains four consecutive superimposed sweeps. Note the longer latency of the response recorded in the LS neurons, shown at a larger scale in the inset. **(F)** The peak amplitude, and **(G)** the latency of the EPSCs evoked by contralateral stimulation. The peak amplitude and latency of the responses shown in panels **(B,E)** are highlighted by filled diamonds in panels **(C,D)** and **(F,G)**, respectively.

(non-LS: 285.39 ± 198.53 pA, $n = 25$; LS: 27.35 ± 24.66 pA, $n = 20$; $p < 0.001$). Similar results were observed after stimulation of the contralateral cortex (**Figures 5E,F**): non-LS neurons generated large EPSCs but LS neurons produced significantly smaller EPSCs (non-LS: 194.0 ± 196.63 pA, $n = 22$; LS: 51.91 ± 35.26 pA, $n = 10$; $p = 0.004$). The EPSCs recorded in the LS neurons had longer average latencies than the non-LS neurons in response to contralateral stimulation (**Figure 5G**; non-LS: 8.13 ± 1.23 ms, $n = 17$; LS: 10.76 ± 1.58 ms, $n = 7$; $p = 0.004$), but not in response to ipsilateral stimulation (**Figure 5D**; non-LS: 3.50 ± 1.70 ms, $n = 16$; LS: 4.15 ± 2.29 ms, $n = 16$).

We also measured the rise and decay times of the EPSCs evoked by contralateral stimulation. The rise time was significantly shorter in LS neurons (1.45 ± 0.45 ms, $n = 12$ vs. 3.27 ± 0.68 ms in non-LS neurons, $n = 9$; $p < 0.001$), while the decay time (measured as the time constant for a single exponential fit) was similar in both types of neurons (5.58 ± 2.15 ms in LS, $n = 12$ vs. 7.54 ± 2.53 ms in non-LS neurons, $n = 9$; $p = 0.07$). For the measurement of the EPSC time course in non-LS neurons, we selected cells in which the synaptic current did not show delayed di- or polysynaptic responses to make possible the fitting of the decay phase to a single exponential. In this sample of neurons, the peak amplitude was smaller in LS compared to non-LS neurons (50.12 ± 41.72 pA, $n = 12$; 218.11 ± 186.53 pA, $n = 9$; $p = 0.021$). The different magnitude of the synaptic responses correlated with the very different probabilities of the firing action potentials in response to ipsilateral or contralateral stimuli. Before going into the voltage-clamp mode, we checked whether electrical stimuli were able to evoke suprathreshold responses and action potential firing in a sample of neurons. We found that ipsilateral stimuli caused action potential to fire in 0 out of 30 (0%) LS and 12 out of 15 (80%) non-LS neurons, whereas with contralateral stimuli, action potentials fired in 0 out of 31 (0%) LS neurons and 5 out of 43 (12%) non-LS neurons.

Our results suggest that LS neurons receive less excitatory synaptic contacts that originated in long-range cortico-cortical axons. For a more accurate estimate of the range over which LS and non-LS neurons receive afferents, we studied the synaptic responses evoked in both types of neurons by the local glutamate

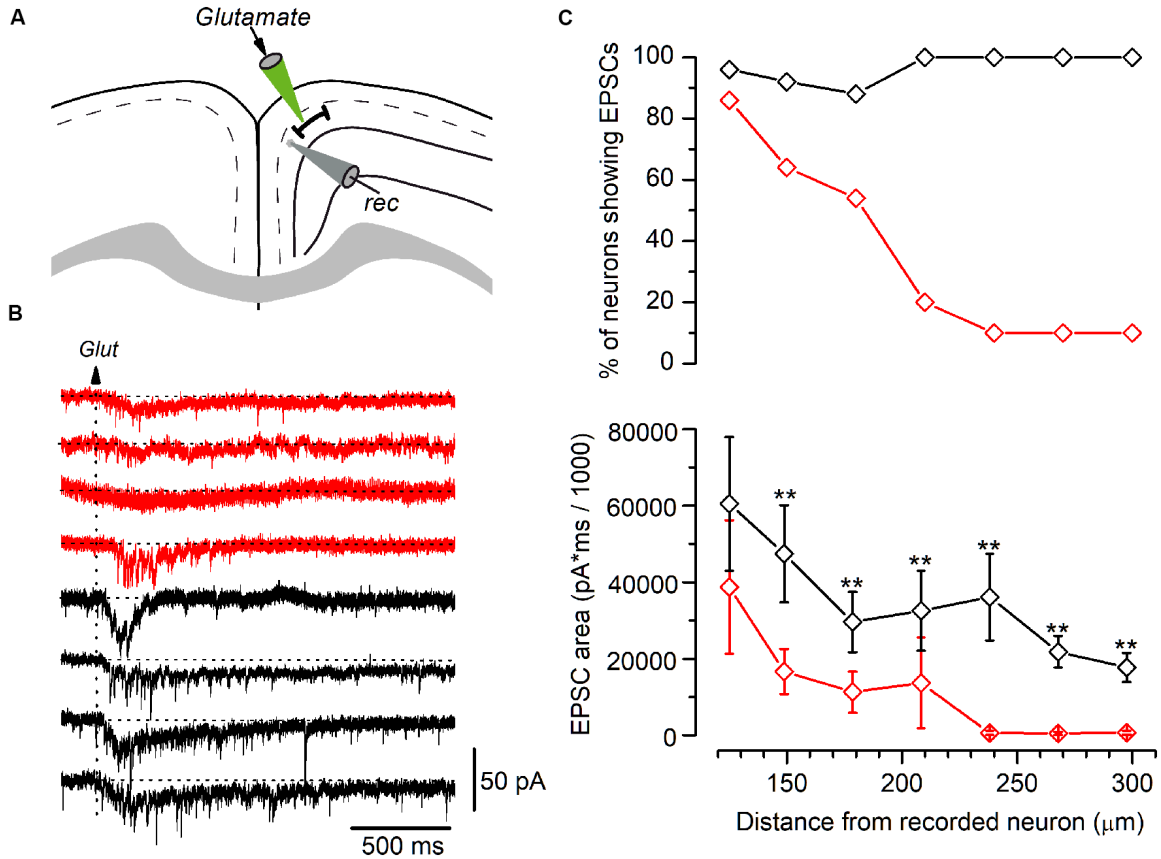

FIGURE 6 | Synaptic currents elicited by glutamate application in LS and non-LS pyramidal neurons. **(A)** The diagram of a GRSC coronal slice showing the positions of the recording electrode (gray) and the pipette used to apply glutamate pressure puffs (green). **(B)** The synaptic currents elicited in four LS neurons (red traces) and four non-LS neurons (black traces) by a puff of glutamate applied at 180 μm from the soma of the recorded neurons (arrow). **(C)** The percent of neurons showing glutamate-evoked EPSCs (upper plot) and the average area of the EPSCs (lower plot) at different distances from the soma, where red symbols represent the LS neurons (125 μm: $n = 28$, show EPSCs $n = 24$; 150 μm: $n = 28$, show EPSCs $n = 18$; 180 μm: $n = 28$, show EPSCs $n = 15$; 210 μm: $n = 10$, show EPSCs $n = 2$; 240 μm: $n = 10$, show EPSCs $n = 1$; 270 μm: $n = 10$, show EPSCs $n = 1$; 300 μm: $n = 10$, show EPSCs $n = 11$), and black symbols the non-LS neurons (125 μm: $n = 26$, show EPSCs $n = 25$; 150 μm: $n = 24$, show EPSCs $n = 22$; 180 μm: $n = 24$, show EPSCs $n = 21$; 210 μm: $n = 11$, show EPSCs $n = 11$; 240 μm: $n = 11$, show EPSCs $n = 11$; 270 μm: $n = 11$, show EPSCs $n = 11$; 300 μm: $n = 11$, show EPSCs $n = 11$); $^{**}p < 0.01$. At < 100 μm or shorter glutamate evoked large currents due to its direct effect on the recorded neurons' somata. The area of the synaptic responses was measured by the integration of the current trace over time (1 s) from the baseline [horizontal dotted lines in panel **(B)**]; the baseline was calculated from the current average of the 200 ms previous to the glutamate application.

application. Glutamate was applied using pressure puffs by placing the tip of patch electrodes at different distances from the recorded neurons. This approach allowed us to activate neurons close to the tip of the glutamate pipette and therefore determine the maximum distance from which both types of neurons received excitatory axons, as shown in **Figure 6**. For each recorded neuron we explored the synaptic responses evoked by applying glutamate on layer 2/3 at 100–300 μm from the soma of the recorded neuron. Synaptic responses were recorded within this range in 88–100% of non-LS neurons; however, they were mostly recorded when glutamate was applied at distances of less than 200 μm in LS neurons (54–86% of the LS neurons). The number of LS neurons that responded to glutamate decreased drastically when glutamate was applied at distances of more than 200 μm (20% to 10% of the LS neurons). These data showed that the LS neurons were innervated by axons originated in nearby layer 2/3 neurons (within 250 μm); in contrast, non-LS neurons receive axons from layer 2/3 neurons located further away.

The above data were recorded and pooled from neurons individually recorded in different slices. Given that the stimulating electrode was not always placed in the same position in different slices and the efficacy of the electrical stimuli varied, the pooling of data from different slices introduced a variability factor that could affect the results, including the differences in the latencies of the evoked responses (**Figure 5E**). Also, in some neurons of this set of experiments the latency could not be measured reliably. To confirm our results and eliminate any variability introduced by differences in the stimuli among slices, we conducted a series of experiments based on the simultaneous recording of pairs of neurons. The position of the stimulating electrode and the stimulus strengths were exactly the same for both neurons in each pair of recorded neurons. The distance between the somata of simultaneously

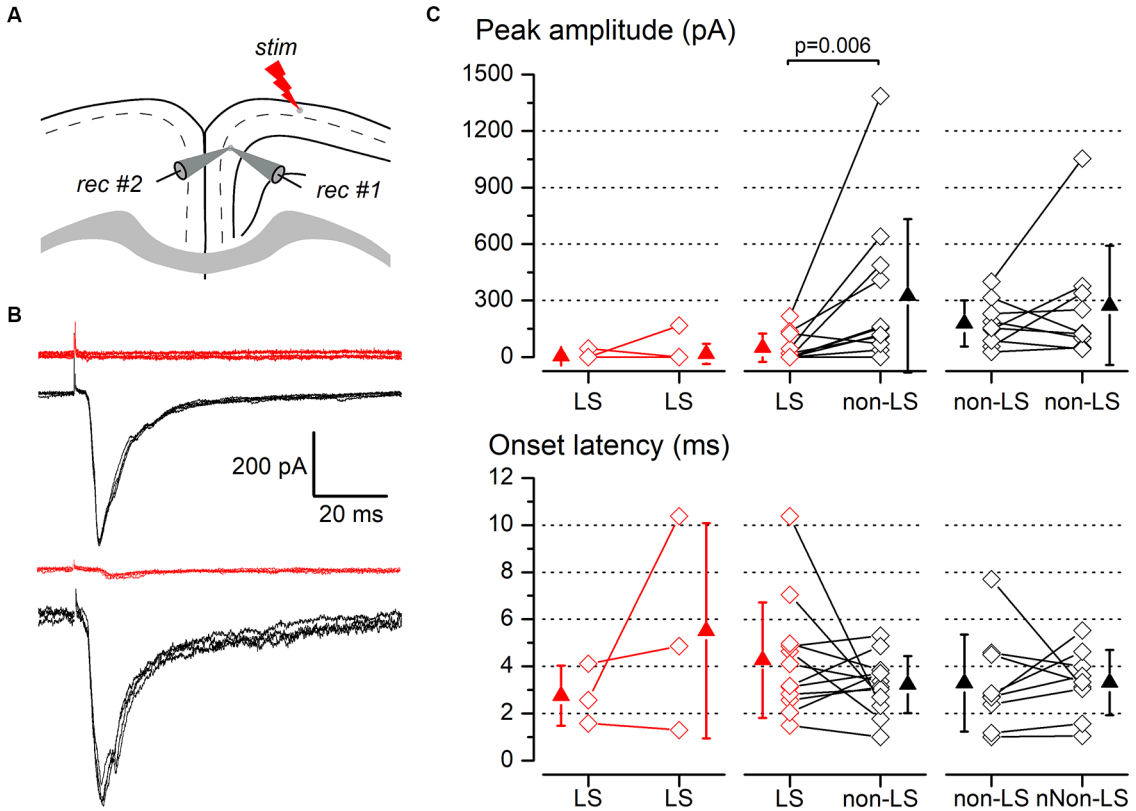

FIGURE 7 | Synaptic responses to ipsilateral stimulation of simultaneously recorded pairs of layer 2/3 pyramidal neurons. **(A)** The diagram of a coronal slice of the GRSC showing the positions of the stimulus and recording electrodes. **(B)** Examples of synaptic responses recorded in two neuron pairs, each formed with one LS (red traces) and one non-LS neuron (black traces); in the upper pair, the LS neuron did not respond and in the lower pair, the LS showed a small EPSC. Each panel comprises five consecutive superimposed responses. **(C)** Peak amplitude (upper panels) and onset latency (lower panels) of the synaptic responses recorded in neuron pairs formed with two LS neurons (left panels), one LS and one non-LS neuron (middle panels), and two non-LS neurons (right panels). The diamonds show the data from individual neurons and the triangles show the mean ± s.d.

recorded neuron pairs was 109.23 ± 81.08 μm (range 20–320 μm; n = 78). All recorded neuron pairs were checked for synaptic connection between the neurons forming the pair. In a total of 78 pairs recorded (28 formed by LS—LS neurons, 27 by LS—non-LS neurons, and 23 by non-LS—non-LS neurons) we detected only six cases of synaptic connections; five were from LS to non-LS and one was from non-LS to non-LS (this latter connection was only unidirectional). In response to either long-range ipsilateral stimulation (**Figure 7**) or contralateral stimulation (**Figure 8**), we found that LS neurons received excitatory inputs of significantly smaller amplitudes when comparing neurons from pairs formed by a non-LS and an LS neuron (ipsilateral stimulation: non-LS, 325.02 ± 406.88 pA; LS, 49.26 ± 75.28 pA; n = 11 pairs; p = 0.006. Contralateral stimulation: non-LS, 215.05 ± 245.63 pA; LS, 28.68 ± 44.81 pA; n = 15 pairs; p = 0.002). In homogeneous pairs, there were no differences in the EPSC peak amplitude of both neurons in response to ipsilateral or contralateral stimuli (Ipsilateral stimuli: LS/LS pairs 4.52 ± 14.29 pA vs. 16.74 ± 52.93 pA, n = 10 pairs; non-LS/non-LS pairs: 178.44 ± 121.74 pA vs. 273.87 ± 316.37 pA, n = 9 pairs. Contralateral stimulation: LS/LS pairs 26.04 ± 30.20 pA vs. 26.64 ± 40.49 pA, n = 18 pairs; non-LS/non-LS pairs: 205.16 ± 2,012.07 pA vs. 195.66 ± 216.15 pA, n = 14 pairs). The EPSCs recorded in response to contralateral stimulation had longer latencies in LS neurons (**Figure 8C**) when comparing the latencies in LS/non-LS pairs (LS: 10.25 ± 1.18 ms; non-LS: 8.09 ± 1.14 ms n = 6 pairs; p = 0.034); however, the EPSCs recorded in response to ipsilateral stimulation in LS neurons also had, on average, longer latencies, but the difference was not statistically significant (**Figure 7C**; LS: 4.27 ± 2.45 ms, non-LS: 3.2 3 ± 1.21 ms, n = 11 pairs). In LS/LS and non-LS/non-LS pairs, there were no differences between the latencies of the neurons forming a pair, either in response to ipsilateral (LS/LS pairs: 2.75 ± 1.27 ms vs. 5.51 ± 4.58 ms, n = 3 pairs; non-LS/non-LS pairs: 3.29 ± 2.06 ms vs. 3.32 ± 1.39 ms, n = 9 pairs) or contralateral stimulation (LS/LS pairs: 9.21 ± 2.48 ms vs. 10.79 ± 1.90 ms, n = 5 pairs; non-LS/non-LS pairs: 7.35 ± 1.08 ms vs. 7.45 ± 1.02 ms, n = 6 pairs).

Excitatory/Inhibitory Balance Was Similar in LS and Non-LS Pyramidal Neurons

Another mechanism that could contribute to the different size of the synaptic currents is a smaller excitatory/inhibitory balance (E/I balance) in LS compared to non-LS neurons. Neuronal

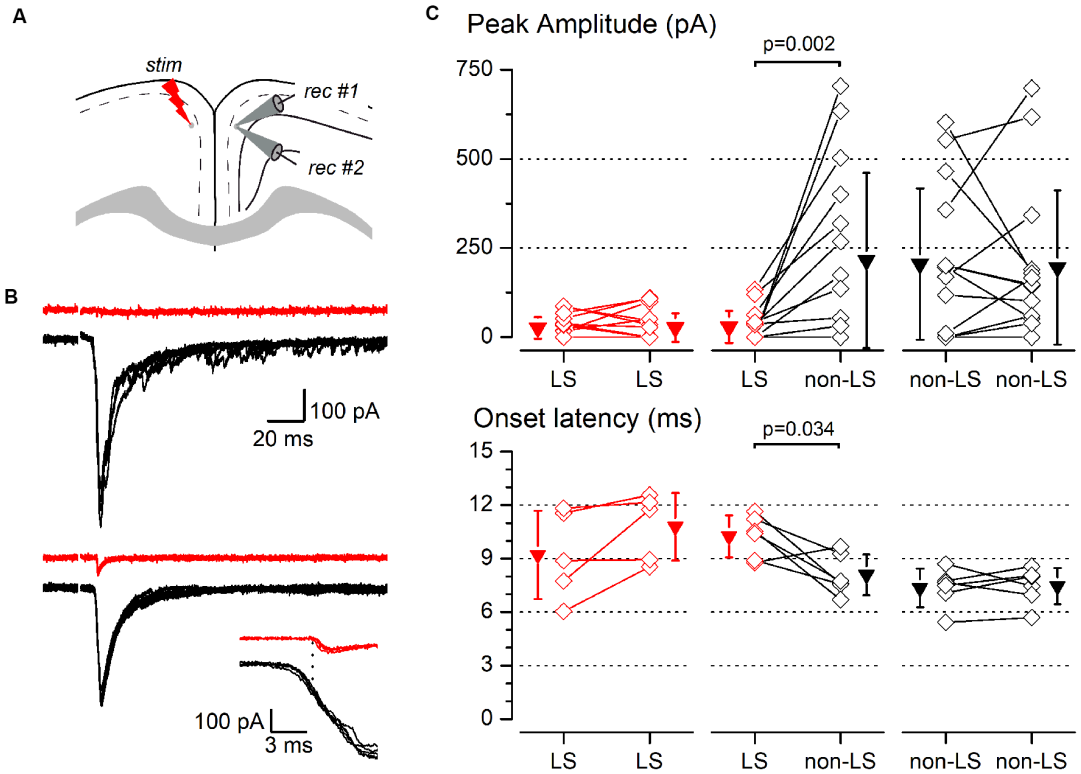

FIGURE 8 | Synaptic responses to contralateral stimulation of simultaneously recorded pairs of layer 2/3 pyramidal neurons. **(A)** The diagram of a coronal slice of the GRSC showing the positions of the stimulus and recording electrodes. **(B)** Examples of synaptic responses recorded in two neuron pairs, each formed with one LS (red traces) and one non-LS neuron (black traces); in the upper pair, the LS neuron did not respond and in the lower pair, the LS showed a small EPSC. The inset shows the onset phase of the responses of the lower example plotted on a larger time scale to highlight the difference in the onset latencies. Each panel shows five consecutive superimposed responses. **(C)** Peak amplitude (upper panels) and onset latency (lower panels) of the synaptic responses recorded in neuron pairs formed by two LS neurons (left panels), one LS and one non-LS neuron (middle panels), and two non-LS neurons (right panels). Comparisons were made with the signed-rank test for paired samples. The diamonds show the data from individual neurons and the triangles show the mean ± s.d.

microcircuits in superficial cortical layers are characterized by a powerful feed-forward inhibitory system arising from parvalbumin-expressing fast-spiking GABAergic interneurons (Holmgren et al., 2003; Avermann et al., 2012). As in the dysgranular RSC (Sempere-Ferràndez et al., 2019), the activation of afferent axons in layer 2/3 of the GRSC evoked a large feed-forward inhibitory component, in both LS and non-LS pyramidal neurons. The presence of this feed-forward inhibition means the net action of afferent axons on the postsynaptic neurons depends on the balance between the direct excitatory input and the feed-forward inhibition. In GRSC pyramidal neurons the E/I balance was measured from the excitatory and inhibitory conductance of the synaptic responses evoked by ipsilateral or contralateral stimulation in a sample of LS and non-LS neurons (**Figure 9**). Excitatory conductance was measured at the peak of the EPSCs recorded at −70 mV (a value close to the chloride equilibrium potential under our experimental conditions), while the inhibitory conductance was measured at the peak of the IPSCs recorded at 0 mV (a potential close to the AMPA receptors reversal potential of). The E/I balance was generally <1 in both LS and non-LS neurons (**Figure 9C**; LS: 0.44 ± 0.32, n = 15; non-LS: 0.87 ± 0.90, n = 25) and there was no difference in E/I balance between LS and non-LS neurons (**Figure 9C**). This result confirms that differences in the E/I balance were not responsible for the different magnitudes observed in the synaptic responses evoked by long-range axons in LS and non-LS neurons.

The Excitatory Responses to Contralateral Stimuli Recorded in LS Neurons Were Disynaptic

We measured the latencies of the EPSCs and IPSCs evoked by contralateral stimuli (**Figures 9E,F**; examples shown in **Figures 9A,D**). In LS neurons, EPSCs and IPSCs latencies were 10.58 ± 2.16 ms (n = 22) and 10.82 ± 1.00 ms (n = 18), respectively; and in non-LS neurons they were: 8.62 ± 1.79 ms (n = 47) in EPSCs and 11.30 ± 3.23 ms (n = 31) in IPSCs. These differences were also apparent in simultaneously recorded neuron pairs (n = 3; **Figure 9F**), with an EPSC of 10.59 ± 1.48 ms, and an IPSC of 10.81 ± 1.09 ms in LS neurons, compared to an EPSC of 8.14 ± 0.99 ms, and an IPSC of 10.49 ± 1.45 ms in non-LS neurons. The latencies were compared with the Kruskal–Wallis ANOVA on ranks, using Dunn's test for pairwise comparisons (**Figure 9E**). This

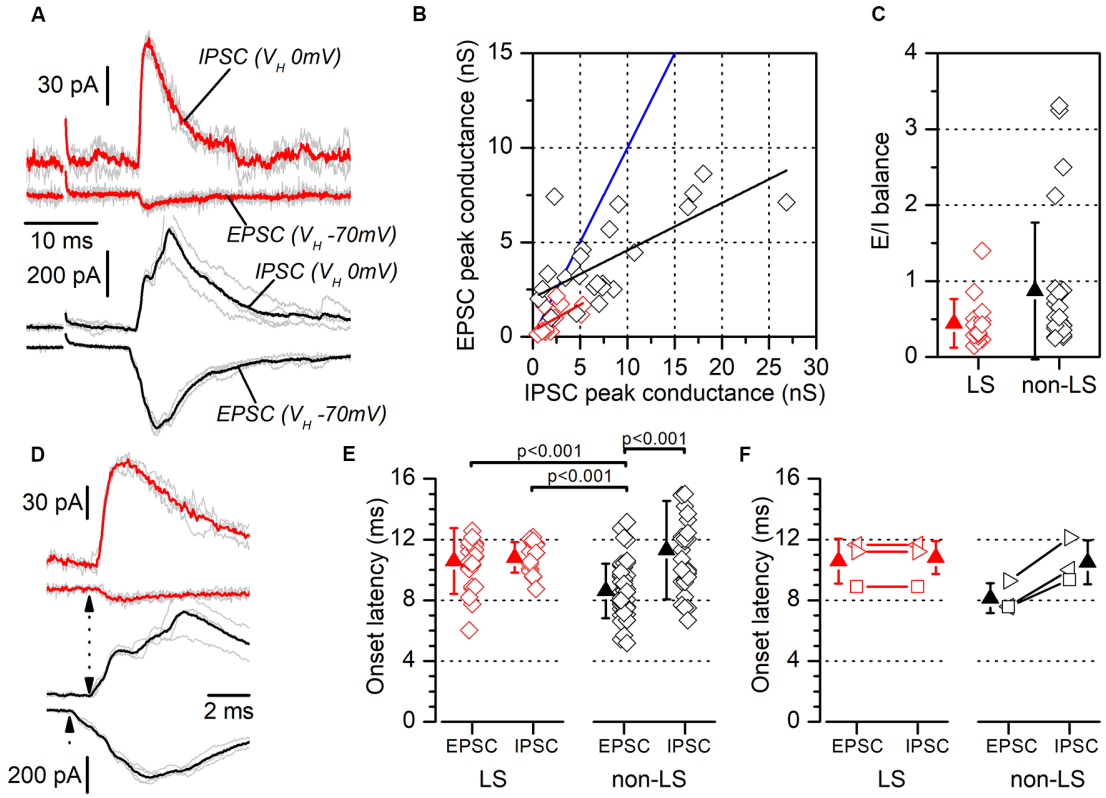

FIGURE 9 | Excitatory/inhibitory balance and latency of responses evoked by contralateral stimuli. **(A)** Examples of recordings of EPSCs and feed-forward IPSCs evoked in a neuron pair formed with one LS neuron (red traces) and one non-LS neuron (black traces). The EPSCs were recorded at a holding potential of −70 mV and the IPSCs at 0 mV. Each panel shows five consecutive responses (gray traces) and their average (thick, red, or black traces). **(B)** EPSC peak conductance vs. IPSC peak conductance measured in individual neurons (LS, red; non-LS, black symbols). Linear fit to data from non-LS neurons: black line, slope: 0.251, R^2: 0.44; linear fit to data from LS neurons: red line, slope: 0.277, R^2: 0.29. The blue line is the identity line. **(C)** E/I balance measured in LS (red) and non-LS (black) neurons. **(D)** The rising phase of the synaptic responses for panel **(A)** plotted on an enlarged time scale to highlight the differences in the EPSC and IPSC onset latencies (dotted arrows). **(E)** EPSCs, and the IPSCs onset latencies recorded in LS (red symbols) and non-LS neurons (black symbols) neurons. For comparison with the IPSC latencies, in this figure, we have pooled the EPSC onset latencies recorded from individual recordings (data in **Figure 5G**) and paired recordings (data in **Figure 8C**). The onset latencies were compared using the Kruskal–Wallis one-way ANOVA on ranks and we used Dunn's test for pairwise comparisons. **(F)** The onset latencies for the three neuron pairs formed with one LS and one non-LS neuron that both responded to contralateral stimuli. As in panel **(E)**, the EPSC onset latency data are taken from **Figure 5G**. In this panel each type of symbol represents the two neurons forming a simultaneously recorded pair.

analysis showed that the latencies of the EPSCs recorded in non-LS neurons were significantly shorter than the latencies measured for the IPSCs in non-LS neurons and the EPSCs and IPSCs from LS neurons. These values suggest that the EPSCs recorded in non-LS neurons were monosynaptic, while the EPSCs recorded in LS neurons (feed-forward excitation) and the IPSCs recorded in both neuron types were disynaptic since the average latency of the latter group of responses was 2.7–3 ms longer than that of the non-LS EPSCs. What is more, the disynaptic nature of the IPSCs is consistent with their feed-forward mechanisms.

DISCUSSION

In this work, we have studied the electrophysiological properties of layer 2/3 pyramidal neurons in the mouse GRSC, as well as their synaptic responses to cortico-cortical axons. We have identified the presence of two electrophysiological types of pyramidal neurons in the dorsal part of this cortical area. Some neurons, about 60% of the whole sample, showed a prominent late-spiking firing pattern similar to that of layer 2/3 pyramidal neurons in the rat GRSC (Kurotani et al., 2013), while the remaining neurons had a regular spiking pattern that was very similar to that of layer 2/3 pyramidal neurons located in other cortical areas, including the dysgranular RSC (area 30; Sempere-Ferràndez et al., 2018). Our data from simultaneous paired recordings show that the LS and non-LS pyramidal neurons were readily intermingled in the dorsal GRSC, as we often found neuron pairs formed by an LS and a non-LS neuron whose somata were separated by 100 μm on average. This neuron mixture suggests that the dorsal portion of the GRSC is an area of transition between the more ventral GRSC (where layer 2/3 comprises almost exclusively LS neurons: 94% in the rat GRSC according to Kurotani et al., 2013) and the dorsally located dysgranular (which contains only regular spiking pyramidal neurons: Sempere-Ferràndez et al., 2018). However, we do not

have further data supporting the hypothesis that the dorsal part of the GRSC is a transition area with the dysgranular RSC.

We have shown that the LS and non-LS pyramidal neurons were integrated with different neuronal circuits, even though these two types of neurons were found in proximity. Our data on glutamate application and the stimulation of long-range cortico-cortical axons (of either ipsilateral or contralateral origin) show that non-LS neurons receive cortico-cortical synaptic contacts from both local and long-range origin (over 250 μm) that generate complex EPSCs with mono- and polysynaptic components (see examples in **Figures 5**, **7**); however, LS neurons were, by contrast, innervated mainly by cortico-cortical axons of local origin, but not by long-range axons. This finding is reinforced by the results for the synaptic responses evoked by the stimulation of long-range cortico-cortical axons, either ipsilaterally or contralaterally. The large difference in the magnitudes of the EPSCs and the proximity of LS and non-LS neurons implies that non-LS pyramidal neurons are selectively innervated by incoming long-range axons acting on layer 2/3 of the dorsal part of the GRSC. This selective long-range axonal innervation of non-LS neurons implies that LS and non-LS pyramidal neurons are integrated with different neuronal circuits, and therefore participate in different functions. The non-LS neurons fired intensely during epileptiform discharges evoked in the dis-inhibited cortex, while LS neurons only showed subthreshold synaptic responses.

An alternative explanation of the different magnitudes of the synaptic responses recorded in LS and non-LS neurons is that afferents originated in long-range axons were similar for both types of neurons, but the somatodendritic localization differed. In the LS neurons, the synapsis could be located in distal dendrites; whereas in the non-LS neurons, the synapsis could be located in proximal dendrites. It has been shown in thick tufted layer 5 pyramidal neurons that synaptic contacts formed on the apical dendrite do not correspond to the distance from the soma and therefore distal contacts generate smaller somatic synaptic responses than proximal contacts (Williams and Stuart, 2002). We cannot rule out this explanation, but the values of the rise and decay times of the EPSCs from LS and non-LS neurons are not fully consistent with different synaptic localization. Decay times were similar in both types of neurons, while rise times were even shorter for LS neurons. However, it is important to note that the EPSCs had polysynaptic components that may lengthen their time course in non-LS neurons.

Neurons with a late-spiking firing pattern have been found in other cortical areas of rodents related to the RSC and implicated in spatial information processing. Pyramidal-like neurons with a clear late-spiking pattern have been reported in the superficial layers of the presubiculum (Abbasi and Kumar, 2013), which is reciprocally connected to the GRSC (Wyss and Van Groen, 1992). In the medial entorhinal cortex, which receives connections from the RSC (Wyss and Van Groen, 1992), layer 2 non-stellate pyramidal-like neurons have also shown an LS pattern (Alonso and Klink, 1993). Finally, small, layer 2/3 pyramidal neurons with an LS firing pattern have been described in the perirhinal cortex (Faulkner and Brown, 1999); there are also LS neurons in layer 6 of this cortical region, but they are not pyramidal. Given that neurons with an LS firing pattern could be involved in the integration of responses with different timing (Kurotani et al., 2013), these neurons may form part of neural circuits equipped with specific signal processing timing capacities.

The characteristics of the synaptic responses evoked in LS and non-LS neurons by long-range cortico-cortical axons show that in the generation of these responses participated complex local neuronal circuits. The values of the onset latencies of the synaptic responses (originated in the contralateral cortex; **Figure 9**) suggests that in LS neurons the EPSCs were disynaptic, while in non-LS neurons the onset of the EPSCs was monosynaptic. On the other hand, in LS neurons the EPSCs were mostly small and had a single component (disynaptic), while in non-LS neurons the EPSCs were mostly large and complex, having an initial monosynaptic component and several delayed polysynaptic components (see recordings shown in **Figures 5**, **7**). The simplest explanation for these findings is that long-range cortico-cortical axons reaching the dorsal part of the GRSC innervated monosynaptically only non-LS neurons; part of these non-LS neurons should fire action potentials and this firing generated the disynaptic EPSCs in LS neurons and the polysynaptic components in non-LS neurons by a feed-forward excitation. This hypothesis is supported by our finding that some non-LS neurons fire action potentials in response to long-range (80–12% of the recorded non-LS neurons in response to ipsi- and contralateral axons, respectively) and by the probability of interconnections between layer 2/3 pyramidal neurons (0.1–0.15, Holmgren et al., 2003; Avermann et al., 2012). However, in our sample of simultaneously recorded neuron pairs, we did not find a single case of non-LS to LS synaptic connections, which suggests that neurons causing the disynaptic responses in LS neurons were placed outside the dorsal part of the GRSC. Overall, these data show the complexity of the local neuronal circuits causing the synaptic responses to cortico-cortical axons in the dorsal part of the GRSC.

Our results may have two limitations associated with the method of recording the synaptic responses. Firstly, concerning the long-range stimulation experiments, the recorded responses (or part of them) may be due to local collaterals from neighboring pyramidal neurons activated antidromically by the electrical stimuli rather than the long-range afferent axons impinging on layer 2/3 neurons. This is particularly important in terms of the contralateral stimulation, given the symmetrical, bilateral structure of the callosal fibers. However, we did not record a single case of antidromic activation in response to contralateral stimulation throughout our entire sample of both LS and non-LS neurons. This observation means it is very unlikely that the synaptic responses recorded after contralateral stimulation could be caused by antidromic activation of the local collateral branches of the neuronal axons. This lack of any antidromic responses contrasted with the dysgranular RSC, where a very small proportion of layer 2/3 pyramidal

neurons fire antidromically (<10% with maximal stimuli, Sempere-Ferràndez et al., 2018). Secondly, we used an intracellular solution based on K^+-gluconate for voltage-clamp recordings, instead of a cesium-based solution. This was because it was impossible to identify LS and non-LS pyramidal neurons with intracellular cesium, given that the firing pattern changes drastically. However, as mentioned previously, the EPSC time course data rule out that small responses recorded in the LS neurons were originated in more distal dendrites than large responses recorded in the non-LS neurons, thus minimizing the relevance of using intracellular cesium.

Our results were obtained in mice aged 14–22 days. At this age, the cortical circuit is still not fully developed and, therefore, we cannot rule out the possibility that further circuit refinement may contribute to the mechanisms controlling the firing of pyramidal neurons and the different coding strategies of layer 2/3 and layer 5 pyramidal neurons. For instance, Angulo et al. (1999) showed that from weeks 3–5 postpartum some changes occur in the excitatory connections from layer 5 pyramidal neurons to fast-spiking interneurons, in particular, a switch from paired-pulse depression to paired-pulse facilitation that confers layer 5 pyramidal neurons wider integrative capabilities at 5 weeks of postnatal age. The fact that cortical circuits are not fully developed at this postnatal development stage means the afferent connections formed on LS and non-LS pyramidal neurons are still susceptible to subsequent refinements.

The innervation of the dorsal dysgranular RSC by callosal axons is denser than the innervation of the GRSC (Sempere-Ferràndez et al., 2018), and this is coincident with the different innervation by contralateral cortico-cortical axons between LS and non-LS neurons that we report here. From a functional point of view, this finding suggests that non-LS neurons could be part of the dorsal dysgranular RSC (their properties were very similar to those of the pyramidal neurons of this area, Sempere-Ferràndez et al., 2018), although they are placed within the morphologically defined GRSC. This would imply that the differences in synaptic responses found between LS and non-LS neurons could represent differences in microcircuit organization between the dorsal dysgranular RSC and the ventral GRSC.

DATA AVAILABILITY STATEMENT

The raw data supporting the conclusions of this article will be made available by the authors, under a reasonable request.

ETHICS STATEMENT

The animal study was reviewed and approved by Ethical Committee for the Experimental Research of the Universidad Miguel Hernández.

AUTHOR CONTRIBUTIONS

RR, SM, and EG-B designed the research. RR, ED-S, and EG-B performed the research. RR and EG-B wrote the manuscript and all the authors revised it. All authors contributed to the article and approved the submitted version.

FUNDING

This work was supported by the Spanish Ministerio de Economía y Competitividad (MINECO/AEI/FEDER, UE; grant number SAF2017-83702-R), the Spanish State Research Agency, through the "Programa Severo Ochoa" for Centers of Excellence in R&D (grant number SEV-2017-0723), and Generalitat Valenciana (program Prometeo II, grant number 2018/041).

ACKNOWLEDGMENTS

We are grateful to Francisca Almagro, Alicia Estirado and Víctor Rodríguez for their excellent technical assistance.

REFERENCES

Abbasi, S., and Kumar, S. S. (2013). Electrophysiological and morphological characterization of cells in superficial layers of rat presubiculum. *J. Comp. Neurol.* 521, 3116–3132. doi: 10.1002/cne.23365

Aggleton, J. P. (2014). Looking beyond the hippocampus: old and new neurological targets for understanding memory disorders. *Proc. Biol. Sci.* 281:20140565. doi: 10.1098/rspb.2014.0565

Alonso, A., and Klink, R. (1993). Differential electroresponsiveness of stellate and pyramidal-like cells of medial entorhinal cortex layer II. *J. Neurophysiol.* 70, 128–143. doi: 10.1152/jn.1993.70.1.128

Angulo, M. C., Staiger, J. F., Rossier, J., and Audinat, E. (1999). Developmental synaptic changes increase the range of integrative capabilities of an identified excitatory neocortical connection. *J. Neurosci.* 19, 1566–1576. doi: 10.1523/JNEUROSCI.19-05-01566.1999

Avermann, M., Tomm, C., Mateo, C., Gerstner, W., and Petersen, C. C. (2012). Microcircuits of excitatory and inhibitory neurons in layer 2/3 of mouse barrel cortex. *J. Neurophysiol.* 107, 3116–3134. doi: 10.1152/jn.00917.2011

Cooper, B. G., and Mizumori, S. J. (1999). Retrosplenial cortex inactivation selectively impairs navigation in darkness. *Neuroreport* 10, 625–630. doi: 10.1097/00001756-199902250-00033

Epstein, R. A. (2008). Parahippocampal and retrosplenial contributions to human spatial navigation. *Trends Cogn. Sci.* 12, 388–396. doi: 10.1016/j.tics.2008.07.004

Faulkner, B., and Brown, T. H. (1999). Morphology and physiology of neurons in the rat perirhinal-lateral amygdala area. *J. Comp. Neurol.* 411, 613–642. doi: 10.1002/(sici)1096-9861(19990906)411:4<613::aid-cne7>3.0.co;2-u

Holmgren, C., Harkany, T., Svennenfors, B., and Zilberter, Y. (2003). Pyramidal cell communication within local networks in layer 2/3 of rat neocortex. *J. Physiol.* 551, 139–153. doi: 10.1113/jphysiol.2003.044784

Ichinohe, N. (2012). Small-scale module of the rat granular retrosplenial cortex: an example of the minicolumn-like structure of the cerebral cortex. *Front. Neuroanat.* 5:69. doi: 10.3389/fnana.2011.00069

Ichinohe, N., Knight, A., Ogawa, M., Ohshima, T., Mikoshiba, K., Yoshihara, Y., et al. (2008). Unusual patch-matrix organization in the retrosplenial cortex of the reeler mouse and Shaking rat Kawasaki. *Cereb. Cortex* 18, 1125–1138. doi: 10.1093/cercor/bhm148

Jones, B. F., Groenewegen, H. J., and Witter, M. P. (2005). Intrinsic connections of the cingulate cortex in the rat suggest the existence of multiple functionally segregated networks. *Neuroscience* 133, 193–207. doi: 10.1016/j.neuroscience.2005.01.063

Kurotani, T., Miyashita, T., Wintzer, M., Konishi, T., Sakai, K., Ichinohe, N., et al. (2013). Pyramidal neurons in the superficial layers of rat retrosplenial cortex exhibit a late-spiking firing property. *Brain Struct. Funct.* 218, 239–254. doi: 10.1007/s00429-012-0398-1

Marx, M., Gunter, R., Hucko, W., Radnikow, G., and Feldmeyer, D. (2012). Improved biocytin labelling and neuronal 3D reconstruction. *Nat. Protc.* 7, 394–407. doi: 10.1038/nprot.2011.449

Miller, A. M., Vedder, L. C., Law, L. M., and Smith, D. M. (2014). Cues, context, and longterm memory: the role of the retrosplenial cortex in spatial cognition. *Front. Hum. Neurosci.* 8:586. doi: 10.3389/fnhum.2014.00586

Rovira, V., and Geijo-Barrientos, E. (2016). Intra- and interhemispheric propagation of electrophysiological synchronous activity and its modulation by serotonin in the cingulate cortex of juvenile mice. *PLoS One* 11:e0150092. doi: 10.1371/journal.pone.0150092

Sempere-Ferràndez, A., Andrés-Bayón, B., and Geijo-Barrientos, E. (2018). Callosal responses in a retrosplenial column. *Brain Struct. Funct.* 223, 1051–1069. doi: 10.1007/s00429-017-1529-5

Sempere-Ferràndez, A., Martínez, S., and Geijo-Barrientos, E. (2019). Synaptic mechanisms underlying the intense firing of neocortical layer 5B pyramidal neurons in response to cortico-cortical inputs. *Brain Struct. Funct.* 224, 1403–1416. doi: 10.1007/s00429-019-01842-8

Shibata, H., Honda, Y., Sasaki, H., and Naito, J. (2009). Organization of intrinsic connections of the retrosplenial cortex in the rat. *Anat. Sci. Int.* 84, 280–292. doi: 10.1007/s12565-009-0035-0

Shibata, H. (1998). Organization of projections of rat retrosplenial cortex to the anterior thalamic nuclei. *Eur. J. Neurosci.* 10, 3210–3219. doi: 10.1046/j.1460-9568.1998.00328.x

Shibata, H. (2000). Organization of retrosplenial cortical projections to the laterodorsal thalamic nucleus in the rat. *Neurosci. Res.* 38, 303–311. doi: 10.1016/s0168-0102(00)00174-7

Shibata, H., and Naito, J. (2008). Organization of anterior cingulate and frontal cortical projections to the retrosplenial cortex in the rat. *J. Comp. Neurol.* 506, 30–45. doi: 10.1002/cne.21523

Sripanidkulchai, K., and Wyss, J. M. (1986). Thalamic projections to retrosplenial cortex in the rat. *J. Comp. Neurol.* 254, 143–165. doi: 10.1002/cne.902540202

Sripanidkulchai, K., and Wyss, J. M. (1987). The laminar organization of efferent neuronal cell bodies in the retrosplenial granular cortex. *Brain Res.* 406, 255–269. doi: 10.1016/0006-8993(87)90790-6

Sugar, J., Witter, M. P., van Strien, N. M., and Cappaert, N. L. (2011). The retrosplenial cortex: intrinsic connectivity and connections with the (para)hippocampal region in the rat. An interactive connectome. *Front. Neuroinform* 5:7. doi: 10.3389/fninf.2011.00007

Sutherland, R. J., Whishaw, I. Q., and Kolb, B. (1988). Contributions of cingulate cortex to two forms of spatial learning and memory. *J. Neurosci.* 8, 1863–1872. doi: 10.1523/JNEUROSCI.08-06-01863.1988

Tamamaki, N., Yanagawa, Y., Tomioka, R., Miyazaki, J.-I., Obata, K., and Kaneko, T. (2003). Green fluorescent protein expression and colocalization with calretinin, parvalbumin and somatostatin in the GAD67-GFP knock-in mouse. *J. Comp. Neurol.* 467, 60–79. doi: 10.1002/cne.10905

van Groen, T., Kadish, I., and Wyss, J. M. (2004). Retrosplenial cortex lesions of area Rgb (but not of area Rga). impair spatial learning and memory in the rat. *Behav. Brain Res.* 154, 483–491. doi: 10.1016/j.bbr.2004.03.016

Van Groen, T., Vogt, B. A., and Wyss, J. M. (1993). "Interconnections between the thalamus and retrosplenial cortex," in *Neurobiology of Cingulate Cortex and Limbic Thalamus*, eds B. A. Vogt and M. Gabriel (Boston: Birkha user), 123–150

van Groen, T., and Wyss, J. M. (1990). Connections of the retrosplenial granular a cortex in the rat. *J. Comp. Neurol.* 300, 593–606. doi: 10.1002/cne.903000412

van Groen, T., and Wyss, J. M. (1992). Connections of the retrosplenial dysgranular cortex in the rat. *J. Comp. Neurol.* 315, 200–216. doi: 10.1002/cne.903150207

van Groen, T., and Wyss, J. M. (2003). Connections of the retrosplenial granular b cortex in the rat. *J. Comp. Neurol.* 463, 249–263. doi: 10.1002/cne.10757

Vann, S. D., and Aggleton, J. P. (2002). Extensive cytotoxic lesions of the rat retrosplenial cortex reveal consistent deficits on tasks that tax allocentric spatial memory. *Behav. Neurosci.* 116, 85–94. doi: 10.1037/0735-7044.116.1.85

Vann, S. D., and Aggleton, J. P. (2004). Testing the importance of the retrosplenial guidance system: effects of different sized retrosplenial cortex lesions on heading direction and spatial working memory. *Behav. Brain Res.* 155, 97–108. doi: 10.1016/j.bbr.2004.04.005

Vann, S. D., and Aggleton, J. P. (2005). Selective dysgranular retrosplenial cortex lesions in rats disrupt allocentric performance of the radial-arm maze task. *Behav. Neurosci.* 119, 1682–1686. doi: 10.1037/0735-7044.119.6.1682

Vann, S. D., Aggleton, J. P., and Maguire, E. A. (2009). What does the retrosplenial cortex do? *Nat. Rev. Neurosci.* 10, 792–802. doi: 10.1038/nrn2733

Vogt, B. A. (2014). "Cingulate cortex and pain architecture," in *The Rat Nervous System*, 4th Edn. ed. G. Paxinos (New York: Academic Press), 575–599.

Vogt, B. A., and Paxinos, G. (2014). Cytoarchitecture of mouse and rat cingulate cortex with human homologies. *Brain Struct. Funct.* 219, 185–192. doi: 10.1007/s00429-012-0493-3

Vogt, B. A., and Peters, A. (1982). Form and distribution of neurons in rat cingulate cortex: areas 32, 24, and 29. *J. Comp. Neurol.* 195, 603–625. doi: 10.1002/cne.901950406

Vogt, B. A., Vogt, L., and Farber, N. B. (2004). "Cingulate cortex and disease models," in *The Rat Nervous System*, 3rd Edn. ed. G. Paxinos (New York: Academic Press), 705–727.

Whishaw, I. Q., Maaswinkel, H., Gonzalez, C. L., and Kolb, B. (2001). Deficits in allothetic and idiothetic spatial behavior in rats with posterior cingulate cortex lesions. *Behav. Brain Res.* 118, 67–76. doi: 10.1016/s0166-4328(00)00312-0

Williams, S. R., and Stuart, G. J. (2002). Dependence of EPSP efficacy on synapse location in neocortical pyramidal neurons. *Science* 295, 1907–1910. doi: 10.1126/science.1067903

Wyss, J. M., and Van Groen, T. (1992). Connections between the retrosplenial cortex and the hippocampal formation in the rat: a review. *Hippocampus* 2, 1–11. doi: 10.1002/hipo.450020102

Conflict of Interest: The authors declare that the research was conducted in the absence of any commercial or financial relationships that could be construed as a potential conflict of interest.

Annex of results

8. ANNEX OF RESULTS

In section 1 and 2 of annex of results, I describe unpublished results which were obtained in my last period of graduate student. These results are directly related with the above paper, and they continue and complete this work.

8.1. SECTION 1. Properties and innervation of L5 thick tufted pyramidal neurons of the granular retrosplenial cortex. Comparison with L2/3 pyramidal neurons

We have shown that the synaptic responses recorded in LS neurons in response to ipsilateral or contralateral stimulation were disynaptic; one possible source of these disynaptic responses in LS neurons could be the thick-tufted large pyramidal neurons of L5; in the dorsal dysgranular RSC these neurons fire strongly in response to contralateral inputs (Sempere-Fernàndez et al., 2018, 2019), and this firing could cause the EPSCs recorded in L2/3 LS neurons through synaptic connections between L5 and L2/3 pyramidal neurons. To test this possibility, we made simultaneous recordings of neuron pairs formed by a L5 thick-tufted neurons and a L2/3 pyramidal neurons (either LS or non-LS). With these experiments we tried to determine whether 1) L5 thick-tufted pyramidal neurons of the GRSC fired action potentials in response to cortico-cortical inputs, and 2) there were monosynaptic connections between L5 and L2/3 pyramidal neurons that could cause the disynaptic responses in LS neurons.

We selected for recording pyramidal neurons of the upper part of L5b because their responses were larger than those laying in the lower half of L5b; these neurons show the standard pyramidal cell morphology. Also, these neurons were relatively easy to identify, due to their characteristic morphology (thick-tufted apical dendrite) and their firing pattern (Figure 8.1). Compared with GRSC pyramidal neurons in L2, those in L5 of the GRSC has a more positive resting membrane potential, and a lower input resistance. In this type of neuron, it has been described that even with a depolarizing current just above threshold, the latency of the first action potential is shorter than that of LS neurons; also, these neurons show adaptation during repetitive firing and lower maximum firing frequencies (Sempere-Fernàndez et al., 2019). It is important to note that in these experiments (similarly to the experiments recording the IPSCs described below) there were few LS neurons that showed synaptic responses; LS neurons not showing synaptic responses were included as having 0 mA peak amplitude, but in these neurons no latency could be measured and for this reason in Figures 8.4 and 8.5 the number of LS neurons having latency is lower than the number of LS neurons having peak amplitude.

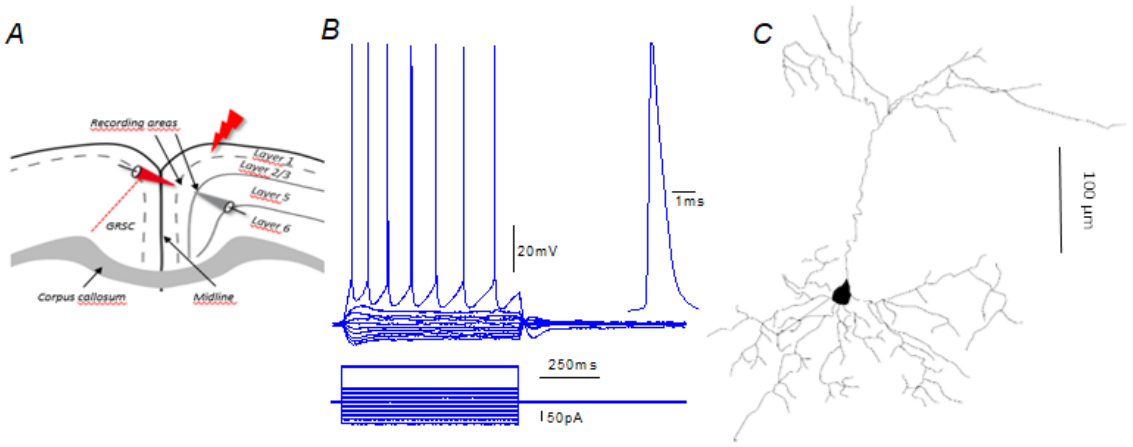

Figure 8.1. Firing pattern and morphology of pyramidal neurons recorded in L5 of the GRSC.

(A) Coronal drawing of the GRSC cortex of the mouse indicating the recording area, in this case in L5. The dotted red line shows the approximate limit between the GRSC and the dorsal dysgranular RSC. This limit has been set according to Vogt & Paxinos, 2014. **(B)** Responses to hyper- and depolarizing current pulses of pyramidal neurons recorded in L5 of the GRSC. Inset: action potential shown at larger time scale. Scale bars in the right apply to the panel recording in the three panels. **(C)** Neurolucida drawing of L5 pyramidal neuron with its scale bar of 100 µm.

To check for the possibility that the small disynaptic responses recorded in L2/3 LS neurons were originated in L5 pyramidal neurons (which fire strongly to contralateral inputs: Sempere-Fernàndez et al., 2019) we made a series of simultaneous recordings in L2/3 and L5 pyramidal neurons to look for the possibility of L5 to L2/3 synaptic

connections. However, we did not find any interconnection between L2/3-5: 0 out of 33 pairs formed by LS - L5 pyramidal neurons and 0 out of 17 pairs formed by non-LS - L5 pyramidal neurons. This finding is against the possibility that the disynaptic responses recorded in LS neurons were originated in L5 pyramidal neurons responding to the incoming stimuli.

From the above mentioned recordings (simultaneous paired recordings) we also analyzed and compared the synaptic responses to ipsi and contralateral stimulation; these data are shown in Figures 8.2 (ipsilateral stimulation) and 8.3 (contralateral stimulation). In both figures panel A shows a sketch of the experiment, panel B shows examples of recording pairs, and panels C and D show the values of EPSC peak amplitude and onset latency of L2/3 LS – L5 pyramidal neuron pairs and L2/3 non-LS – L5 pyramidal neuron pairs.

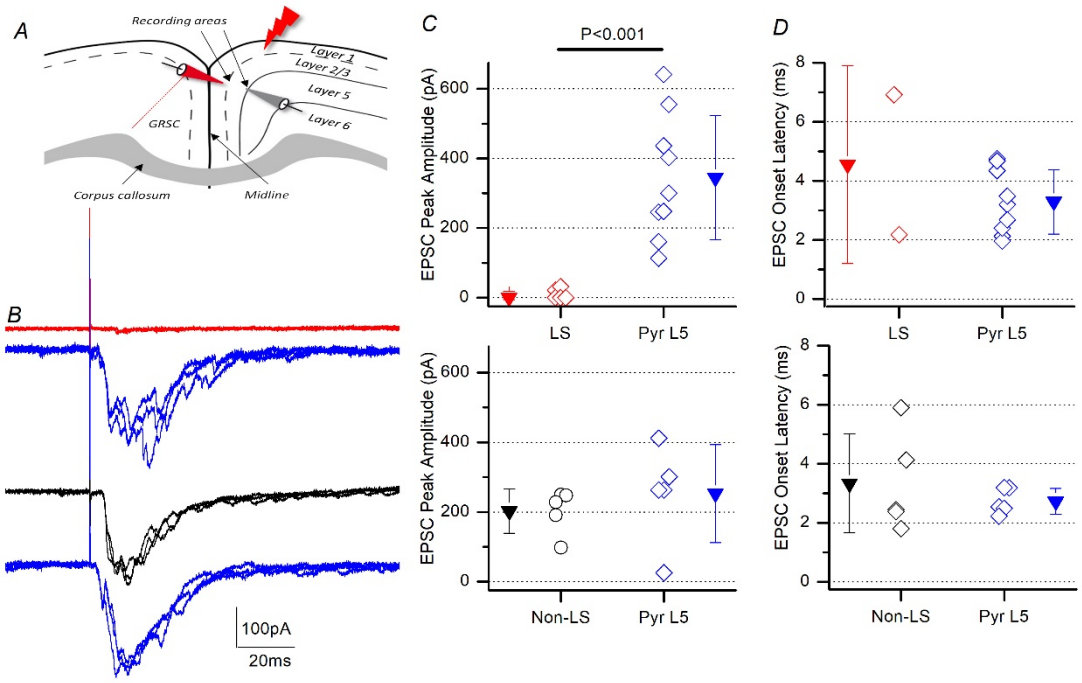

Figure 8.2. Excitatory synaptic currents evoked by ipsilateral electrical stimulation in simultaneous paired recordings between L2/3 pyramidal neurons and L5 pyramidal neurons of the GRSC.

(A) Drawing of a coronal slice from the GRSC showing the arrangement of recording and stimulation electrodes for ipsilateral stimulation and simultaneous recording of L2/3 and L5 neurons. **(B)** Examples of EPSCs recorded in response to ipsilateral electrical stimuli applied at 1.2 mm from the both types of recorded pairs of neurons, three consecutive sweeps superimposed in each panel: a LS neuron (red traces) with a L5b pyramidal neuron (blue traces); and a non-LS neuron of L2/3 with a L5b pyramidal neuron (blue traces). **(C)** peak amplitude and **(D)** latency of the EPSCs recorded in LS pyramidal neurons (red symbols; n=9 and 2 respectively),

non-LS pyramidal neurons (black symbols; n=5), and L5 pyramidal neurons (blue symbols; n=9).

In response to ipsilateral stimulation, the average peak amplitude of the EPSC was larger in L5b pyramidal neurons than in L2/3 LS neurons (344.71±177.7 pA, n=9 versus 5.9±11.99 pA, n=9; paired t test $p<0.001$) (Figure 8.2C upper panel). The average onset latency of the responses recorded in upper L5b pyramidal neurons and L2/3 LS neurons was similar (Figure 8.2D upper panel) (3.29±1.09 ms, n=5 versus 4.75±3.35 ms, n=2); however, the number of neurons responding to ipsilateral stimuli was very low (only two neurons) and this makes this result not absolutely clear because. This finding of few responses in LS neurons was similar to the finding reported above. When comparing non-LS L2/3 pyramidal neurons and upper L5b pyramidal neurons from neuron pairs, the average EPSC peak amplitude of the responses recorded in L5 pyramidal neurons and in non-LS neurons was similar (Figure 8.2C, lower panel) (252.82±140.80 pA, n=5 versus 202.64±63.17 pA, n=5). The average latency of the responses recorded in L5 pyramidal neurons and in L2/3 non-LS neurons was also similar (Figure 8.2D, lower panel; 2.73±0.44 ms, n=5 versus 3.34±1.67 ms, n=5).

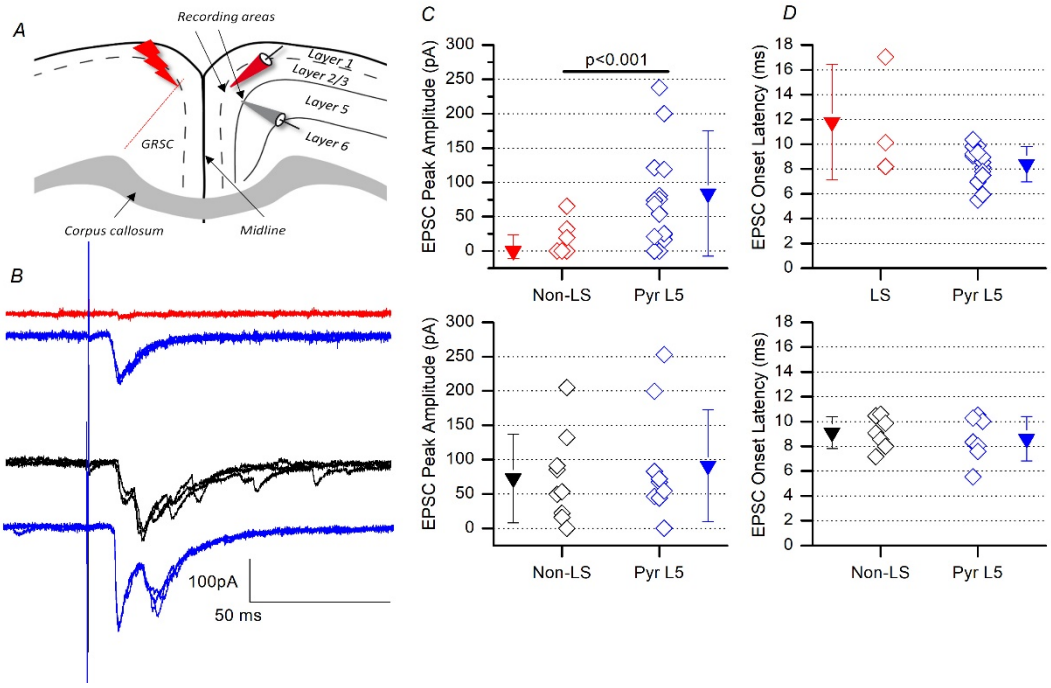

Figure 8.3. Excitatory synaptic currents evoked by contralateral electrical stimulation in simultaneous paired recordings between L2/3 pyramidal neurons and L5 pyramidal neurons of the GRSC.

(A) Drawing of a coronal slice from the GRSC showing the arrangement of recording and stimulation electrodes for contralateral stimulation. **(B)** Examples of recorded EPSCs in response to contralateral electrical stimuli applied at 1.2 mm from the both types of recorded pairs of neurons: one type of pair from non-LS neuron (black traces) versus L5b pyramidal neuron (blue traces), and another type of pair from LS neuron (red traces) versus L5b pyramidal neuron (blue traces); three consecutive sweeps superimposed in each panel. **(C)** Peak amplitude and **(D)** latency of the recorded EPSCs in LS (red symbols; n=18 and 3 respectively) and L5 pyramidal neurons (blue symbols; n=18) and in non-LS pyramidal neurons (black

symbols; n=9 and 7 respectively) and L5 pyramidal neurons (blue symbols; n=9 and 7 respectively).

In response to contralateral stimulation, the average of EPSCs peak amplitude was larger in L5b pyramidal neurons than in L2/3 LS neurons too (83.79 ±91.31 pA, n=9 versus 6.50±17.02 pA, n=9; paired t test $p<0.001$) (Figure 8.3C upper panel). If we look at the mean of average of onset latency from the responses recorded in upper L5b pyramidal neurons was similar than in L2/3 LS neurons (Figure 8.3D upper panel) (8.39±1.42 ms, n=5 versus 11.79±4.64 ms, n=5), but we only got three responses of LS pyramidal neurons. In this case again, these results were not clear because we also need to increase the number on LS pyramidal neurons recorded to get more LS responses and then compare them. Our problem was that just few neurons of the whole sample responded to the stimulus in all the experiments. When comparing non-LS L2/3 pyramidal neurons and upper L5b pyramidal neurons from neuron pairs, the average of EPSCs peak amplitude of the responses recorded in L5 pyramidal neurons was similar than in non-LS neurons (Figure 8.3C, lower panel) (91±81.21 pA, n=5 versus 72.68±64.8 pA, n=5). The average latency of the responses recorded in L5 pyramidal neurons was similar than in non-LS neurons too (Figure 8.3D, lower panel) (8.61±1.69 ms, n=5 versus 9.09±1.28 ms, n=5).

In the case of EPSC peak amplitudes of LS and non-LS pyramidal neurons compared to L5b pyramidal neurons, we obtained almost the same results than recorded pairs of L2/3-2/3, these numbers could mean that these type of pyramidal neurons are not in the same local circuit and we suppose that they play different roles with different functions.

8.1.1. Inhibitory responses in L2/3 and L5 pyramidal neurons

In neuron pairs formed by a L2/3 pyramidal neuron and a L5b pyramidal neuron we studied also the feed forward inhibitory responses evoked by cortico-cortical axons and the E/I balance.

The IPSCs evoked in simultaneously recorded pairs of neurons in response to ipsilateral electrical stimuli applied at 1.2 mm of the recorded neurons or to contralateral electrical stimuli were measured at a holding potential 0 mV (Figures 8.4 and 8.5, respectively). It is important to note that in these experiments (similarly to the experiments recording the EPSCs described above) there were few LS neurons that showed synaptic responses; LS neurons not showing synaptic responses were included as having 0 mA peak amplitude, but in these neurons no latency could be measured and for this reason in Figures 8.4 and 8.5 the number of LS neurons having latency is lower than the number of LS neurons having peak amplitude.

The properties of the IPSCs recorded in response to ipsilateral stimulation are shown in Figure 8.4. IPSCs peak amplitude was larger in L5b pyramidal neurons than in LS pyramidal neurons (Figure 8.4C, upper panel) (611.21±319.73 pA, n=9 versus 3.25±9.76 pA, n=9 and 1 respectively). In contrast, IPSC peak amplitude was similar in non-LS and L5 pyramidal neurons (Figure 8.4C, lower panel) (608.62±466.54 pA, n=5 versus 381.32±260.90 pA, n=5). In pairs formed by an LS and L5b pyramidal neuron, the average of onset latency from the responses recorded in L5b pyramidal neurons was 4.39±1.17 ms (n=9), while in the only LS neuron that showed an IPSC the latency was 7.58 ms (n=1). In pairs formed by a non-LS and and L5 pyramidal neuron the average onset latency was similar in both neuron types (non-LS 4.55±0.68 ms, n=5; L5 5.16±2.41 ms, n=5).

Since we only had the latency of one LS pyramidal neuron responses, we could not say that these values showed that IPSC recorded in LS pyramidal neurons were disynaptic, however it was 3.5 ms longer than the average of IPSCs latency of L5b pyramidal neurons. It would be interesting try to get more LS responses in order to measure more latency values and compare them.

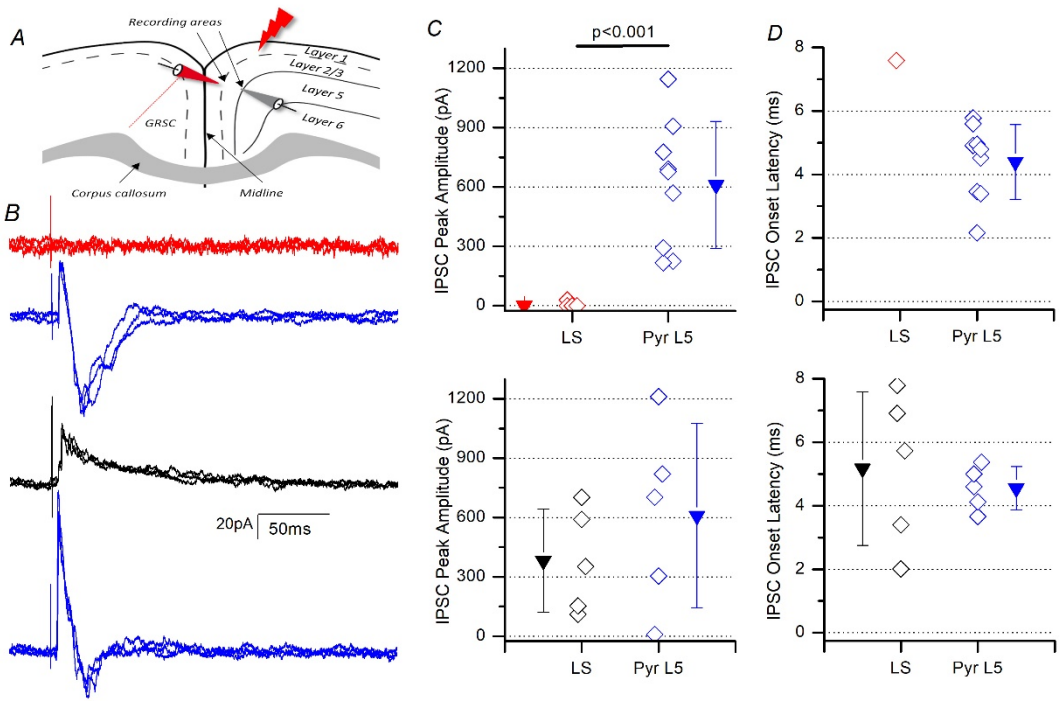

Figure 8.4. Inhibitory synaptic currents evoked by ipsilateral electrical stimulation in simultaneous paired recordings between L2/3 pyramidal neurons and L5 pyramidal neurons of the GRSC.

(A) Drawing of a coronal slice from the GRSC showing the arrangement of recording and stimulation electrodes for ipsilateral stimulation. **(B)** Examples of recordings of feed-forward IPSCs evoked in neuron pairs, three superimposed sweeps in each panel: a LS neuron (red traces) with a L5b pyramidal neuron (blue traces); and a non-LS neuron of L2/3 with a L5b pyramidal neuron (blue traces). The IPSCs were recorded at a holding potential 0 mV responding to ipsilateral electrical stimuli at 1.2 mm from recorded neuron pairs, three consecutive superimposed sweeps are shown in panel B, a non-LS neuron (black traces) with L5

pyramidal neuron (blue traces), and a LS neuron (red traces) with L5 pyramidal neuron (blue traces); three consecutive sweeps superimposed in each panel. **(C)** Peak amplitude and **(D)** latency of the IPSCs recorded in LS (red symbols; n=9 and 1) and L5 (black symbols; n=9) pyramidal neurons, in non-LS pyramidal neurons (black symbols; n=5) and L5 pyramidal neurons (black symbols; n=5).

Figure 8.5 shows the results of the recordings of feed-forward IPSCs evoked in neuron pairs in response to contralateral stimulation. The IPSCs were recorded at a holding potential of 0 mV recorded in response to electrical stimuli applied to the homotopic L2/3 of the contralateral hemisphere from both types of simultaneously recorded pairs of neurons: non-LS pyramidal neurons with upper L5b pyramidal neurons, and LS pyramidal neurons with upper L5b pyramidal neurons. Regarding peak amplitude and onset latency of the IPSCs recorded in LS and upper L5b, the average IPSC peak amplitude of the responses recorded in upper L5b pyramidal neurons was larger than in LS pyramidal neurons (Figure 8.5C upper panel) (159.56 ± 235.99 pA, n=10 versus 13.18±41.47 pA, n=10). However, the latency of the responses recorded in upper L5b and LS pyramidal neurons were similar (Figure 8.5D upper panel) (11.44 ± 1.41 ms, n=5 versus 10.08 ms, n=1). On the other hand, in the case of non-LS pyramidal neurons and upper L5b pyramidal neurons, the average of EPSC peak amplitude of the responses recorded in L5 pyramidal neurons was similar than in non-LS neurons (Figure 8.5C lower panel) (188 ± 293.96pA, n=6 versus 17.48 ± 24.03 pA, n=6). The onset latency of the

responses recorded in upper L5b and in non-LS neurons was similar too (Figure 8.5D lower panel) (12.07±1.86ms, n=3 versus 12.49±2.49 ms, n=3).

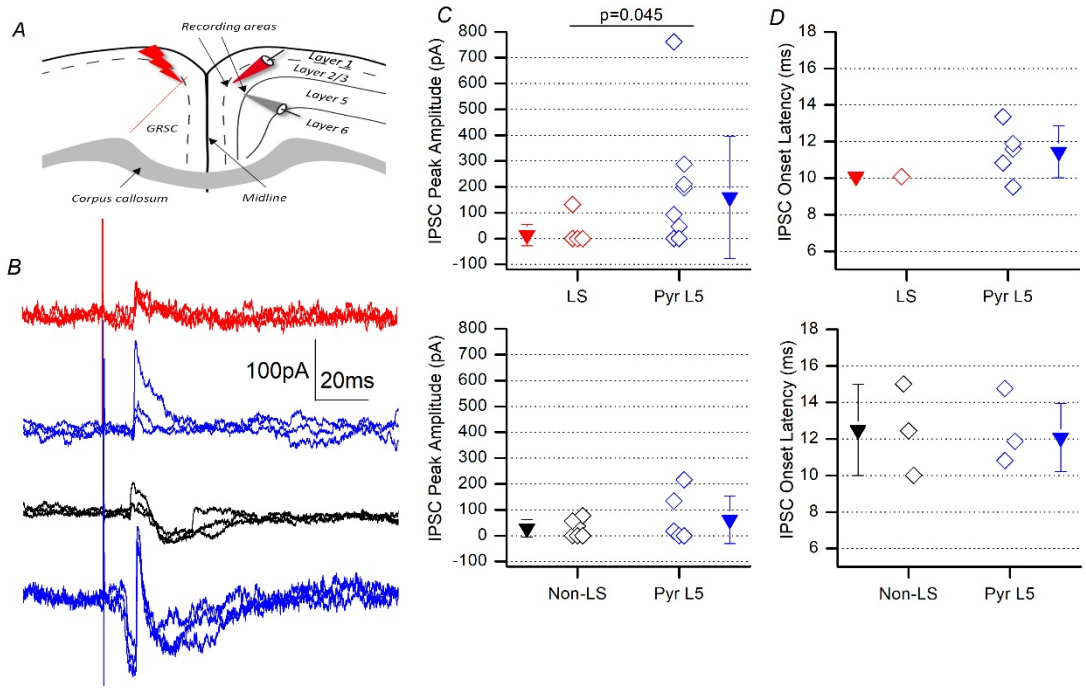

Figure 8.5. Inhibitory synaptic currents evoked by contralateral electrical stimulation in simultaneous paired recordings between L2/3 pyramidal neurons and L5 pyramidal neurons of the GRSC.

(A) Drawing of a coronal slice from the GRSC showing the arrangement of recording and stimulation electrodes for contralateral stimulation. **(B)** Examples of recordings of feed-forward IPSCs evoked in a neuron pairs. The IPSCs were recorded at a holding potential of 0 mV in response to contralateral electrical stimuli applied at the homotopic side of the other hemisphere from the both types of recorded pairs of neurons: non-LS neuron (black traces) with L5 pyramidal

neurons (blue traces), and a LS neuron (red traces) with L5 pyramidal neuron (blue traces); three consecutive sweeps superimposed in each panel. **(C)** Peak amplitude and **(D)** latency of the IPSCs recorded in LS (red symbols; n=10 and 1 respectively) and L5 (black symbols; n=10 and 5 respectively) pyramidal neurons and in non-LS pyramidal neurons (black symbols; n=6 and 3 respectively) and L5 pyramidal neurons (blue symbols; n=6 and 3 respectively).

8.1.2. Comparison of the E/I balance in pyramidal neurons of L2/3 and L5

As in the experiments of pairs formed by L2/3 LS and non-LS pyramidal neurons, E/I balance was measured from the excitatory and inhibitory conductance of the synaptic responses evoked by either ipsi- or contralateral stimulation (Figures 8.6 and 8.7) in neuronal pairs formed by L2/3 versus L5 pyramidal neurons. Conductance was measured from the peak of the EPSCs recorded at -70 mV, a potential close to the equilibrium potential for chloride in our experimental conditions; and from the peak of the inhibitory component recorded at 0 mV, a potential close to the reversal potential of AMPA receptors.

Values of the excitatory and inhibitory conductances of the responses to ipsilateral stimulation recorded from the different type of neurons studied are shown in Figures 8.6A and B. In LS neurons (n = 10, only 2 with excitatory conductance and 1 with inhibitory conductance because of the lack of response in 8 out of them) the excitatory conductance was 0.36 ± 0.07 nS and the inhibitory conductance was 0.42 nS. In non-LS neurons (n = 5) the excitatory and inhibitory conductances were respectively 4.68 ± 0.1.87 nS and 5.44 ± 3.73 nS. In upper L5b pyramidal neurons (n = 15) the excitatory and inhibitory conductances were respectively 4.42 ± 1.93 nS and 10.08 ± 5.49 nS, ($p = 0.002$, Mann-Whitney rank sum test); note that, in contrast to L2/3 pyramidal neurons (both LS and non-LS), in upper L5 pyramidal neurons the excitatory conductance was lower that the inhibitory conductance being statistically different between non-LS pyramidal neurons and upper L5 pyramidal neurons ($p = 0.009$, Mann-Whitney rank sum test). From these values of excitatory and inhibitory conductance the E/I balance were (Figure 8.6C): LS pyramidal neurons 0.738 (n = 1), non-LS pyramidal neurons 1.16 ± 0.84 (n = 5), and upper L5b pyramidal neurons 0.52 ± 0.30 (n = 14). Mostly, the average E/I balance was <1 or very close to 1 in LS, non-LS and upper L5b pyramidal neurons (Figure 8.6C). Our data shows that upper L5 pyramidal neurons had a smaller E/I balance than L2/3 non-LS neurons; however, we were unable to compare the E/I balance from LS neurons due to the very small number of these neurons that showed synaptic responses.

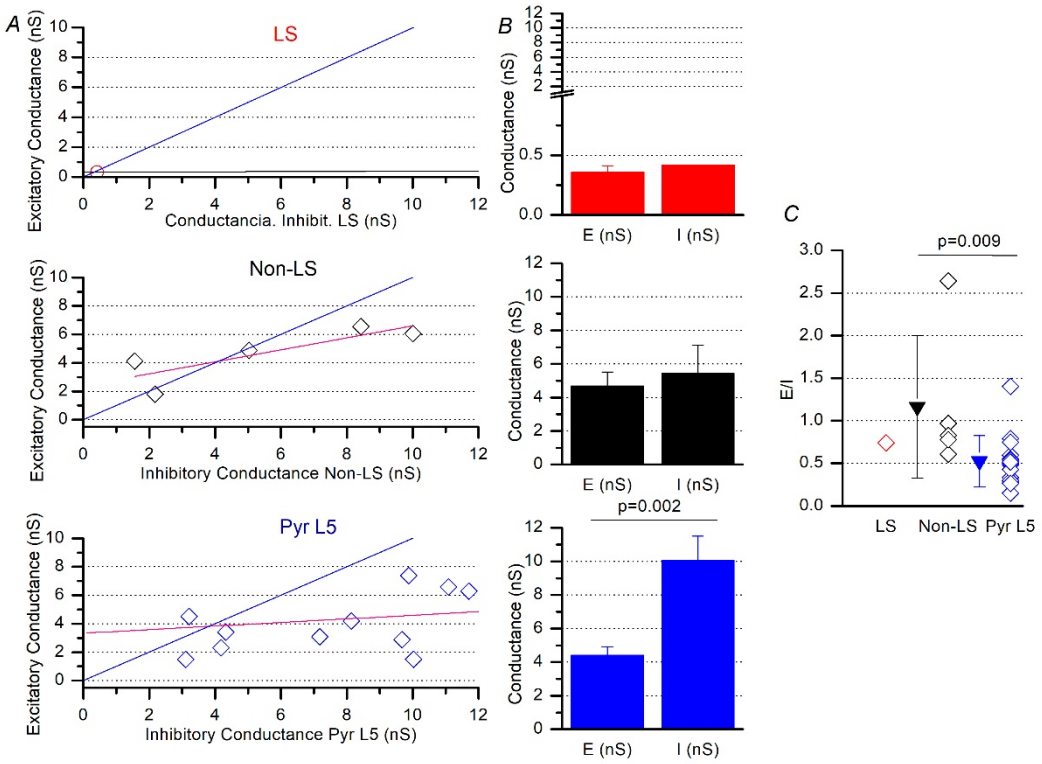

Figure 8.6. Excitatory/inhibitory balance of the responses evoked by ipsilateral stimuli.

(A) EPSCs peak conductance values versus IPSCs peak conductance values measured in individual neurons (LS red symbols, non-LS black symbols, upper L5 blue symbols). Linear fit to data of non-LS pyramidal neurons: pink line, slope: 0.421, R^2: 0.601; linear fit to data of upper L5 pyramidal neurons: pink line, slope: 0.126, R^2: 0.036. The blue line is the identity line. **(B)** Values of excitatory and inhibitory conductance from the different types of pyramidal neurons studied: LS n=2 and 1; non-LS n=5; L5 pyramidal neuron n=14. Notice the break in upper panel B on vertical axis in order to enlarge the vertical scale. **(C)** E/I balance measured in LS (n = 1), non-LS (n = 5), and L5 pyramidal neurons (n=15). Notice the break in panel B due to the small LS conductance in order to appreciate it better.

Values of excitatory and inhibitory conductance and the E/I balance of the responses evoked by contralateral stimuli are shown in Figure 8.7. In LS neurons (note that from a total of 27 recorded LS pyramidal neurons only 3 had responses, n=3) the excitatory conductance was 0.142 ± 0.37 nS and the inhibitory conductance was 0.140 ± 0.43 nS. In non-LS neurons (from 13 recorded non-LS pyramidal neurons only 3 had response, n=3) the excitatory and inhibitory conductances were respectively 0.99 ± 0.85 nS and 0.07 ± 0.16 nS. Finally, in upper L5b pyramidal neurons (from 35 recorded upper L5 pyramidal neurons only 14 had response, n=14) the excitatory and inhibitory conductances were respectively 1.76 ± 1.72 nS and 1.640 ± 3.37 nS. For contralateral stimulation, the E/I balance measured in three types of neurons is shown in Figure 8.7C; LS 0.97 ± 0.89 (n=3), non-LS 7.58 ± 9.45 (n=3), and upper L5b pyramidal neurons 1.24 ± 1.21 n=14. In the case of contralateral stimulation, mostly the E/I balance was >1 in non-LS neurons and upper L5b pyramidal neurons, but it was close to 1 in LS pyramidal neurons and there was no difference in E/I balance among them. These values of E/I balance are explained by the finding that inhibitory conductance was bigger than excitatory conductance in non-LS pyramidal neurons, in contrast to LS and upper L5 pyramidal neurons that they had approximately the same values between excitatory and inhibitory conductance.

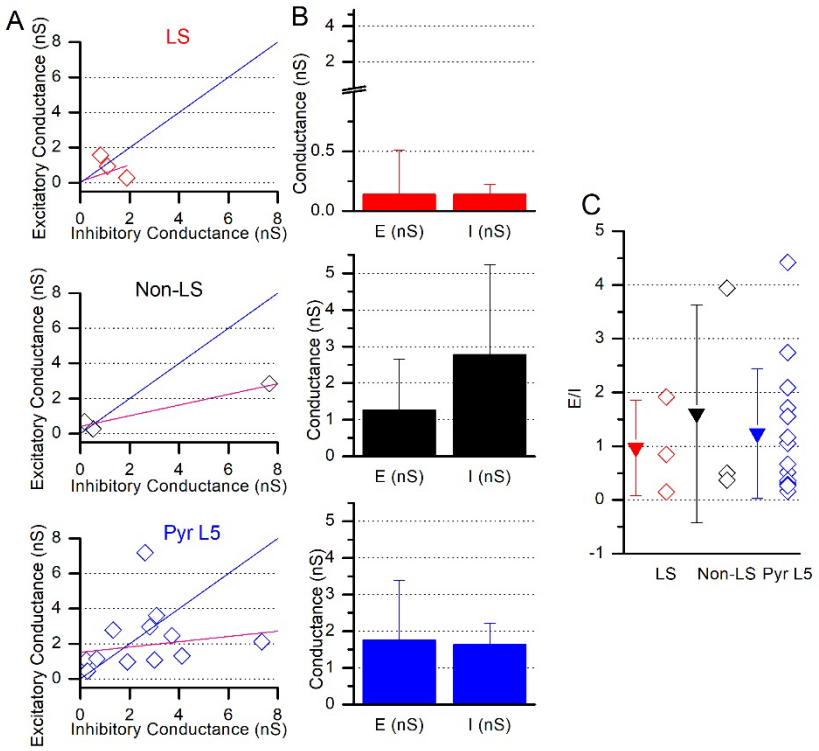

Figure 8.7. Excitatory/inhibitory balance of the responses evoked by contralateral stimuli.

(A) Values of EPSC peak conductance versus IPSC peak conductance measured in individual neurons (LS red, non-LS black symbols, upper L5 pyramidal neurons blue symbols). Linear fit to data from non-LS neurons: pink line, slope: -0.456, R^2: 0.279; linear fit to data from LS neurons: pink line, slope: 0.470, R^2: -0.09; linear fit to data from upper L5 pyramidal neurons: pink line, slope: 0.150, R^2: 0.070. The blue line is the identity line. **(B)** Values of excitatory and inhibitory conductance from the different type of neurons studied (mean±SD): LS (red) n=3; non-LS (black) neurons n=3; and upper L5b pyramidal neurons (blue) n=14. Notice the break in upper panel B on vertical axis in order to enlarge the vertical scale. **(C)** E/I

balance (mean±SD) measured in LS (red) n=3, non-LS (black) neurons n=3; and upper L5b pyramidal neurons (blue) n=14.

8.2. SECTION 2. Role of $GABA_B$ receptors in the local neuronal circuits of the GRSC L2/3

8.2.1. Inhibitory responses recorded in LS pyramidal neurons during the propagation of epileptiform discharges

In slices bathed with mACSF and in the presence of 10 μm Bicuculline (a blocker of $GABA_A$ receptors; see material and methods above) there are generated large oscillatory epileptiform discharges that propagated along L2/3 in response to the stimulation of L1 (see Results section). We observed the presence of inhibitory components as part of these discharges in both LS and non-LS neurons; one example of these responses, in an LS neuron, is shown in Figure 8.8. The voltage-dependence of the synaptic responses recorded during the propagation of epileptiform discharges is shown in Figures 8.8A and B. When studied in detail, we noted that the synaptic responses recorded in LS neurons had a late component that reversed at approximately -70 mV (Figure 8.8C). This reversal potential was similar to the equilibrium potential of Chloride calculated in our experimental conditions (Cl^-_{Erev} = -68 mV) and less negative than the

equilibrium potential for potassium (K^+_{Erev} = -87 mV): this shows the presence of an inhibitory component dependent on $GABA_A$ receptors.

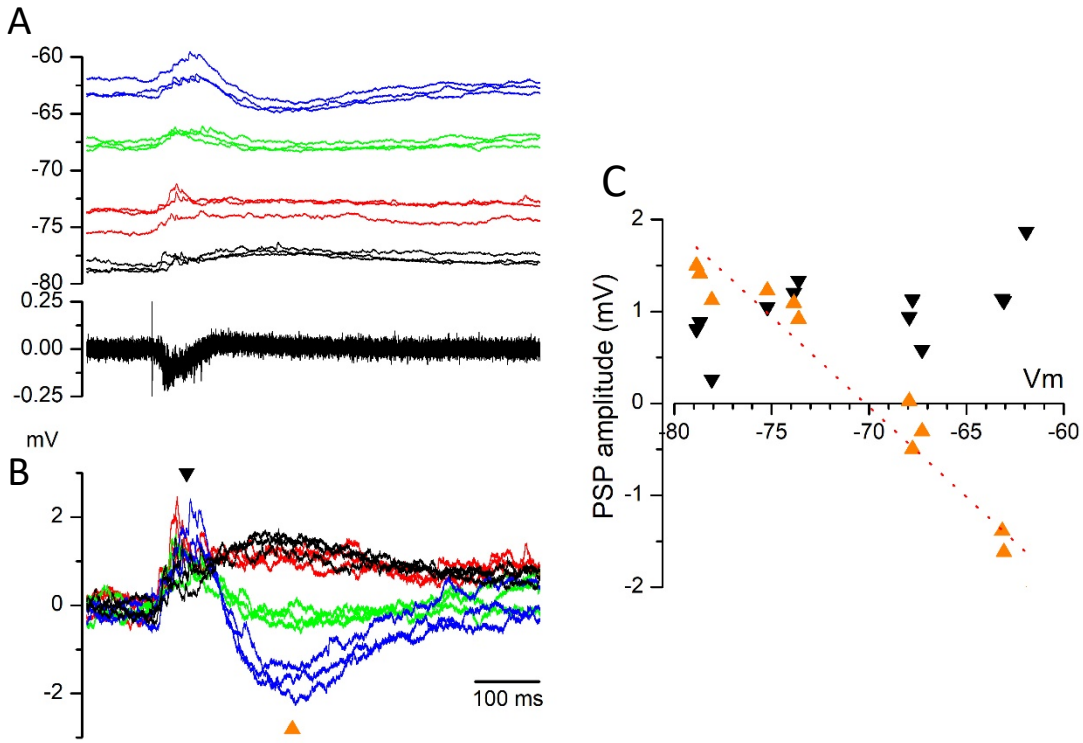

Figure 8.8. Voltage-dependence of the synaptic responses recorded in LS pyramidal neurons during the propagation of epileptiform discharges.

(A) Synaptic responses obtained in a LS neuron during the propagation of epileptiform discharges recorded at different membrane potentials. **(B)** Same recordings of panel A but superimposed and shown at an enlarged vertical scale to show the voltage-dependence of the synaptic responses. The amplitude of the synaptic responses respect to the baseline was measured at the peak of the initial excitatory component (black triangles) and at the peak of the late component (orange triangles). **(C)** Peak amplitude of the early (black triangles) and late (orange triangles)

components of the recordings shown in C plotted respect to the membrane potential; the dotted red line is the linear regression of the amplitudes of the late component, showing a reversal potential close to -70 mV. The early excitatory component did not show a clear voltage dependence in range of membrane potential studied.

8.2.2. Effects of $GABA_B$ receptor blockers

The late component that reversed at -70 mV suggests the presence of a large inhibitory component mixed with the EPSPs in LS neurons, which could be the cause of the small subthreshold amplitude of these responses in LS neurons. Since the presence of Bicuculline should block, at least partially, the inhibition due to $GABA_A$ receptors, we checked the possible presence of an additional inhibitory component due to the activation of $GABA_B$Rs. This was done using two specific blockers of $GABA_B$Rs: CGP55845 and CGP52432; these two blockers had the same effect either on LS or non-LS neurons. Therefore, in Figure 8.9 we show the results obtained with either CGP55845 or CGP52432 pooled together because of this same effect. CGP 55845 (5μM) or CGP 52432 (10μM) were added to the perfusion solution (mACSF). The different concentrations were due to the Tocris recommendation on their datasheets to use it (Tocris, Bio-Techne R&D Systems, S.LU).

Figure 8.9 shows the effect of $GABA_B$ blockers on LS neurons and Figure 8.10 on non-LS neurons. In each neuron, the synaptic responses recorded during the propagation of epileptiform discharges were recorded for an initial period of 5 min in control solution with Bicuculline (10μM); then CGP 55845 (5μM) or CGP 52432 (10μM) was added to the extracellular solution during 10 min and finally the $GABA_B$ blocker was washed out. The effect of CGP 55845 or CGP 52432 was not fully reversed after 25 min of wash out, preventing us to record more than one cell from each slice. In these recordings we noticed that the hyperpolarization present in LS pyramidal neurons disappear in the presence of $GABA_B$ blockers (Figure 8.9), leading to the firing of action potentials by a previously silent neurons (Figure 8.9A, B). This suggest that in LS neurons the $GABA_B$ component was causing, at least in part, the small excitatory synaptic responses recorded in these neurons. In non-LS neurons (Figure 8.10) the $GABA_B$ blockers did increase the action potential firing during epileptiform discharges (Figure 8.10A, B) but the effect on the initial part of the synaptic response was smaller and delayed in time (Figure 8.10C); however, further experiments are necessary to confirm this observation.

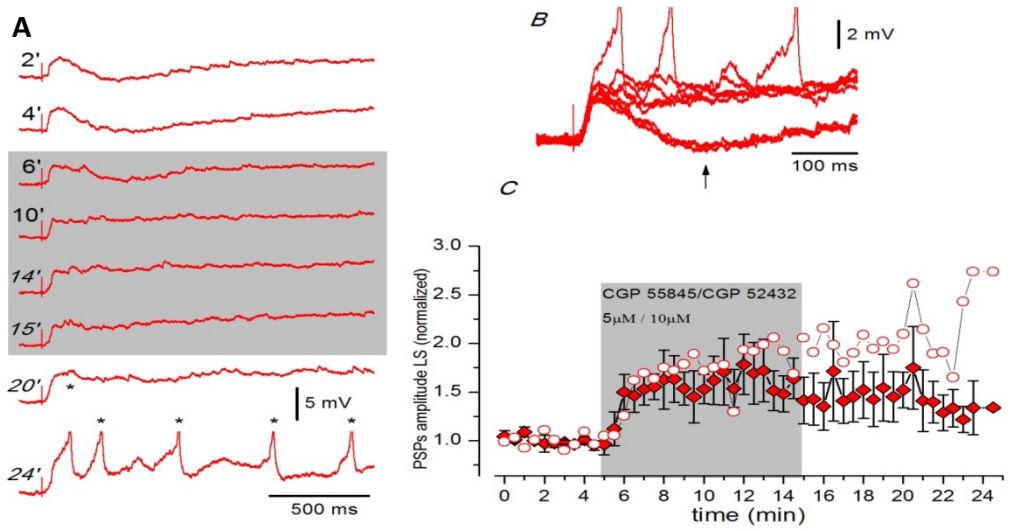

Figure 8.9. Effect of $GABA_BR$ blockers in LS pyramidal neurons.

(A) Recordings of the synaptic responses obtained in a LS neurons during the propagation of epileptiform activity in control conditions (recordings taken at 2' and 4'), during the application of 5 μM CGP 55845 (recordings at 6' – 15') and during the washout period (recordings at 20' and 24'). The synaptic response increased in amplitude and finally evoked the firing of action potentials, shown truncated (and marked with asterisks) at the 24' trace. **(B)** Same recordings than panel A shown superimposed and at an enlarged vertical scale. **(C)** Normalized amplitudes (respect to average values during the control period) of the late component of the synaptic response in LS neurons; the amplitude was measured respect to the baseline at the time shown in panel B by an arrow. White circles show the values of the neuron shown in panels A and B, and red diamonds show the mean ± S.E.M. of the LS neurons studied (pooling the data obtained with CGP 55845 n=3 and CGP 52432 n = 5).

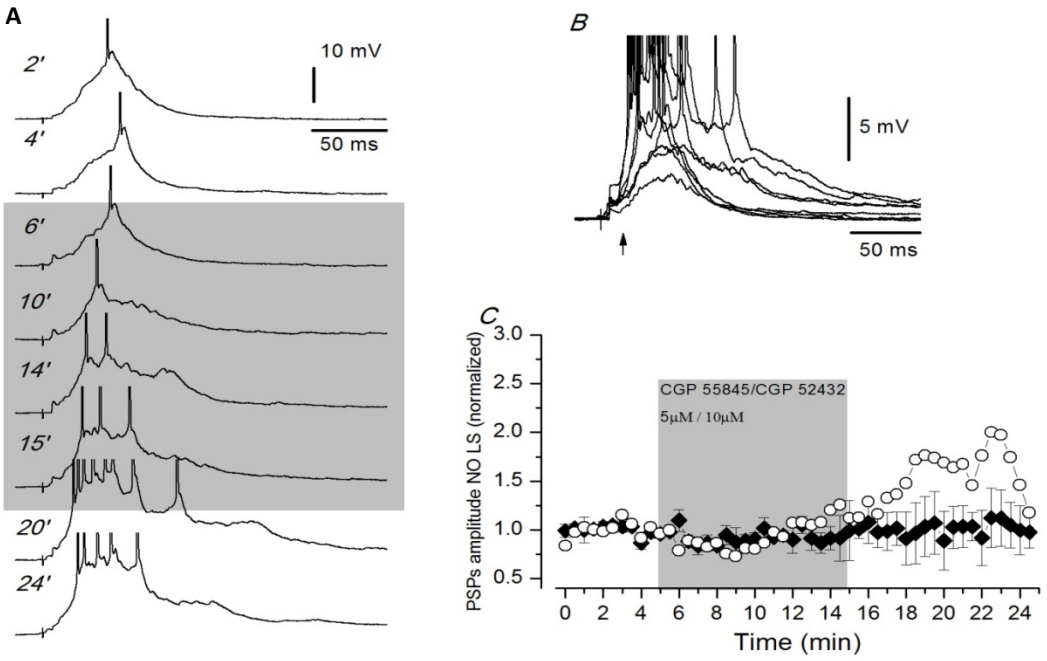

Figure 8.10. Effect of $GABA_BR$ blockers in non-LS pyramidal neurons.

(A) Recordings of the synaptic responses obtained in a non-LS neurons during the propagation of epileptiform activity during the control period (recordings taken at 2' and 4'), during the application of 5 μM CGP 55845 (recordings at 5' – 15') and during the washout period (recordings at 20' and 24'). **(B)** Same recordings than panel A shown superimposed and at an enlarged vertical scale. **(C)** Normalized amplitudes (respect to average values during the control period) of the late component of the synaptic response in non-LS neurons; the amplitude was measures respect to the baseline at the time shown in B by an arrow. White circles show the values of the neuron shown in panels A and B, and red diamonds show the mean ± S.E.M. of the non-LS neurons studied (pooling the data obtained with CGP 55845 n =1 and CGP 52432 n = 4).

Figure 8.11 shows the comparison of the effects of $GABA_B$ blockers on LS and non-LS pyramidal neurons; the data in this figure is reproduced from the data in Figures 8.9C and 8.10C. Comparing the control period (using 10 sweeps, 5 minutes) versus CGP application (last 10 sweeps, 5 minutes), we had statistical differences in both populations of pyramidal neurons (LS cells: mean and standard deviation for control period 0.992±0.972 and CGP application 1.588±1.537, p-value<0.001 n=10); and non-LS cells: mean and standard deviation for control period 1.000±0.0527 and CGP application 0.944±0.0578, p-value=0.035 n=10) proving that in both cases there is an effect of CGP application. The interesting point is that blocking $GABA_B$Rs let LS pyramidal neurons fire action potentials activating then the regulated local neuronal circuit. If you compare the normalize averages of both time frames (control and CGP) it goes from 0.983 to 1.538 in the LS pyramidal neurons, and in the non-LS pyramidal neurons the averages go from 0.996 to 0.928). This indicates that the difference in the LS cells is much greater and it seems that it has a more relevant role than in the non-LS cells where only the increase in amplitude or frequency is seen, but they fire anyway, while in the LS pyramidal neurons the $GABA_B$Rs have a regulatory role since they go from not firing to fire when you block

these receptors. So that, we suggest an important and specific role of $GABA_BRs$ on LS pyramidal neurons.

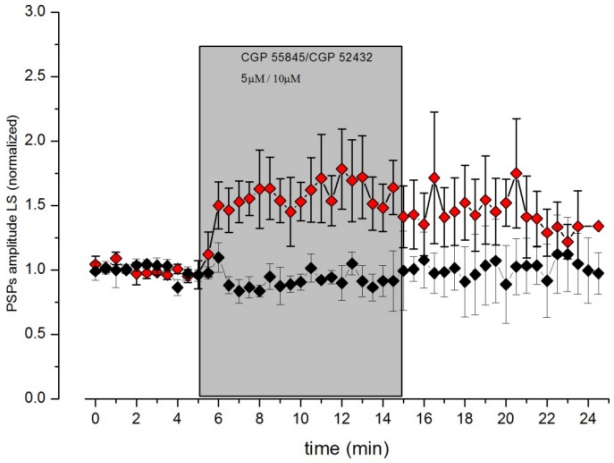

Figure 8.11. Comparison of the effect of $GABA_BR$ blockers on LS and non-LS pyramidal neurons.

For comparison between LS and non-LS neurons in this figure we show superimposed the same average data taken plotted in figures 8.9C and 8.10C; red symbols are for LS pyramidal neurons and black symbols for non-LS pyramidal neurons.

8.2.3. Currents evoked by the direct application of GABA on LS and non-LS pyramidal neurons

The above experiments using $GABA_BRs$ blockers suggest the presence of an inhibitory response caused by this type of receptors. To disclose the presence of responses caused by $GABA_BRs$ in LS neurons we recorded the currents caused by the direct activation of these receptors by direct GABA application; with this experiment we tried to isolate the membrane currents generated by $GABA_BRs$ and to analyze their properties. To do that we recorded the currents evoked in LS and non-LS neurons by the direct application of GABA on the recorded neuron. GABA was applied by pressure pulses (20 ms duration) delivered with a Picospritzer and using patch pipettes filled with 1 or 0.1 mM GABA dissolved in mACSF. First, we did some recordings using pipettes filled with mACSF in order to prove that there was no mechanical effect of the direct application of drugs by pressure pulses. Next, we added to the mACSF 10 μM CNQX (a competitive AMPA/kainate receptor antagonist) in order to block possible response due to glutamate receptors and isolate the currents carried by GABA Rs ($GABA_ARs$ and $GABA_BRs$) (Figure 8.12A). Then, we recorded currents evoked by GABA in different conditions (Figure 8.12A): mACSF + 10 μM CNQX (figure 8.12A) blocking the AMPA/kainite currents; mACSF + 10 μM CNQX + 10 μM CGP52432 (blocking $GABA_BRs$ and isolating $GABA_A$ currents; figure 8.12B), and mACSF + 10 μM CNQX + 20 μM Bicuculline (blocking $GABA_A$ receptors and isolating $GABA_B$ currents; figure 8.12C).

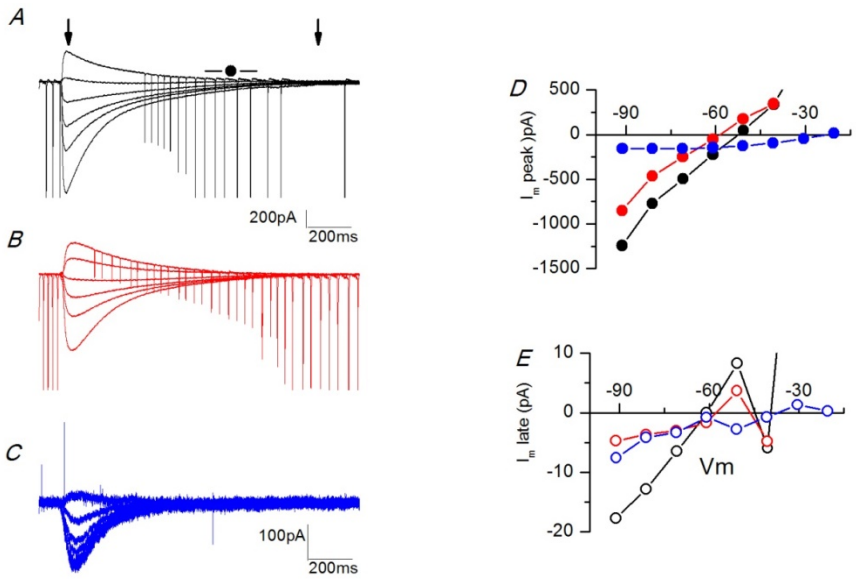

Figure 8.12. Membrane currents recorded in a LS pyramidal neuron evoked by the direct application of GABA. (A-C) Membrane currents recorded at different membrane potentials in mACSF + 10 µM CNQX (panel A), in mACSF + 10 µM CNQX + 10 µM CGP 52432 (panel B) and in mACSF + 10 µM CNQX + 20 µM Bicuculline (panel C). The pressure pulse that ejected GABA from the ejection pipette preceded in approximately 10 ms the onset of the currents. The current traces are shown superimposed respect to the baseline just before the onset of the currents. The downward deflections in A and B are action currents evoked by large depolarizing voltage pulses. A and B are from the same neuron. **(D)** Current measured at the peak (left arrow in A) in panels A (black symbols), B (red symbols) and C (blue symbols) plotted respect to the membrane potential. **(E)** Current measured at the end of the response (right arrow in A) in panels A (black symbols), B (red symbols) and C (blue symbols) plotted respect to the membrane potential.

We did this type of experiment in LS and non-LS neurons and the reversal potentials of the currents evoked by GABA in these conditions were calculated from the linear regression of the plot of the current versus the membrane potential, and the values obtained are given in table 1.

	mACSF	mACSF + Bic	mACSF + CGP
LS neurons	-55.6 ± 3.5 n = 7	-23.5 n = 1	-59.3 ± 1.7 n = 2
Non-LS neurons	-55.8 ± 4.4 n = 9	-26.2 n = 1	-56.5 ± 6.7 n= 4

Table 8.1. Reversal potentials (in mV) of the currents evoked by the application of GABA in LS and non-LS pyramidal neurons.

These data show the presence of a clear component due to the activation of $GABA_A$ receptors, which was blocked by Bicuculline and had a reversal close to the Cl^- reversal potential in our experimental conditions (-68 mV), but does not reveal any current caused by the activation of $GABA_B$Rs, since in the presence of CGP 52432 there was no change in the reversal potential of the GABA evoked currents. However, the

number of neurons studied was low, and we cannot also discard that the presence of small $GABA_B$ currents relative to very large $GABA_A$ currents, which should produce a very small change in reversal potential when blocked by CGP 52432. We do not know the origin of the small currents recorded in the presence of Bicuculline (Figure 8.12C) that had reversal potential of -23.5 or -26.2 mV; however, this experiment was done only in one LS and in one non-LS pyramidal neurons and this result was not conclusive.

Discussion

9. DISCUSSION

During this thesis project we have studied the electrophysiology of the pyramidal neurons of GRSC L2/3 in mice and their synaptic responses to cortico-cortical axons. We revealed the presence of two electrophysiological types of pyramidal neurons in the dorsal part of this cortical area: several neurons, about 60% of the whole sample, showed a prominent LS firing pattern similar to the pyramidal neurons of L2/3 of GRSC in the rat (Kurotani et al., 2013); these particular cells were classified as "LS pyramidal neurons". The remaining pyramidal neurons presented a RS pattern very similar to the pyramidal neurons located in L2/3 of other cortical areas, involving the dysgranular RAC (area 30; Sempere-Fernàndez et al., 2018) and were classified as "non-LS pyramidal neurons".

Since it was quite common to find neurons pairs formed by an LS pyramidal cell and a non-LS pyramidal cell whose soma was separated by less than 50 μm, we could say that our data from simultaneous paired recordings revealed that LS and non-LS pyramidal neurons were readily merged in the dorsal part of the GRSC. This neuron mixture proposes that the dorsal part of the GRSC is a transition area between the more ventral GRSC (where only are LS neurons in L2/3) and the dysgranular RSC placed dorsally, where only RS pyramidal neurons are found.

9.1. Classification of pyramidal neurons in L2/3 of the GRSC

We classified as a first step choosing the smaller pyramidal soma as LS pyramidal neuron and then we compared it using intracellular parameters as they are described in rat as a classificatory criterion (Kurotani et al., 2013). Moreover, we added more parameters to the list from the previous study. However, apart from statistical differences, we had a limitation because of the overlapped values in some cases. Fortunately, we found one parameter which was not overlapped in any case: the time to fire the first spike.

Additionally, we can complete and improve this classification using our cell reconstructions by Neurolucida software in order to quantify the morphological parameters such as soma, dendrites, arborizations of our cells, etc, by Imaris software afterwards as a next step. A good improvement would be to carry out quantitative analysis of these morphological characteristics.

9.2. Electrophysiological properties of LS pyramidal neurons and differences with non-LS pyramidal neurons in L2/3 of the GRSC

As we said above, in a previous study it has been said that there are a distinctive population of neurons in layers 2/3 of the rat RSC, with a common output, strong apical

dendritic bundling, and shared unusual firing properties (Kurotani et al., 2013). Similarly, we found the same population in layers 2/3 of the mice RSC at 14-22 postnatal days.

Our results showed a higher input resistance in LS neurons comparing to non-LS neurons in L2/3 of mice RSC. These values are comparable to those of Kurotani's laboratory in rat. On the one hand, the rat LS cells have an elevated input resistance too, but the value is higher than mice and, on the other hand, non-LS cells exhibit a similar value between both animal genus (Kurotani et al., 2013). Regarding to the duration of action potential at half amplitude (50%), we have obtained shorter values in LS cells and in non-LS neurons unlike the longer results in rat (Kurotani et al., 2013). Furthermore, we also found in mice more significant differences as duration of action potential at baseline being shorter in LS cells; the time to fire the first action potential by depolarizing pulses is longer in LS neurons than in non-LS neurons; the threshold is more positive in LS neurons than in non-LS neurons; the posthiperpolarization (measured from threshold to peak) is bigger in LS neurons than in non-LS pyramidal neurons; the adaptation in firing frequency (first versus last ISI at 2x rheobase) is smaller in LS pyramidal neurons than in non-LS neurons; and finally, the voltage sag from hyperpolarizing current injections is smaller too in LS pyramidal neurons, in fact, there is no voltage sag almost in these cells comparing to non-LS pyramidal neurons. Nevertheless, the most important measure is the time to fire the first spike because of being the only one without overlapped as it is said above.

It has been shown the presence of neurons presenting a LS firing pattern in other rodent cortical areas related to the RSC and involved in spatial formation processing. In the superficial layers of the presubiculum, where is reciprocally connected with the GRSC (Van Groen & Wyss, 1992), there are pyramidal-like neurons with a clear LS firing pattern (Aabbasi et al., 2013). In the medial entorhinal cortex, where connections from the RSC are received (Van Groen & Wyss, 1992), L2 non-stellate pyramidal-like neurons also present a LS firing pattern (Alonso & Klink, 1993). Finally, in the perirhinal cortex there have been reported small pyramidal neurons in L2/3 with LS firing pattern too (Faulkner & Brown, 1999); in this cortical area there are also LS neurons in L6, but not pyramidal in this case. Considering neurons showing a LS firing pattern could be involved in the integration of responses with distinct timing (Kurotani et al., 2013), in other words, these neurons could be part of neural circuits provided with specific timing capabilities for signal processing. A master student from our laboratory, did experiments regarding I_A, which is a fast-activating and inactivating outward K^+ subthreshold voltage activated current that activates at Vm=-50mV approximately and works against depolarization. It generates a change in membrane voltage enough to delay the action potential firing and generates the LS firing pattern. The I_A current is known to be a regulator of the repetitive action potential firing and membrane excitability in other neuron types and other cortical regions as we said to. Moreover, apart from persistent and transient inward currents, repetitive firing and the waveform of the action potential depends on the K^+ channels expressed in particular cell types. These K^+ channels have a principal role in determining the interspike interval and in that way in setting the neuron firing frequency.

Furthermore, they regulate the shape of action potentials too determining Ca^{2+} influx at presynaptic terminals. A good review of cellular signaling properties in microcircuits in 2005 (Toledo-Rodríguez et al., 2005) explained that Kv1, Kv2 and KV4 subfamilies are activated at membrane potentials under the spike threshold (low-voltage-activated, delayed and delayed-rectifying channels). Channels which are classified under the delayed-rectifying Kv3 subfamily activate only at membrane potentials well over the spike threshold. In addition, other types of K^+ channels are activated by intracellular Ca^{2+} (SK family channels), a combination of voltage and Ca^{2+} (BK channels), or Na^{2+} (Slo2 channels). But the most powerful intrinsic factor determining the frequency of firing neurons is the late afterhyperpolarization following each action potential. Deep and prolonged afterhyperpolarizations characterize neurons with low regular firing, while small afterhyperpolarizations favor high firing rates. Curiously, the expression of Kv3.4 and Kv3.1 also supports high-frequency firing, and could involve Kv2.1 in spike repolarization at high firing frequencies in some cells. Other correlations involve expression of A-type K^+ channel Kv4.2 with delayed firing onset and accommodation and expression of delayed-rectifier K^+ channel Kv1.1 with suttering and irregular spiking behavior (Toledo-Rodríguez et al., 2005). In other study, it was published that the excitatory interneurons interact to promote a burst, and its activity terminates in a predictable way. This research showed that the main cause is spike-train adaptation, resulting from activation of Ca^{2+}-dependent K^+ channels, which generates the post-spike after-hyperpolarization, which is the main determinant of firing frequency. The post-spike afterhyperpolarizations are summated, which results in a frequency adaptation that

is greater the large the post-spike afterhyperpolarizations. In addition, Ca^{2+} entry through NMDA channels leads to a general activation of Ca^{2+}-dependent K^+ channels, which promotes burst termination (Grillner et al., 2005). So that, this findings support the fact that the specific LS firing pattern due to K^+ channels let LS pyramidal neurons play a sizeable and precise role in these cortical circuits.

9.3. Innervation of LS and non-LS pyramidal neurons by cortico-cortical axons

Our finding that LS neurons had very different responses than non-LS neurons during the propagation of epileptiform discharges as it is shown in Figure 7.4 of our paper (Robles et al., 2020). This strongly suggests that both types of pyramidal neurons, while being closely placed in the dorsal part of the GRSC, had very different axonal afferences, since LS showed late small (always subthreshold EPSPs) and non-LS showed early, large (always suprathreshold) EPSPs that fired bursts of action potentials. This result also suggests the presence of different local neuronal circuits involving LS and non-LS neurons and opens two important questions respect to the role of LS neurons in the GRSC. First, which mechanisms cause this smaller synaptic response during epileptiform discharges? And second, are the interconnections of LS pyramidal neurons within the GRSC different from those of non-LS pyramidal neurons?

To investigate these possibilities with more detail we studied the responses of LS and non-LS neurons to two different examples of incoming cortico-cortical axons: (1) contralateral axons (originated in the homotopic contralateral cortex) that are a model of long-range axons and (2) ipsilateral horizontal axons (activated by stimuli applied to the ipsilateral L2 at different distances from the recorded neuron), which are an example of both short- and long-range axons (depending of the distance between the stimuli and the recording neuron). With these experiments we tried to disclose differences in the innervation of LS and non-LS neurons.

As it is mentioned in our publication (Robles et al., 2020), some groups like Boucsein's laboratory suggest that the bulk of axons targeting pyramidal neurons most likely originate from outside this local range, emphasizing the importance of horizontal connections in rat neocortex. The decay space constant of horizontal connectivity was highest in layers 2/3 and 6A, showing that these layers are the principal sources of horizontal projections to pyramidal neurons of L5b (Schnepel et al., 2015). It is known the vast majority of synaptic connections, about 50-75%, a neuron receives actually inputs originated from outside the local volume. In other words, it has been hypothesized that horizontal projections could even dominate cortical network dynamics. Finally, these projections may also serve to reduce noise correlations and trial-by-trial variability and thereby improve signal detection in the neocortex (Churchland et al., 2010; Cohen & Kohn, 2011; Schnepel et al., 2015). In addition, the apparent lack of specificity may also suggest a more general role for horizontal projections, which is probably more accessible

through statistical descriptions and modeling of cortical network dynamics (Schnepel et al., 2015). However, until few years ago, cortical information processing at the cellular level has predominantly been studied in local networks, which are dominated by strong vertical connectivity between layers. For that we expanded L2/3 experiments recording pair of neurons between L2/3 versus L5b in order to discard if the small PSPs of LS neurons of L2/3 were due to afferents from pyramidal neurons of L5b. Along these lines of thinking, strong local connectivity will generally lead to strongly correlated activity in subnetworks of the neocortex, whereas a broader dispersion of presynaptic cells tends to reduce correlations and the overall amplitude of membrane potential fluctuations caused by the so-called ongoing activity.

Our results may have two potential problems related with the way of recording of synaptic responses. First, in the experiments of long-range stimulation it was possible that the recorded responses (or part of them) could be caused, not by long-range afferent axons impinging on L2/3 neurons, but by local collaterals of neighboring pyramidal neurons activated antidromically by the electrical stimuli; this is particularly important with respect to the contralateral stimulation, given the symmetrical bilateral structure of the callosal fibers. In our whole sample of neurons, we did not record a single case of antidromic activation in response to contralateral explanation, nor in LS neither in non-LS neurons. This observation makes very unlikely that the synaptic responses recorded after contralateral stimulation could be caused by local collateral branches of the axon of neurons activated antidromically. This lack of antidromic responses was in contrast with

the dysgranular RSC, where a very small proportions of L2/3 pyramidal neurons fire antidromically (<10% with maximal stimuli) (Sempere-Fernàndez et al., 2018). Second, for voltage-clamp recordings we used an intracellular solution based on K-gluconate, instead of a solution based on cesium as the main intracellular cation. The reason for doing that is that with intracellular cesium it was impossible to identify LS and non-LS pyramidal neurons, given that the firing pattern changed drastically. However, as we have noted before, the data on the time course of the synaptic responses discard that small responses recorded in LS neurons were located in distal dendrites in comparison with large responses recorded in non-LS neurons, making less relevant the use of intracellular cesium. Also, the increase of input membrane resistance caused by the use of cesium would be more relevant in non-LS neurons making larger the synaptic responses recorded in these neurons and thus further increasing the difference with LS neurons.

In primary sensory systems, horizontal projections have been implicated in several mechanisms, ranging from spatio-temporal information processing over surround suppression to sensorimotor interactions. Since all types of principal neurons as well as interneurons in all layers are possible targets of horizontal projections (Schnepel et al., 2015), it will be crucial to investigate the horizontal connectivity of other cell types. The laminar targeting of L2/3 axons is therefore likely to be determined by the molecular identity of the postsynaptic neurons, rather than by patterns of activity or diffusible gradients (Petreanu et al., 2007). We provide evidences that LS and non-LS pyramidal

neurons were integrated in different neuronal circuits, despite that the fact that these two types of neurons were at close proximity. Our data on glutamate application and stimulation of long-range axons (of both ipsi- and contralateral origin) showed that non-LS neurons received cortico-cortical synaptic contacts originated in both local and long-range axons (more than 250 μm); in contrast, cortico-cortical axons of local origin (less than 250 μm) innervate LS pyramidal neurons. Long-range mean axon originated in the contralateral cortex (callosal axons) or axons originated in the same hemisphere but no longer than 250 μm from the recorded neuron. In addition, the results of the analysis of synaptic responses evoked by stimulation of long-range cortico-cortical axons, either ipsilaterally or contralaterally, reinforced this finding. The big difference in EPSC size and the close proximity of LS and non-LS neurons imply that incoming long-range axons arriving in L2/3 of the GRSC selectively innervate non-LS pyramidal neurons. The fact the E/I balance was similar in LS and non-LS neurons discard that the size difference of the synaptic responses was caused by intrinsic synaptic mechanisms. This selective innervation by long-range axons implies that LS and non-LS pyramidal neurons are integrated in different neuronal circuits, accordingly participating in different functions. During epileptogenic discharges evoked in the disinhibited cortex, non-LS fired intensely, whereas LS only presented subthreshold synaptic responses.

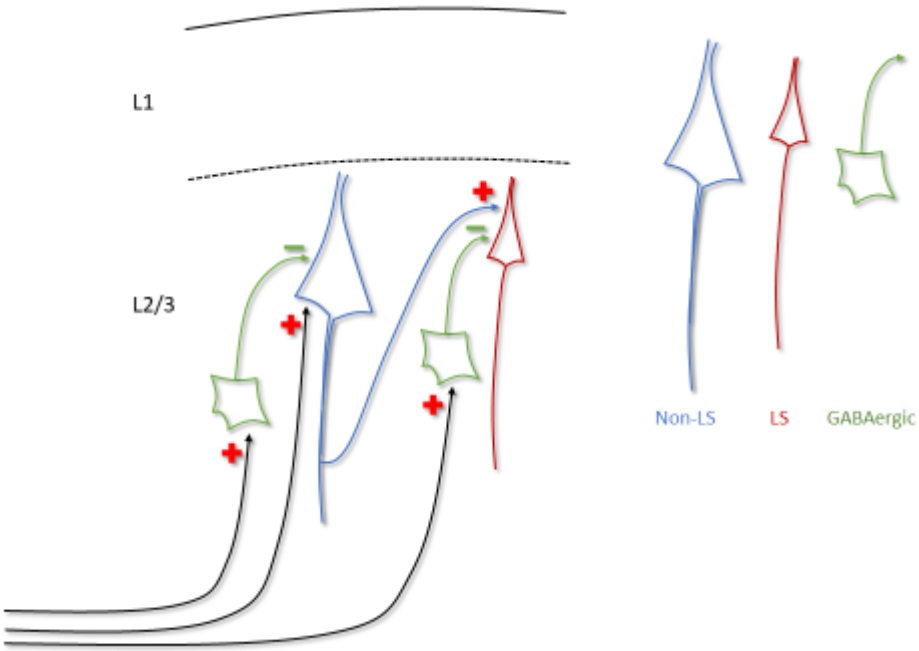

Figure 9.3.1. Local neuronal circuit scheme of L2/3 GRSC.

Another reason to the distinct size in the synaptic recorded LS and non-LS pyramidal neurons is that afferences originated in long-range axons were similar for both types of neurons but having different somato-dendritic localization in both types of pyramidal neurons. In LS pyramidal neurons the synapsis may be located in distal dendrites whereas in non-LS pyramidal neurons the synapsis might be located in proximal dendrites. In fact, in L5 thick tufted pyramidal neurons, it has been described that synaptic contacts formed on the apical dendrite are not scaled in respect to the distance from the soma and thus distal contacts produce smaller somatic synaptic responses than proximal contacts (Williams & Stuart, 2002). However, this possibility is unlikely because the rise time values and the time course of the decay phase of the EPSCs

from LS and non-LS did not support this possibility; in fact, the decay time was similar in both neuron types and the rise time was even shorter in LS neurons.

Comparing to other cortical areas, what happens between LS and non-LS pyramidal neurons of L2/3 of the GRSC, could be similar to what happen in L2 of the medial entorhinal cortex. Witter's lab suggests that the lack of evidence for excitatory stellate cell to stellate cell connectivity was not due to a cutting artifact of the slice preparation or a biased sample of only local connections between spatially associated clusters (Couey et al., 2013). And they also proposed that the fact that a minimal inhibitory connectivity pattern between L2 stellate cells is present in medial entorhinal cortex, and that a model based on a network with these biological properties could generate grid activity, raises the possibility that similar mechanisms are used in other parts of the cortex where pattern formation is considered to be a crucial component in information processing. Moreover, at Jeffery's laboratory it was observed the dominance of neural activity by local environmental cues even when these conflict with the global head direction signal (Jacob et al., 2017). This support our thinkings of separated local circuits between non-LS neurons, because the vast majority of them are in dysgranular RSC, and LS neurons, almost all of them, are in the GRSC.

Regarding development, the data was obtained from 14 to 22 postnatal days in mice and it is known that the postnatal development of the cortical circuit is still not completed at this age and thus we cannot exclude the possibility that further circuit

refinement might participate in the mechanisms controlling pyramidal neurons firing and the different coding strategies of L2/3 and L5 pyramidal neurons. However, we did the same experiments of individual recordings in two P30 mice, and we obtained exactly the same results. A next step could be to check if we have the same local circuits at different ages studying this in adult mice. An example could be what Angulo et al., (1999) presented with changes in the L5 pyramidal neurons to FS interneuron excitatory connections from 3 to 5 postnatal weeks, particularly a switch from paired-pulse depression to paired-pulse facilitation that confers L5 pyramidal neurons wider integrative capabilities at 5 weeks of postnatal age. So that, the possibility of later refinements of the afferent connections formed on LS and non-LS pyramidal neurons is opened since cortical circuits are not fully developed at this postnatal developmental stage. In addition, there is a study related to maturation reporting that L2 GRSC neurons are developmentally distinctive, characterized by late migration from the subventricular zone during the first postnatal week (Zraggen et al., 2011). So that we think that we should do more experiments in adult mice to be completely sure that these differences are permanent with age.

9.4. Role of inhibition in LS and non-LS pyramidal neurons

Thanks to the analysis of the latencies of the excitatory and inhibitory synaptic responses evoked by cortico-cortical axons, it is suggested that the responses to

contralateral axons were disynaptic in LS pyramidal neurons, in contrast to non-LS pyramidal neurons, making a sort of feed-forward excitation. We do not know the origin of these disynaptic responses on LS neurons, but a reasonable possibility is that they are originated in those neighbouring non-LS neurons firing in response to large EPSCs. The proportion of non-LS neurons firing in response to ipsi- or contralateral stimuli was really higher than LS-neurons and the probability of interconnections of L2/3 pyramidal neurons (0.1-0.15, Avermann et al. 2012; Holmgren et al. 2003) would support this possibility. However, we must say that we did not find a single case of non-LS to LS monosynaptic connection among our sample of simultaneously recorded neuron pairs. Moreover, in our lab it has been reported that PV-FS interneurons from superficial layers responded larger PSPs and were more often recruited by the stimulus than L5 PV-FS interneurons from GRSC (Sempere-Fernàndez et al., 2019). So that, there is more inhibitory activity on L2/3 according to the smaller responses of the LS pyramidal neurons on L2/3 of the GRSC. According with these results, we can think that LS pyramidal neurons play a sizeable and unique role in a local manner and these neurons are really controlled by inhibitory system.

For better understanding that cortical neurons operated the synaptic nature of the integration process during sensory processing, it was crucial to set up quantitative methods which allow inferring the level of conductance change evoked by the sensory stimulation and, consequently, the dynamics of the E/I balance. We know that each neuron received 2500 excitatory and 500 inhibitory inputs from the recurrent network,

in other words, 1/5 of neuron connections are inhibitory (Schnepel et al., 2015). So that a quantification step is to measure conductance changes seen at the soma, reflecting more directly the functional impact of synaptic input on the spike trigger mechanism. A research (Koch et al., 1993) estimated that the shunting inhibitory effect would significantly reduce the amplitude of the EPSP but somatic input conductance increased. Large rises in input conductance, after electrical stimulation of the cortical surface and during exogenous iontophoretic application of GABA, were found in cortical neurons up to 300% (Monier et al., 2008). *In vitro*, using also the current pulse injection, it was demonstrated during electrically evoked hyperpolarization in slices of rat and cat visual cortex that huge conductances increases (Berman et al., 1991). As well as it was revealed that 200% changes in input conductance during electrically evoked inhibition in cortical pyramidal neurons (Connors et al., 1988). These distinct results extensively supported the point that excitation and inhibition would interact in different ways in the *in vitro* slice and the intact *in vivo* network as Frégnac's laboratory proposed (Monier, et al., 2008).

To support that, as it has been commented before, there is a study from Witter's laboratory where using whole-cell cluster recordings and a simplified uniform inhibitory attractor model in rat entorhinal cortex, they reached the conclusion that inhibitory microcircuitry between stellate cells, principal cell type in L2 grid network of medial entorhinal cortex, is sufficient to generate grid-cell firing patterns in L2 of the medial entorhinal cortex (Couey et al., 2013). Moreover, the last study demonstrated that these grid cells are mainly interconnected via inhibitory interneurons and its grid firing can

emerge from a simple recurrent inhibitory network. Furthermore, other research concluded that the absence of grid cells in lateral entorhinal cortex predicts a different organization of the L2 principal cell microcircuit if the local microcircuit design of L2 medial entorhinal cortex excitatory cells is crucial for generating grid cell firing. Considering the fact that inhibition control microcircuits of both pyramidal and stellate cells in medial entorhinal cortex, although supplied by different interneuron types, similar cell types in lateral entorhinal cortex (e.g. the fan and pyramidal cell) might have a circuit structure where monosynaptic connectivity prevails. Their data from pair recordings of fan cells suggests that direct communication is present, but not prevalent, between cells of this type. Synaptic interactions is limited between stellate cell and pyramidal cell networks according to said in available data about the little monosynaptic connectivity between stellate and pyramidal cells (Ohara et al., 2019). This indicate the presence of two isolated subcircuits within L2 of the medial entorhinal cortex. Nevertheless, it must be taken into consideration that networks might be coordinated through one of the intermediate cell types, like intermediate pyramidal cells, which have been described to form synaptic connections with both stellate and pyramidal cells. This could be comparable to our research.

Our results could be compared and supported by the research of Schmitz's laboratory where they concluded that the network topology contributes to the functional diversity of subicular pyramidal cells observed during sharp-wave associated ripples since they showed that in the subiculum a subset of pyramidal neurons is activated, while

another subset is inhibited during ripples. The cell subtype is what predetermined these functionally subgroups. The cell subtype specific discrepancies extend into the local network topology, being reflected in an asymmetric wiring scheme where bursting cells and regular firing cells are recurrently connected among themselves but connections between subtypes exist from regular to bursting cells exclusively. Moreover, it is known that inhibitory connections are more numerous onto regular firing cells than onto bursting cells (Böhm et al., 2015).

Finally, another point of view could be that membrane properties variations ultimately determine the way in which these neurons integrate multiple synaptic afferents from different sources as it is proposed in a research from Gaspar's laboratory where they saw changes in the expression of glutamatergic, GABAergic or peptide membrane receptors among the sample of 153 5-HT (5-hydroxytryptamine or serotonin) raphe neurons analyzed through scRT-PCR analysis. Therefore, variations in the expression of in excitatory/inhibitory receptor do not contribute to the differences in excitability that were observed in other study (Fernández et al., 2016).

To sum up, we think that LS pyramidal neurons are silent and controlled by interneurons in standard conditions. According to that, Kurotani's laboratory concluded that the transverse propagation of IPSPs in coronal slices is mediated by GABAergic interneurons, which possibly suppress or modulate superficial neuronal cascade activities (Nixima et al., 2017).

9.5. Site of action of $GABA_B$ dependent inhibition

9.5.1. GABA Blockers

We can say that LS cells display a change in their response against two distinct and specific $GABA_B$ blockers unlike the rest of the cells of L2/3 mice GRSC. Nevertheless, it would be interesting to do more experiments to increment the number of cell of each type of neuron to complete this pack of experiments.

Besides we have got along sweeps the increment of value amplitudes of PSPs in both types of neurons when we applied the two different specific $GABA_B$ blockers. On this occasion we remark that in the case of LS cells there is a clear increase of amplitudes of EPSPs unlike other cells. The effect of $GABA_B$ blockers is more sizeable in LS cells than non-LS cells again. Nevertheless, we should measure with the non-LS response in front to specific $GABA_B$ blocker in order to compare responses in a better way because we appreciate an increment in frequency and a change in response, but we measured like a simple small LS depolarizations without taking into account the spikes from non-LS neurons.

According with that, it is known from developmental studies in L2/3 of rat somatosensory and visual cortex that polysynaptic excitation is regulated by slow

inhibition because, on the one hand, in the feedback pathway large-amplitude polysynaptic EPSPs were longer lasting and showed a late component whose onset coincided with that of slow IPSPs. On the other hand, in forward pathway these late EPSPs were only seen with stimulus intensities that were below the activation threshold of slow IPSPs (Shao & Burkhalter, 1999). So the hyperpolarization that we can see may be an effect of $GABA_BRs$. It has been proposed that a constant release of the transmitter is enabled by the high-frequency firing of GABAergic interneurons, leading to diminish the neuron excitability of the microcircuit. Targeting Kv3 channels using modulators or mutations interfer with the firing of these inhibitory neurons compromising the release of GABA (Toledo-Rodríguez et al., 2005). This fact impairs the function of the microcircuit due to the changes in the excitability.

Generally, the effects of GABA-mediated inhibition on neural circuit function are multifaceted (Sebe et al., 2014a). Thanks to baclofen disinhibitory effects in the cerebral cortex proposes that $GABA_BR$ might be important regulators of synaptic plasticity in many brain regions (Mott & Lewis, 1992). While many antiepileptic medications act by increasing synaptic GABAergic current, elevated levels of extrasynaptic GABA current are associated with epilepsy (Sebe et al., 2014a).

First, in a study in 2014, it was seen difference between effects against $GABA_BRs$ agonist SFK97541 on cortical and hippocampal after discharges and they said that it might be due to different distribution on interneurons and their relationship with principal

neurons in the two structures. In addition, they suggested that this distribution has more tight connections in neocortex (Fábera & Mareš, 2014). We think that it is possible that there is a distinct distribution on interneurons and their relationship with principal neurons between LS cells and the rest of cells in L2/3 of mice RSC at 14-22 postnatal days. Maybe LS cells are more connected with interneurons than non-LS cells. Therefore, the effect of inhibitory system seems more valuable on LS cells. Third, functionally, the data of Kinney's lab agreed that proper functioning of $GABA_BR$ is crucial for numerous learning and memory tasks and that targeting this system via pharmacological may benefit several clinical populations (Heaney & Kinney, 2016).

Second, in an investigation of ontogeny of $GABA_B$ binding in rat brain in 1994, it was described that $GABA_B$ binding peaked in the neocortex and thalamus is leaded at postnatal day 14 and binding decreased at postnatal day 28. $GABA_BRs$ antagonist CGP 54626A, however, inhibited binding thalamus and neocortex strongly at postnatal day 7 than in the adult brain (Turgeon & Albin, 1994). Because of that it is credible that there are discrepancies between LS cells and non-LS cells in our region at 14-22 postnatal days in mice. In the last study, it was revealed thanks to saturation analyses two binding sites with comparable affinities in both immature and mature adult brain, showing that postnatal modulation of $GABA_B$ binding reflects changes in binding site density rather than modulation of binding site affinity. This argues that GABA binding sites might have a different pharmacological profile in immature brains (Turgeon & Albin, 1994). An important point to take into account is that in interneurons the reversal potential for

chloride ions changes as they mature, and so that GABA becomes hyperpolarizing when it occurs. This variation turns ambient GABA into a stop signal for migrating interneurons since hyperpolarizing GABA diminishes the intracellular calcium transients frequency (Bartolini et al., 2013). That makes us think that it is possible that there may be a different level of maduration between LS cells and non-LS cells in the region of study. To support that, another publication in 2006 of Mares mentions that the role of $GABA_B$-mediated inhibition in epileptogenesis depends on the type of seizures and also on the stage of maduration too (Mares & Slamberová, 2006). There is a developmental irregularity because we can see opposite effects or failures of agonists and antagonists of $GABA_BRs$ between early postnatal days (e.g. 12 and 18) and 25 posnatal day, in other words, between immature and mature brain (Ben-Ari, 2013; Bolton et al., 2015; Fábera & Mareš, 2014; Mares & Slamberová, 2006; Sebe et al., 2014a; Turgeon & Albin, 1994).

All these suggestions coincides with the general information about circuits which are generally in agreement that circuits during development are more readily engaged in epilepsies and seizure manifestations than adult circuits as we said in the introduction. So all voltage and transmitter gated currents vary in young and adult neurons virtually (Ben-Ari, 2013). Then at 15 postnatal day it is performable the epileptiform activity and different level of maturation between cells, being non-LS cells the most excitables and immatures than LS cells. To understand that, one reason may be that GABA operates differently because of a difference in chloride gradient as immmature neurons have a higher intracellular concentration of chloride. This is due to early expression of a chloride

cotransporter, NKCC1, which loads immature neurons with chloride and delayed expression of a chloride extruder, NKCC2 (Ben-Ari, 2013; Bolton et al., 2015). Moreover, KCC2 is expressed earlier in female rodents, suggesting a sexually dimorphic maturation of the developing nervous system (Bolton et al., 2015). The consequence of this difference is that a major source of inhibitory drive is lacking in immature neurons and this entrains a lower threshold for seizures generations. Another general reason is the earlier maduration of GABAeric signals that precede the formation of glutamatergic synapses like a pioneer system that operates by default with its synapses being automatically formed when the pre and postsynaptic elements meet (Ben-Ari, 2013). The last paper also affirms that these variations during development are characterized in humans and animals with a unique difference being that these variations mainly occur during the fetal stages of development in humans, while there is a shift towards the postnatal period in rodents, showing that is is more related to brain development rather than to birth.

An irregular development of pre- and postsynaptic $GABA_BRs$ and at least quantitative variations if these receptors in pharmacological sensitivity in the cerebral cortex were demonstrated. Release of both glutamate and GABA is suppressed by presynatic $GABA_BRs$ and the effects on inhibitory and excitatoory presynaptic terminals may be change during ontgeny. In rat cerebral cortex, the representation of two $GABA_BR$ splice variants show opposite developmental trends- GB1a diminishes and GB2b rises with age. Laminar distribution of $GABA_BR$ protein in the somatosensory cortex varies too during early development, the affinity of both GB1a and GB1b for baclofen rises with age.

Accordingly, it supports as we said that LS cells are more mature cells than non-LS cells and have $GABA_BRs$ more developed to respond more specifically to agonists and antagonist, with more affinity in mice. We tried to do immunohistochemistry with commercial antibodies but we did not obtain clear result. For that, we should create a handmade antibody discriminating both subunits of $GABA_BRs$ thanks to the sequence of aminoacids showed in several studies (Calver et al., 2000) because it is an heteroreceptor and it is known that $GABA_B1$ isoforms, present only in neurons (Kasten & Boehm, 2015), exhibit pharmacological and/or functional differences *in vivo* (Vigot et al., 2006). We would be interested in $GABA_B1a$ due to it is the one which inhibits Glutamate release presynaptically on axon terminals and dendritic branches and it is involved in hyperactivity, seizure activity, protection of depressive phenotypes, and memory maintenance. In contrast, $GABA_B1b$ that mediates postsynaptic inhibition on dendritic spines is involved in susceptibility to depression-like phenotypes and impaired memory formation (Kasten & Boehm, 2015; Vigot et al., 2006). These findings could be interesting to see the distribution of $GABA_BR$ in the whole RSC so that we could distribute and compare with other techniques several frequent pathologies associated with this receptor type like cognitive, anxiety and depressive impairments (Kasten & Boehm, 2015).

Regarding to this, in adult rodent, oscillatory function and numerous behavioural domains have been linked with $GABA_BRs$ activation (Bolton et al., 2015; Heaney et al., 2013). Furthermore, the majority of inhibitory tone in early postnatal life is provided by $GABA_BRs$ during rodent development. So that, the role of $GABA_BRs$ is particularly

important in the absence of $GABA_AR$-driven inhibition considering that synaptic connections begin around the time of birth and adult-like features (extensive growth of axons and dendrites) (Bolton et al., 2015). This is the same that we found in our experiments because at the last day of second postnatal week and the beginning of the third postnatal week with an antagonist of $GABA_AR$, Bicuculline, it appears an essential effect on $GABA_BR$ in LS cells to let their to fire action potentials.

9.5.2. GABA Application

Our experiments of direct GABA application apparently discord the possibility of a postsynaptic component, therefore the action of $GABA_B$ could be presynaptic. The depolarization of human neocortex nerve terminals which are evoked by Glutamate and GABA release can be affected distinctively through pharmacologically different $GABA_BRs$, and $GABA_B$ autoreceptors sited on GABA-releasing terminals vary pharmacologically from the $GABA_B$ heteroreceptors sited on glutamate-releasing terminals (Bonanno et al., 1997; Chalifoux & Carter, 2011; Fábera & Mareš, 2014). In other study, application of CGP52432 slightly suppressed optical responses to early pulses, whereas it enhanced responses to later pulses, suggesting that $GABA_BR$ activation reduced polysynaptic $GABA_AR$ activation indirectly via inhibition of presynaptic GABA release (Fujita et al., 2011) like CGP56999A (Bonanno et al., 1997). Moreover, $GABA_BRs$ might work as a filter that passes high activities in the cerebral cortex, not low, and maybe this is what it happening in our conditions in LS cells. The findings of Fujita and his lab

mates reinforce the chance that $GABA_BR$ agonists might suppress moderate excitatory propagation in cerebral cortex. Nevertheless, $GABA_BR$ agonists may be ineffective as suppressors of excitation in response to more intense neural activity (Fujita et al., 2011). Regarding this, another possibility could be that non-LS cells have more activity and $GABA_BR$ is not able to suppress that activity completely.

Finally, activation $GABA_B$ and 5-HT receptors produces presynaptic inhibition at glutamatergic terminals in the rat neocortex (Torres-Escalante et al., 2004). So it would be interesting to do experiments with all these receptors together in order to understand what is happening. Furthermore, it was demonstrated that Gabapentin activates presynaptic $GABA_B$ heteroreceptors, but not $GABA_B$ autoreceptors (Parker et al., 2004), and it may be useful ligand to discriminate between presynaptic $GABA_BRs$ subtypes.

Another study showed that deletion of the Neuregulin Receptor (ErbB4) from chandelier and basket cells, the two principal classes of fast-spiking interneurons, produces thin but consistent synaptic defects. Unexpectedly, these small wiring abnormalities boost cortical excitability, rise oscillatory activity and disrupt synchrony across cortical regions. It is thought that increased locomotor activity, abnormal emotional responses, impaired social behavior and impaired cognitive function are possible factors for these functional deficits. These results support the idea that cortical fast-spiking interneurons dysfunction may be central to the schizophrenia pathophysiology (Del Pino et al., 2013). So that, it could explain why in human patients

with schizophrenia it is very activated the RSC. For that, we can think that LS pyramidal neurons which form local neuronal circuits in GRSC are really regulated by GABAergic system and when this inhibitory system is altered, the LS pyramidal neurons are activated and then they could play an interesting role in schizophrenia.

Last but not least, a research raised the chance that $GABA_B$-mediated disinhibition may happen *in vivo* during normal theta activity, thus LTP facilitation in dentate gyrus. Frequency of the stimuli used to induce LTP could be modified by $GABA_B$Rs effects on LTP induction. Hyperpolarizing $GABA_B$ IPSPs could relate the enhancement of LTP by $GABA_B$ antagonists to the suppression of NMDA currents. Furthermore, it was demonstrated that $GABA_B$Rs from CA1 of hippocampus facilitates LTP induction too. These studies and the disinhibitory effects of baclofen in the cerebral cortex propose that $GABA_B$Rs might be crucial regulators of synaptic plasticity in several brain regions (Mott & Lewis, 1992).

9.6. Future studies

Considering our results and their limitations, we plan the following studies concerning the electrophysiology of LS neurons:

First, to disclose the structure of the local micro-circuits involving LS neurons in the RSC. This is a complex problem, but we plan two initial approaches. Given that the latency of the synaptic responses in LS is longer than in non-LS, one possibility is that horizontal collateral of pyramidal neurons (from which depend the horizontal propagation of epileptiform discharges) only form monosynaptic connections on LS neurons while LS neurons are only innervated by feed-forward horizontal axon coming from local non-LS neurons. The other possibility (approach) is that that the axonal convergence on LS neurons is lower than on non-LS neurons and / or the single axon EPSPs are smaller. Bringing together whole-cell recordings of synaptic currents and photostimulation allows to map circuits between presynaptic neurons (by ChR2 expression) and postsynaptic neurons (targeted patching). Using ChR2-assisted circuit mapping (CRACM) technique to map from L2/3 of the somatosensory cortex the long-rage callosal projections, it was showed that L2/3 axons connect with L2/3, L5 and L6 in both ipsilateral and contralateral cortex, but not L4. Moreover, L2/3 to L5 projection is stronger in both hemispheres than L2/3-to-L2/3 projection. The results of Svoboda's laboratory (Petreanu et al., 2007) propose that a possible identical laminar specificity for both long-range and local cortical projections.

In addition, until 2016, RSC was considered to be troublesome for *in vivo* two photon imaging. However, a study from Czajkowski's laboratory got good results with Thy1-GFP transgenic mouse line making possible to research the correlation of behavioural manipulations with variations *in vivo* in neuronal morphology. It was

combined a mCherry-expressing recombinant adeno-associated virus (rAA mCherry injection into the dorsal hippocampus and the cranial window implantation over the RSC, and the mCherry expression spreads out from the dorsal hippocampus too the RSC to axonal projections allowing to see the changes in both presynaptic axonal boutons and postsynaptic dendritic spines (Lukasiewicz et al., 2016). This methodology sorts out the poor accuracy that we have got using optogenetics with our apparatus.

Second, to check the different postnatal development and distribution of $GABA_BRs$, their subunits as well as modulation of their affinity to GABA, it could be interesting to do recording pairs experiment in adult mice and also between 5-14 postnatal days. So it could be possible explanation for ambiguous effect of $GABA_B$ on L2/3 of mice RSC.

Third, to clarify the role of the $GABA_B$ dependent inhibition in LS neurons. The actions of $GABA_B$ blockers on the responses recorded during epileptiform activity shows the presence of a $GABA_B$ dependent component. However, the results of the experiments of recording the currents evoked by direct application of GABA do not show a postsynaptic current depending on $GABA_BRs$ and this opens the possibility that the action of $GABA_BRs$ is dependent on presynaptic $GABA_BRs$ that inhibit the release of glutamate. So that we could check effects that depend on presynaptic $GABA_BRs$ with a ligand as Gabapentin which activates presynaptic $GABA_B$ heteroreceptors but not $GABA_B$

autoreceptors (Parker et al., 2004) and discriminate between presynaptic $GABA_BR$ subtype.

We did immunohistochemistry against $GABA_B$, the problem that we had was that the results were not clear, it was not well labelled after several modifications. However, we found several researches where it is showed the oligonucleotids from each subunit of $GABA_BRs$ and TaqMan fluorogenic probes and developed polyclonal antisera specific to two splice variants of the $GABA_{B1}$ subunits, $GABA_{B1a}$ and $GABA_{B1b}$, as well antiserum to the $GABA_{B2}$ subunit (Calver et al., 2000; Charles et al., 2001), so that we can build a specific handmade antibody to improve our results.

Finally, a tempting goal is to get a general model integrating defined anatomical, neurochemical and electrophysiological features and to recognize functionally crucial neuron types. Consolidating retrograde tracing and single-cell RT-PCR patch-clamp recordings, we may achieve multiple neurochemical and electrophysiological properties of a single LS pyramidal neuron and obtain the first unbiased classification of these ones based on multiple criteria.

Conclusions

10. CONCLUSIONS/CONCLUSIONES/ CONCLUSIONS

10.1. Conclusions

1. In the mice GRSC there is a sub-population of pyramidal neurons that show a LS firing pattern (LS neurons) and that are located in the superficial L2/3. In addition to the firing pattern, these neurons have other electrophysiological differences with the rest of pyramidal neurons in this cortical area (higher input resistance and shorter action potentials).

2. LS neurons have a different electrophysiological response than non-LS neurons during the propagation of epileptiform discharges along L2/3: they show subthreshold postsynaptic potentials that never fire action potentials in contrast to non-LS neurons, which always fire action potentials in synchrony with the epileptiform discharges.

3. Long range excitatory axons, either ipsilateral or contralateral, innervate preferably non-LS pyramidal neurons in L2/3 of the GRSC. In addition, local

excitatory axons which innerve LS pyramidal neurons are originated in neurons placed at < 250 μm from the soma.

4. The excitatory responses recorded in LS pyramidal neurons in response to the activation of long-range axons are disynaptic and probably it is originated in nearby firing non-LS pyramidal neurons.

5. The E/I balance between the EPSCs and the feed-forwarded activated IPSCs were similar in LS and in non-LS pyramidal neurons.

6. However, this E/I balance was larger in response to ipsilateral than to contralateral stimulation; this suggests that, in the GRSC, both types of pyramidal neurons in L2/3 would fire preferently in response to inputs from the ipsilateral hemisphere that to inputs carried by the corpus callosum.

7. Simultaneously pairs recorded between L2/3 and L5 pyramidal neurons discard the possibility that pyramidal neurons from upper L5b send inputs to LS

pyramidal neurons of L2/3 due to, on the one hand, the responses of LS neurons did not change and, on the other hand, the probability of these connected pairs is too low.

8. The application of $GABA_BR$ blockers increases the synaptic potentials generated during the epileptiform discharges in LS neurons; this increase is large enough to reach the threshold and to fire action potentials. This action of $GABA_BR$ blockers is probably mediated by presynaptic $GABA_BRs$.

9. These results are the initial step to study the way in which LS neurons are integrated in the local cortical microcircuits, as well as to study the role of the $GABA_BRs$ in the electrophysiology of GRSC.

10.2. Conclusiones

1. En la GRSC de ratón hay una subpoblación de neuronas piramidales que muestran un patrón de disparo LS (neuronas LS) que se encuentran en la capa superficial 2/3. Además del patrón de disparo, estas neuronas tienen otras diferencias electrofisiológicas con el resto de neuronas piramidales de corteza (mayor resistencia de entrada y potenciales de acción más cortos, entre otros).

2. Las neuronas LS tienen respuesta electrofisiológica diferente respecto a las neuronas no-LS durante la propagación de descargas epileptiformes a lo largo de la capa 2/3: muestran potenciales postsinápticos por debajo del umbral que nunca llegan a disparar potenciales de acción a diferencia de las neuronas no-LS, las cuales siempre disparan potenciales de acción en sincronía con dichas descargas epileptiformes.

3. Los axones excitatorios de largo alcance, tanto ipsilaterales como contralaterales, inervan preferiblemente las neuronas piramidales no-LS de la capa 2/3 de la GRSC. Además, los axones locales excitatorios que inervan las neuronas piramidales LS son originados en neuronas situadas a < 250 μm desde el soma.

4. Las respuestas excitadoras registradas en las neuronas piramidales LS en respuesta a la activación de axones de largo alcance son disinápticas y probablemente originadas por los disparos de las neuronas piramidales no-LS vecinas.

5. El balance E/I entre la activación de las EPSCs y de las IPSCs fue similar en las neuronas piramidales LS y no-LS.

6. Sin embargo, el balance E/I fue mayor en la respuesta a estimulación ipsilateral que en la contralateral; sugiriendo que, en la GRSC, ambos tipos de neuronas en la capa 2/3 dispararían preferiblemente en respuesta a aferencias desde el hemisferio ipsilateral que a aferencias procedentes a través del cuerpo calloso.

7. Los registros pareados simultáneos entre neuronas piramidales de L2/3 y L5 de la GRSC descartan la posibilidad de que las neuronas piramidales de la capa superior L5b envían aferencias a las neuronas piramidales LS de L2/3 debido a, por un lado, las respuestas de las LS no cambian y, por otro lado, la probabilidad de que estos pares estén conectados es muy baja.

8. La aplicación de bloqueantes de $GABA_BR$ aumenta los potenciales sinápticos generados en descargas epileptiformes en neuronas LS; este aumento es suficientemente grande para conseguir el umbral y disparar potenciales de acción. Esta acción del bloqueante de $GABA_BR$ es probablemente mediado por los $GABA_BRs$ presinápticos.

9. Estos resultados son el paso inicial para estudiar la vía en que las neuronas LS se integran en los microcircuitos corticales locales, así como para estudiar el papel de los $GABA_BRs$ en la electrofisiología de la GRSC.

10.3. Conclusions

1. En la GRSC de ratolí hi ha una subpoblació de neurones piramidals que mostren un patró de tret LS (neurones LS) que es troben en la capa superficial 2/3. A més del patró de tret, aquestes neurones tenen altres diferències electrofisiològiques amb la resta de neurones piramidals d'escorça (major resistència d'entrada i potencials d'acció més curts, entre d'altres).

2. Les neurones LS tenen resposta electrofisiològica diferent respecte a les neurones no-LS durant la propagació de descàrregues epileptiformes al llarg de la capa 2/3: mostren potencials postsinàptics per davall del llindar que mai arriben a disparar potencials d'acció a diferència de les neurones no-LS, les quals sempre disparen potencials d'acció en sincronia amb aquestes descàrregues epileptiformes.

3. Els axons excitatoris de llarg abast, tant ipsilaterals com contralaterals, innerven preferiblement les neurones piramidals de la capa 2/3 de la GRSC. A més a més, els axons locals excitatoris que innerven les neurones piramidals LS són originats en neurones situades a < 250 mm del soma de les neurones LS.

4. Les respostes excitadores registrades en les neurones piramidals LS en resposta a l'activació d'axons de llarg abast són disinàptiques i probablement originades pels trets de les neurones piramidals no-LS veïnes.

5. El balanç E/I de l'activació entre les EPSCs i les IPSCs va ser similar en les nurones piramidals LS y no-LS.

6. No obstant això, el balanç E/I va ser major en la resposta a estimulació ipsilateral que en la contralateral; suggerint que, en la GRSC, tots dos tipus de neurones en la capa 2/3 dispararien preferiblement en resposta a aferències des de l'hemisferi ipsilateral que a aferències procedents a través del cos callós.

7. Els registres apariats simultanis entre neurones piramidals de L2/3 i L5 de la GRSC descarten la possibilitat que les neurones piramidals de la capa superior L5b envien aferències a les neurones piramidals LS de L2/3 a causa de, d'una banda, les respostes de les neurones LS no canvien i, d'altra banda, la probabilitat de què aquests parells estiguen connectats és molt baixa.

8. L'aplicació de bloquejants de $GABA_BR$ augmenta els potencials sinàptics generats en descàrregues epileptiformes en neurones LS; este augment és suficientment gran per aconseguir l'umbral i disparar potencials dacció. Esta acció del bloquejant de $GABA_BR$ és probablement degut als $GABA_BRs$ presinàptics.

9. Aquests resultats són el pas inicial per a estudiar la via en què les neurones LS s'integren en els microcircuits corticals locals, així com per estudiar el paper dels $GABA_BRs$ en l'electrofisiologia de la GRSC.

Bibliographic references

10. BIBLIOGRAPHIC REFERENCES

Abbasi, S., & Kumar, S. S. (2013). Electrophysiological and morphological characterization of cells in superficial layers of rat presubiculum. *Journal of Comparative Neurology*, *521*(13), 3116–3132. https://doi.org/10.1002/cne.23365

Agabio, R., & Colombo, G. (2015). GABAB receptor as therapeutic target for drug addiction: From baclofen to positive allosteric modulators. *Psychiatria Polska*, *49*(2), 215–223. https://doi.org/10.12740/PP/33911

Aggleton, J. P., & Nelson, A. J. D. (2014). Why do lesions in the rodent anterior thalamic nuclei cause such severe spatial deficits? *Neuroscience and Biobehavioral Reviews*, *54*, 131–144. https://doi.org/10.1016/j.neubiorev.2014.08.013

Agster, K. L., & Burwell, R. D. (2009). Cortical efferents of the perirhinal, postrhinal and entorhinal cortices of the rat. *Hippocampus, 19*(12), 1159–1186. https://doi.org/10.1002/hipo.20578

Albertson, A. J., Williams, S. B., & Hablitz, J. J. (2013). Regulation of epileptiform discharges in rat neocortex by HCN channels. *Journal of Neurophysiology*, *110*(8), 1733–1743. https://doi.org/10.1152/jn.00955.2012

Alezander, A., & Nitz, D. A. (2017). Spatially Periodic Activation Patterns of Retrosplenial Cortex Encode Route Sub-spaves and Distance Traveled. *Current Biology, 27*(11), 1551-1560.e4. https://doi.org/10.1016/j.cub.2017.04.036

Alonso, A., & Klink, R. (1993). Differential electroresponsiveness of stellate and pyramidal-like cells of medial entorhinal cortex layer II. *J. Neurophysioly, 70*(1):128-43. https://doi.org/10.1152/jn.1993.70.1.128.

Angulo, M. C., Rossier, J., & Audinat, E. (1999). Postsynaptic glutamate receptors and integrative properties of fast-spiking interneurons in the rat neocortex. *Journal of Neurophysiology*, *82*(3), 1295–1302. https://doi.org/10.1152/jn.1999.82.3.1295

Ash, J. A., Lu, H., Taxier, L. R., Long, J. M., Yang, Y., Stein, E. A., & Rapp, P. R. (2016). Functional connectivity with the retrosplenial cortex predicts cognitive aging in rats. *Proceedings of the National Academy of Sciences oof the United States oof America, 113*(43), 12286–12291. https://doi.org/10.1073/pnas.1525309113

Auger S. D., Zeidman, P., & Maguire, E. A. (2015). A central role for the retrosoplenial cortex in de novo environmental learning. *ELife, 4,* 1-26. https://doi.org/10.7554/eLife.09031

Auger S. D., Zeidman, P., & Maguire, E. A. (2017). Efficacy of navigation may be influenced by retrosplenial cortex-mediated learning of landmark stability. *Neuropsychologia, 104,* 102-112. https://doi.org/10.1016/j.neuropsychologia.2017.08.012

Avermann, M., Tomm, C. Mateo, C., Gerstner, W., & Petersen. C. C. H. (2012). Microcircuits of excitatory and inhibitory neurns in layer 2/3 of mouse barrel cortex. *Juornal of Neurophysioloogy, 107*(11), 3116-3134. https://doi.org/10.1152/jn.00917.2011

Bartolini, G., Ciceri, G., & Marín, O. (2013). Integration of GABAergic Interneurons into Cortical Cell Assemblies: Lessons from Embryoos and Adults. *Neuron, 79*(5), 849-864. https://doi.org/10.1016/j.neuron.2013.08.014

Beloozerova, I.N., Sirota, M. G., & Swadlow, H. A. (2003a). Activity of different classes of neurons of the motor cortex during locomotion. *Journal of Neuroscience, 23*(3), 1087-1097. https://doi.org/10.1523/jneurosci.23-03-01087.2003

Beloozerova, I.N., Sirota, M. G., & Swadlow, H. A. (2003b). Activity of different classes of neurons of the motor cortex during locomotion. *Journal of Neuroscience, 23*(3), 1087-1097. https://doi.org/10.1523/jneurosci.23-03-01087.2003

Ben-Ari, Y. (2013). The developing cortex. In *Handbook of clinical neurology* (1st ed., Vol. 111). Elsevier B.V. https://doi.org/10.1016/B978-0-444-52891-9.00045-2

Benke, D. (2013). GABAB receptor trafficking and interacting proteins: targets for the development of highly specific therapeutic strategies to treat neurological disorders? *Biochemical Pharmacology*, *86*(11), 1525–1530. https://doi.org/10.1016/j.bcp.2013.09.016

Benke, D., Balakrishnan, K., & Zemoura, K. (2015). Regulation of cell surface GABA(B) receptors: contribution to synaptic plasticity in neurological diseases. In *Advances in pharmacology (San Diego, Calif.)* (1st ed., Vol. 73). Elsevier Inc. https://doi.org/10.1016/bs.apha.2014.11.002

Berman, N.J., Douglas, R.J., Martin, K. A. C., & Whitteridge, D. (1991). Mechanisms of inhibition in cat visual cortex. Journal of Physiology, 440, 697-722.

Bicanski, A., & Burgess, N. (2016). Environmental anchoring of head direction in a computational model of retrosplenial cortex. *Journal of Nueroscience, 36*(46). 11601-11618. https://doi.oorg/10.1523/JNeurosci.0516-16.20167

Bluhm, R., L., Miller, J., Lanius, R. A., Osuch, E. A., Boksman, K., Neufeld, R. W. J., Théberge, J., Schaefer, B., & Williamson, P. C. (2009). Retrosplenial cortex connectivity in schizophrenia. *Psychiatry Research-Neuroimaging, 174*(1), 17-23. https://doi.org/10.1016/j.pscychresns.2009.03.010

Böhm, C., Peng, Y., Maier, N., Winterer, J., Poulet, J. F. A., Geiger, J. R. P., & Schmitz, D. (2015). Functional diversity of subicular principal cells during hippocampal ripples. *Journal of Neuroscience, 35*(40), 13608–13618. https://doi.org/10.1523/JNEUROSCI.5034-14.2015

Bolton, M. M., Heaney, C. F., Murtishaw, A. S., Sabbagh, J. J., Magcalas, C. M., & Kinney, J. W. (2015). Postnatal alterations in GABAB receptor tne produce sensorimotor gating ddeficits and protein level differences in adulthood. International Journal oof Developmental Neuroscience: *The Official Journal of the Inetrnational Society for Developmental Neuroscience, 41,* 17-27. https://doi.org/10.1016/j.ijdevneu.2014.10.001

Bonanno, G., Fassio, A., Schmid, G., Severi, P., Sala, R., & Raiteri, M. (1997). Pharmacologically distinct GABA(B) receptors that mediate inhibition of GABA and glutamate release in human neocortex. *British Journal of Pharmacology*, *120*(1), 60–64. https://doi.org/10.1038/sj.bjp.0700852

Bos, J. J., Vinck, M., Van Mourik-Donga, L. A., Jackson, J. C., Witter, M. P., & Pennartz, C. M. A. (2017). Perirhinal firing patterns are sustained across large spatial segments of the task environment. *Nature Communications*, *8*(7491), 1–12. https://doi.org/10.1038/ncomms15602

Boudewijns, Z. S. R. M., Kleele, T., Mansvelder, H. D., Sakmann, B., de Kock, C. P. J., & Oberlaender, M. (2011). Semi-automated three-dimensional reconstructins of individual neurons reveal cell type-specific circits in cortex. *Communicative & Integrative Biology*, *4*(4), 486–488. https://doi.org/10.4161/cib.15670

Bowery, N. G., Hill, D. R., & Hudson, a L. (1983). Characteristics of GABAB receptor binding sites on rat whole brain synaptic membranes. *British Journal of Pharmacology*, *78*(1), 191–206.

Brickley, S. G., Farrant, M., & Swanson, G. T. (2001). *CNQX increases GABA-mediated synaptic transmission in the cerebellum by an AMPA / kainate receptor-independent mechanism*. *41*, 730–736.

Brown, S. & Hestrin, S.P., (2009). Intracortical circuits of pyramidal neurons reflect their long- range axonal targets. *Nature* *457*(7233), 1133–1136. https://doi:10.1038/nature07658

Buchtová, H., Fajnerová, I., Stuchlík, A., & Kubík, Š. (2017). Acute systemic MK-801 induced functional uncoupling between hippocampal areas CA3 and CA1 with distant effect in the retrosplenial cortex. *Hippocampus*, *27*(2), 134–144. https://doi.org/10.1002/hipo.22678

Buckley, M. J., & Mitchell, A. S. (2016). Retrosplenia cortical contributions to anterograde and retrograde memory in the monkey. Cerebral Cortex, *26*(6), 2905–2918. https://doi.org/10.1093/cercor/bhw054

Burles, F., Slone, E., & Iaria, G. (2017). Dorso-medial and ventro-lateral functional specialization of the human retrosplenial complex in spatial updating and orienting. *Brain Structure and Function*, *222*(3), 1481–1493. https://doi.org/10.1007/s00429-016-1288-8

Cajal, S.R. (1911) Histologie du système nerveux de l'homme et des vertébrés. Ed. Française rev. & mise à jour par l'auteur tr. De l'espagnol par L. Azoulay. Paris: Maloin. https://doi.org/10.5962/bhl.title.48637

Calver, A. R., Medhurst, A. D., Robbins, M. J., Charles, K. J., Evans, M. L., Harrinson, D. C., Stammes, M., Hughes, S.A., Hervieu, G., Couve, A., Moss, S. J., Middlemiss, D. N., & Pangalos, M. N. (2000). The expression of GABA(B1) and GABA(B2) receptor subunits in the CNS differs from that in peripheral tissues. *Neuroscience, 100*(1), 155-170. https://doi.org/10.1016/S0306-4522(00)00262-1

Carrasquillo, Y., Burkhalter, A., & Nerbonne, J. M. (2012). A-type K^+ channels encoded by Kv4.2, Kv4.3 and Kv1.4 differentially regulate intrinsic excitability of cortical pyramidal neurons. *Journal of Physiology*, *590*(16), 3877–3890. https://doi.org/10.1113/jphysiol.2012.229013

Chalifoux, J. R., & Carter, A. G. (2011). GABAB receptor modulation of synaptic function. *Current Opinion in Neurobiology*, *21*(2), 339–344. https://doi.org/10.1016/j.conb.2011.02.004

Chan, K. F. Y., Burnham, W. M., Jia, Z., Cortez, M. A., & Snead, O. C. (2006). GABAB receptor antagonism abolishes the learning impairments in rats with chronic atypical absence seizures. *European Journal of Pharmacology*, *541*(1–2), 64–72. https://doi.org/10.1016/j.ejphar.2006.04.012

Charles, K. J., Evans, M. L., Robbins, M. J., Calver, A., R., Leslie, R. A. & Pangalos, M. N. (2001). Comparative immunohistochemical localization of GABAB1a, GABAB1b

and GABAB2 subunits in rat brain, spinal cord and dorsal root ganglion. *Neuroscience, 106*(3), 447–467. https://doi.org/10.1016/S0306-4522(01)00296-2

Chrastil, E. R. (2018). Heterogeneity in human retrosplenial cortex: A review of function and connectivity. *Behavioral Neuroscience, 132*(5), 317-338. https://doi.org/10.1037/bne0000261

Chrastil, E. R., Sherrill, K. R., Aselcioglu, I., Hasselmo, M. E., & Stern, C. E. (2017). Individual differences in human path integrations abilities correlate with gray matter volume in retrosplenial cortex, hippocampus, and medial prefrontal cortex. *ENeuro, 4*(2). https://doi.org/10.1523/ENEURO.0346-16.2017

Chrastil, E. R., Sherrill, K. R., Hasselmo, M. E., & Stern, C. E. (2015). There and back again: hippocampus and retrosplenial cortex track homing distance during human path integration. J*ournal of Neuroscience, 35*(46), 15442-15452. https://doi.org/10.1523/JNEUROSCI.1209-15.2015.

Chu, Z., Galarreta, M., & Hestrin, S. (2003). Synaptic Interactions of Late-Spiking Neocortical Neurons in Layer 1. *The Journal of Neuroscience, 23*(1), 96-102.

Churchland, M. M., Cunningham, J.P., Kaufman, M. T., Ryu, S. I., & Shenoy, K. V. (2010). Cortical Preparatory Activity: Representation of Movement or First Cog in a Dynamical Machine? Nueron, 68(3), 387-400. https://doi.org/10.1016/j.neuron.2010.09.015

Clark, B. J. (2017). Spatial Navigation: Retrosplenial Cortex Encodes the Spatial Structure of Complex Routes. *Current Biology*, *27*(13), R649–R651. https://doi.org/10.1016/j.cub.2017.05.019

Cohen, M., Kohn, A. (2011). Measuring and interpreting neuronal correlations. *Nat Neurosci 14,* 811-819. https://doi.org/10.1038/nn.2842

Connors, B. W., Malenka, R. C., & Silva, L. R. (1988). Two inhibitory postsynaptic potentials, and GABAA and GABAB receptor-mediated responses in neocortex of rat and cat. *The Journal of Physiology*, *406*(1), 443–468. https://doi.org/10.1113/jphysiol.1988.sp017390

Corcoran, R., Mansfield, R., Giokas, T., Hawkins, A., Bamford, L., & Marshall, G. (2017). Places Change Minds: Exploring the Psychology of Urbanicity Using a Brief Contemplation Method. *SAGE Open*, *7*(2). https://doi.org/10.1177/2158244017707004

Couey, J. J., Witoelar, A., Zhang, S. J., Zheng, K., Ye, J., Dunn, B., Czajkowski, R., Moser, M. B., Moser, E. I., Roudi, Y., & Witter, M. P. (2013). Recurrent inhibitory circuitry

as a mechanism for grid formation. *Nature Neuroscience, 16*(3), 318-324. https://doi.org./10.1038/nn.3310

Cowansage, K. K., Shuman, T., Dillingham, B. C., Chang, A., Golshani, P., & Mayford, M. (2014). Direct Reactivation of a Coherent Neoocortical Memory of Context. *Neuron, 84*(2), 432–441. https://doi.org/10.1016/j.neuron.2014.09.022

Crochet, S., & Petersen, C. C. H. (2006). Correlating whisker behavior with membrane potential in barrel cortex of awake mice. *Nature Neuroscience*, *9*(5), 608–610. https://doi.org/10.1038/nn1690

Crochet, S., Poulet, J. F. A., Kremer, Y., & Petersen, C. C. H. (2011). Synaptic mechanisms underlying sparse coding of active touch. *Neuron*, *69*(6), 1160–1175. https://doi.org/10.1016/j.neuron.2011.02.022

Çukur, T., Huth, A. G., Nishimoto, S., & Gallant, J. L. (2016). Functional subdomains within scene-selective cortex: Parahippocampal place area, retrosplenial complex, and occipital place area. *Journal of Neuroscience*, *36*(40), 10257–10273. https://doi.org/10.1523/JNEUROSCI.4033-14.2016

Czajkowski, R., Jayaprakash, B., Wiltgen, B., Rogerson. T., Guzman-Karlsson, M. C., Barth, A. L., Trachtenberg, J. T., & Silva, A. J. (2014). Encoding and storage of sparial information in the retrosplenial cortex. *Proceedings of the National Academy of Sciences of the United States of America, 111*(23), 8661–8666. https://doi.org/10.1073/pnas.1313222111

Larssen, D.D., & Callway, E. M. (2005). Development of Layer-specific Axonal Arborizations in Mouse Primary Somatosensory Cortex. *J Comp Neurol*. 2006 January 20; 494(3): 398–414. doi:10.1002/cne.20754.

DeFelipe, J., & Fariñas, I. (1992). The pyramidal neuron of the cerebral cortex: Morphological and chemical characteristics of the synaptic inputs. Progress in Neurobiooloogy, 39 (6), 563-607. https://doi.org/10.1016/0301-0082(92)90015-7

DeFelipe, J., López-Cruz, P. L., Benavides-Piccione, R., Bielza, C., Larrañaga, P., Anderson, S., Burkhalter, A., Cauli, B. Fairén, A., Feldmeyer, D. Fishell, G., Fitzpatrick, D., Freund, T. F., González-Burgos, G., Hestrin, S., Hill, S., Holf, P. R., Huang, J., Jones, E, G., … Ascoli, G. A. (2013). New insights into the classification and nomenclature oof cortical GABAergic interneurons. *Nature Reviews Neuroscience*, *14*(3), 202–216. https://doi.org/10.1038/nrn3444

Deitcher, Y., Eyal, G., Kanari, L., Verhoog, M. B., Atenekeng Kahou, G. A., Mansvelder, H. D., De Kock, C. P. J., & Segev, I. (2017). Comprehensive morpho-electronic analysis shows 2 distinc classes of L2 and L3 pyramidal neurons in human temporal cortex. *Cerebral Cortex*, *27*(11), 5398–5414. https://doi.org/10.1093/cercor/bhx226

DelPino, I., García-Frigola, C., Dehorter, N., Brotons-Mas, J. R., Alvarez-Salvado, E., MartínezdeLagrán, M., Ciceri, G., Gabaldón., M, Moratal., D., Dierssen, M, Canals, S., Marín, O., & Rico, B. (2013). Erbb4 deletion from fast-spiking internneurons causes schizophrenia-like phenotypes. Neuron, 79(6), 1552-1168. https://doi.org/10.1016/j.neuron.2013.07.010

DelPino, I., & Marín, O. (2014). Sculpting Circuits: CRH Interneurons Modulate Neuronal Integration. *Developmental Cell*, *30*(6), 639–640. https://doi.org/10.1016/j.devcel.2014.09.006

Dillen, K. N. H., Jacobs, H. I. L., Kukolja, J., von Reutern, B., Richter, N., Onur, O. A., Dronse, J., Langen, K. J., & Fink, G. R. (2016). Aberrant functional connectivity differentiates retrosplenial cortex from posterior cingulate cortex in prodromal Alzheimer's disease. *Neurobiology of Aging*, *44*, 114–126. https://doi.org/10.1016/j.neurobiolaging.2016.04.010

Douglas, R. J., & Martin, K. A. C. (2007). Mapping the matrix: the ways of neocortex. *Neuron*, *56*(2), 226–238. https://doi.org/10.1016/j.neuron.2007.10.017

Ebbinghaus, H. (2004). Memory: A contribution to experimental psychology. *Memory: A Contribution to Experimental Psychology.*, *20*(4), 155–156. https://doi.org/10.1037/10011-000

Fábera, P., & Mareš, P. (2014). Effect of GABAB receptor agonist SKF97541 on cortical and hippocampal epileptic afterdischarges. *Physiological Research*, *63*(4), 529–534.

Faulkner, B., **& Brown**, T.H. (1999). Morphology and physiology of neurons in the rat perirhinal-lateral-lateral amygdala area. The Journal of Comparative Neurology, 411(4), 613-642. **https://doi.org/10.1002/(SICI)1096-9861(19990906)411:4<613::AID-CNE7>3.0.CO;2-U**

Fernandez, S. P., Cauli, B., Cabezas, C., Muzerelle, A., Poncer, J. C., & Gaspar, P. (2016). Multiscale single-cell analysis reveals unique phenotypes of raphe 5-HT neurons projecting to the forebrain. *Brain Structure and Function*, *221*(8), 4007–4025. https://doi.org/10.1007/s00429-015-1142-4

Filip, M., & Frankowska, M. (2008). GABA B receptors in drug addiction. *Pharmacol Rep. 60*(6)755–770.

Fink, C. C., & Meyer, T. (2002). Molecular mechanisms of CaMKII activation in neuronal plasticity. *Current Opinion in Neurobiology, 12*(3), 293-299. https://doi.org/10.1016/S.959-4388(02)00327-6

Frizzati, A., Milczarek, M. M., Sengpiel, F., Thomas, K. L., Dillingham, C. M., & Vann, S. D. (2016). Comparable reduction in Zif268 levels and cytochrome oxidase activity in the retrosplenial cortex following mammillothalamic tract lesions. Neuroscience, 330, 39-49. https://doi.org/10.1016/j.neuroscience.2016.05.030

Fujita, S., Koshikawa, N., & Kobayashi, M. (2011). GABAB receptors accentuate neural excitation contrast in rat insular cortex. *Neuroscience, 199,* 259–271. https://doi.org/10.1016/j.neuroscience.2011.09.043

Golchert, J., Smallwood, J., Jefferies, E., Liem, F., Huntenburg, J. M., Falkiewicz, M., Lauckner, M. E., Oligschläger, S., Villringer, A., & Margulies, D. S. (2017). In need of constraint: Understanding the role of the cingulate cortex in the impulsive mind. *NeuroImage, 146*, 804-813. https://doi.org/10.1016/j.neuroimage.2016.10.041

Grillner, S., Markram, H., De Schutter, E., Silberberg, G., & LeBeau, F. E. N. (2005). Microcircuits in action – From CPGs to neocortex. *Trends in Neurosciences, 28*(10), 525-533. https://doi.org/10.1016/j.tins.2005.08.003

Guterstam, A., Björnsdotter, M., Gentile, G., & Ehrsson, H. H., (2015). Posterior cingulate cortex integrates the senses oof self-location and body ownership. *Current Biology, 25*(11), 1416-1425. https://doi.org/10.1016/j.club.2015.03.059

Harland, B. C., Collings, D. A, McNaughton, N., Abraham, W. C., & Dalrymple-Alford, J. C. (2014). Anterior thalamic lesions reduce spine density in both hippocampal CA1 and retrosplenial cortex, but enrichment rescues CA1 spines only. *Hippocampus, 24*(10), 1232-1247. https:/doi.org/10.1002/hipo.22309

Hattox, A. M., & Nelson, S. B. (2007). Layer V neurons in mouse cortex projecting to different targets have distinc physilofical properties. *Journal of Neurophysiology, 98*(6), 3330-3340. https://doi.org/10.1152/jn.00397.2007

Hayakawa, T., Hata, M., Kuwahara-Otani, S., Yamanishi, K., Yagi, H., & Okamura, H. (2016) Fine structure of interleukin 18 (IL-18) receptor-immunoreactuve neurons in the retrosplenial cortex and its changes in IL18 knockout mice. *Journal of Chemical Neuroanatomy, 78*, 96-101. https://doi.org/10.1016/j.jchemneu.2016.08.009

Heaney, C. F., & Kinney, J. W. (2016). Role of GABAB receptors in learning and memory and neurological disorders. *Neuroscience and Biobehavioral Reviews*, *63*, 1–28. https://doi.org/10.1016/j.neubiorev.2016.01.007

Hedberg, T. G., & Stanton, P. K., (1995). Long-term potentiation and depression of synaptic transmission in rat posoterior cingulate cortex. *Brain Research, 670*(2), 181-196. https://doi.org/10.1016/0006-8993(94)01254-F

Helm, K. A., Haberan, R. P. Dean, S. L., Hoyt, E. C., Melcher, T., Lund, P. K., & Gallegher, M. (2005). GABAB receptor antagonist SGS742 improves spatial memory and reduces protein binding to the cAMP response element (CRE) in the hippocampus. *Neuropharmacology, 48*(7), 956-964. https://doi.org/10.1016/j.neuropharm.2005.01.019

Holmgren, C., Harkany, T., Svennenfors, B., & Zilberter, Y. (2003). Pyramidal cell communication within local networks in layer 2/3 of rat neocortex. *Journal of Physiology, 551*(1), 139-153. https://dio.org/10.1113/jphysiol.2003.044784

Honda, Y., Furuta, T., Kaneko, T., Shibata, H., Sasaki, H. (2011). Patterns of axonal collateralization of single layer V cortical projection neurons in the rat presubiculum. *J. Comp. Neurol. 519:* 1395-1412. https://doi:10.1002/cne.22578

Huffman, D. J., & Stark, C. E. L. (2017). The influence of low-level stimulus features on the representation of contexts, items, and their mnemonic associations. *NeuroImage*, *155*(April), 513–529. https://doi.org/10.1016/j.neuroimage.2017.04.019

Ichinohe, N. (2012). Small-scale module of the rat granular retrosplenial cortex: an example of the minicolumn-like structure of the cerebral cortex. *Frontiers in Neuroanatomy, 5*, 69. https://doi.org/10.3389/fnana.2011.00069

Igelström, K. M., Shirlet, C. H., & Heyward, P. M. (2011). Low-magnesium medium induces epileptiorm activity in mouse olfactory bulb slices. *Journal of Neurophysiology, 106*(5), 2593-2605. https://doi.org/10.1152/jn.00601.2011

Jacob, P. Y., Casali, G., Spieser, L., Page, H., Overington, D., & Jeffery, K. (2017). An independent, landmarl-dominated head-direction signal in dusgranular retrosplenial cortex. *Nature Neuroscience, 20*(2), 173-175. https://doi.org/10.1038/nn.4465

Jiang, X., Shen, S., Cadwell, C. R., Berens, P., Sinz, F., Ecker, A. S., Patel, S., & Tolias, A. S. (2015). Principles os connectivity among morphologically, defined cell types in adult neocortex. *Science, 350*(6264). https:/doi.org/10.1126/science.aac9462

Jones, B.F., & Witter, P.M. (2007). Cingulate cortex projections to the parahippocampal region and hippocampal formation in the rat. *Hippocampus*, *17*(10), 957-976. https://doi.org/10.1002/hipo.20330

Kádár, E., Vico-Varela, E., Aldavert-Vera, L., Huguet, G., Morgado-Bernal, I., & Segura-Torres, P. (2016). Increase in c-Fos and Arc protein in retrosplenial cortex after memory-improving lateral hypothalamic electrical stimulation treatment. *Neurobiology of Learning and Memory*, *128*, 117–124. https://doi.org/10.1016/j.nlm.2015.12.012

Kampa, B. M., Letzkus, J. J., & Stuart, G. J. (2006). Cortical feed-forward networks for binding different streams of sensory information. *Nature Neuroscience*, *9*(12), 1472–1473. https://doi.org/10.1038/nn1798

Kanari, L., Ramaswamy, S., Shi, Y., Morand, S., Meystre, J., Perin, R., Abdellah, M., Wang, Y., Hess, K., & Markram, H. (2019). Objective morphological classification of neocortical pyramidal cells. *Cerebral Cortex, 29*(4), 1719–1735. https://doi.org/10.1093/cercor/bhy339

Kasten, C. R., & Boehm, S. L. (2015). Identifying the role of pre-and postsynaptic GABAB receptors in behavior. *Neuroscience and Biobehavioral Reviews*, *57*, 70–87. https://doi.org/10.1016/j.neubiorev.2015.08.007

Katche, C., & Medina, J. H. (2017). Requirement of an Early Activation of BDNF/c-Fos Cascade in the Retrosplenial Cortex for the Persistence of a Long-Lasting Aversive Memory. *Cerebral Cortex (New York, N.Y. : 1991)*, *27*(2), 1060–1067. https://doi.org/10.1093/cercor/bhv284

Kato, K., Nakagawa, C., Murabayashi, H., & Oomori, Y. (2014). Expression and distribution of GABA and GABAB-receptor in the rat adrenal gland. *Journal of Anatomy*, *224*(2), 207–215. https://doi.org/10.1111/joa.12144

Koch, M., Kungel, M., & Herbert, H. (1993). Cholinergic neurons in the pedunculopontine tegmental nucleus are involvd in the mediation of prepulse inhinbition of the acoustic startle response in the rat. *Exp. Brain Res.,* 97, 71–82 (1993). https://doi.org/10.1007/BF00228818

Kerr, D. I. B., & Ong, J. (2003). Potentiation of metabotropic GABAB receptors by L-amino acids and dipeptides in rat neocortex. *European Journal of Pharmacology*, *468*(2), 103–108. https://doi.org/10.1016/S0014-2999(03)01675-3

Kim, H., Jung, S., Son. H., Kim, S., Chol, J., Lee, D. H., Roh, G. S., Kang, S. S., Cho, G. J., Choi, W. S., & Kim, H. J. (2014). The GABAB receptor associates with regulators of

G-protein signaling 4 protein in the mouse prefrontal cortex and hypothalamus. *BMB Reports, 47*(6), 324-329. https:/doi.org/10.5483/BMBRep.2014.47.6.162

Kim, W., & Seo, H. (2014). Baclofen, a GABAB receptor agonist, enhances ubiquitin-proteasome system functioning and neuronal survival in Huntington's disease model mice. *Biochemical and Biophysical Research Communications*, *443*(2), 706–711. https://doi.org/10.1016/j.bbrc.2013.12.034

Kinnavane, L., Amin, E., Olarte-Sánchez, C. M., & Aggleton, J. O. (2017). Medial temporal pathways for contextual learning: Network c-fos mapping in rats with or without perirhinal cortex lesions. Brain and Neuroscience Advances, *1*, 239821281769416. https://doi.org/10.1177/2398212817694167

Knight, R., & Hayman, R. (2014). Allocentric directional in the rodent and human retrosplenia, cortex. *Frontiers in Human Neuroscience, 8,* 135. https://doi.org/10.3389/fnhum.2014.00135

Kononenko, N.L., & Witter, M.P. (2012). Presubiculum layer III conveys retrosplenial input to the medial entorhinal cortex. *Hippocampus*, *22*(4), 881-885.

Kumar, K., Sharma, S., Kumar, P., & Deshmukh, R. (2013). Therapeutic potential of GABA(B) receptor ligands in drug addiction, anxiety, depression and other CNS disorders. *Pharmacology, Biochemistry, and Behavior*, *110*, 174–184. https://doi.org/10.1016/j.pbb.2013.07.003

Kurotani, T., Miyashita, T., Wintzer, M., Konishi, T., Sakai, K., Ichinohe, N., & Rockland, K. S. (2013). Pyramidal neurons in the superficial layers of rat retrosplenial cortex exhibit a late-spiking firing property. *Brain Structure & Function*, *218*(1), 239–254. https://doi.org/10.1007/s00429-012-0398-1

Kwapis, J., Jarome, T., Ferrara, N. *et al.* Updating Procedures Can Reorganize the Neural Circuit Supporting a Fear Memory. *Neuropsychopharmacol* **42,** 1688–1697 (2017). https://doi.org/10.1038/npp.2017.23

Ledergerber, D., & Larkum, M. E. (2010). Properties of layer 6 pyramidal neuron apical dendrites. *Journal of Neuroscience*, *30*(39), 13031–13044. https://doi.org/10.1523/JNEUROSCI.2254-10.2010

Leone, D. P., Srinivasan, K., Chen, B., Alcamo, E., & McConnell, S. K. (2008). The determination of projection neuron identity in the developing cerebral cortex. *Current Opinion in Neurobiology, 18*(1), 28–35. https://doi.org/10.1016/j.conb.2008.05.006

Li, S. P., Park, M. S., Yoon, H., Rhee, K. H., Bahk, J. Y., Lee, J. H., Park, J. S., & Kim, M. O. (2003). Differential distribution of GABAB1 and GABAB2 receptor mRNAs in the rat brain. *Molecules and Cells*, *16*(1), 40–47.

Lin, C. T., Chiu, T. C., & Gramann, K. (2015). EEG correlates of spatial orientation in the human retrosplenial complex. *NeuroImage, 120*, 123-132. https://doi.org/10.1016/j.neuroimage.2015.07.009.

López-Bendito, G., Luján, R., Shigemoto, R., Ganter, P., Paulsen, O., Molnár, Z., Biomédicas, I., & Medicina, DeF. (2003). Blockade of GABA B receptors alters the tangential migration of cortical neurons. *Cerebral Cortex, 13*(9), 932-942. https://doi.org/10.1093/cercor/13.9.932.

Łukasiewicz, K., Robacha, M., Bożycki, Ł., Radwanska, K., & Czajkowski, R. (2016). Simultaneous two-photon in vivo imaging of synaptic inuts and postsynaptic targets in the mouse retrsplenial cortex. *Journal of Visualized Experiments*, *2016*(109), 5–9. https://doi.org/10.3791/53528

Markham, J. A., Morris, J. R., & Juraska, J. M. (2007). Neuron number decreases in the rat ventral, but not dorsal, medial prefrontal cortex between adolescence and adulthood. *Neuroscience*, *144*(3), 961–968. https://doi.org/10.1016/j.neuroscience.2006.10.015

Markram, H., Muller, E., Ramaswamy, S., Reimann, M.W., Abdellah, M., Sanchez, C. A., Aliamaki, A., Alonso-Nanclares, L., Antille, N., Arsever, S., Kahou, G. A. A., Berger, T. K., Bligili, A., Buncic, N., Chalimourda, A., Chindemi, G., Courcol, J., D., Delalondre, F., Delattre, V., Schürmann, F. (2015). Reconstruction and simulation of neocortical microcircuitry. *Cell, 163*(2), 456-492. https://doi.org/10.1016/j.cell.2015.09.029

Malinowska, M., Niewiadomska, M., & Wesierska, M. (2016). Spatial memory formation differentially effects c-fos expression in retrosplenial areas during place avoidance training in rats. *Acta Neurobiologiae Experimentalis*, *76*(3), 244–256. https://doi.org/10.21307/ane-2017-024

Marx, M., & Feldmeyer, D. (2013). Morphology and physiology of excitatory neurons in layer 6b of the somatosensory rat barrel cortex. *Cerebral Cortex (New York, N.Y. : 1991)*, *23*(12), 2803–2817. https://doi.org/10.1093/cercor/bhs254

Mares, P., & Slamberová, R. (2006). Opposite effects of a GABA(B) antagonist in two models of epileptic seizures in developing rats. *Brain Research Bulletin*, *71*(1–3), 160–166. https://doi.org/10.1016/j.brainresbull.2006.08.013

Martin, I., Bowery, N., & Dunn, S. (2009). *CGP 55845, Potent , Selective GABAB Antagonist CGP*.

Mayford, M., Bach, M. E., Huang, Y. Y., Wang, L., Hawkins, R. D., & Kandel, E. R. (1996). Control of memory formation through regulated expression of a CaMKII transgene. *Science, 274*(5293), 1678–1683. https://doi.org/10.1126/science.274.5293.1678

Milczarek, M. M., Vann, S. D., & Sengpiel, F. (2018). Spatial Memory Engram in the Mouse Retrosplenial Cortex. *Current Biology*, *28*(12), 1975-1980.e6. https://doi.org/10.1016/j.cub.2018.05.002

Miller, A. M. P., Vedder, L. C., Law, L. M., & Smith, D. M. (2014). Cues, context, and long-term memory: the role of the retrosplenial cortex in spatial cognition. F*rontiers in Human Neuroscience, 8*, 586. https://doi.org/10.3389/fnhum.2014.00586

Möhler, H. (2012). The GABA system in anxiety and depression and its therapeutic potential. *Neuropharmacology*, *62*(1), 42–53. https://doi.org/10.1016/j.neuropharm.2011.08.040

Monier, C., Fournier, J., & Frégnac, Y. (2008). *In vitro* and *in vivo* measures of evoked excitatory and inhibitory conductance dynamics in sensory cortices. *Journal of Neuroscience Methods*, *169*(2), 323–365. https://doi.org/10.1016/j.jneumeth.2007.11.008

Mott DD, & Lewis DV. (1992). GABAB receptors mediate disinhibition and facilitate long-term potentiation in the dentate gyrus. *Epilepsy Res Suppl.7*:119-34. PMID: 1334658.

Muhchyi, C., Juliandi, B., Matsuda, T., & Nakashima, K. (2013). Epigenetic regulation of neural stem cell fate during corticogenesis. *International Journal of Develpmental Neuroscience: The Official Journal of the International Society for Developmenal Nueroscience, 31*. https://doi.org/10.1016/j.ijdevneu.2013.02.006

Nelson, A. J., Hindley, E. L., Pearce, J. M., Vann, S. D., & Aggleton, J. P. (2015). The effect of retrosplenial cortex lesions in rats on incidental and active spatial learning. Frontiers in Behavioral Neuroscience, 9, 1-16. https://doi.org./10.3389/fnbeh.2015.00011

Nelson, A- J- D., Powell, A. L., Holmes, J. D., Vann, S. D., & Aggleton, J. P. (2015). What does spatial alternation tell us about retrosplenial cortex function? *Frontiers in Behavioral Neuroscinecie, 9*, 1–15. https://doi.org/10.3389/fnbeh.2015.00126

Nixima, K., Okanoya, K., Ichinohe, N., & Kurotani, T. (2017). Fast voltage-sensitive dye imaging of excitatory and inhibitory synaptic transmission in the rat granular

retrosplenial cortex. *Journal of Neurophysiology*, *118*(3), 1784–1799. https://doi.org/10.1152/jn.00734.2016

Nonaka, S., Arai, C., Takayama, M., Matsukura, C., & Ezura, H. (2017). Efficient increase of Γ-aminobutyric acid (GABA) content in tomato fruits by targeted mutagenesis. *Scientific Reports*, *7*(1), 1–14. https://doi.org/10.1038/s41598-017-06400-y

Oda, S., Funato, H., Sato, F., Adachi-Akahane, S., Ito, M., Takase, K., & Kuroda, M. (2014). A subset of thalamocortical projections to the retrosplenial cortex possesses two vesicular glutamate transporter isoforms, VGluT1 and VGluT2, in axon terminals and somata. *The Journal of Comparative Neurology*, *522*(9), 2089–2106. https://doi.org/10.1002/cne.23519

Oess, T., Krichmar, J. L., & Rohrbein, F. (2017). A computational model for spatial navigation based on reference frames in the hippocampus, retrosplenial cortex, and posterior parietal cortex. *Frontiers in Neurorobotics*, *11*(FEB). https://doi.org/10.3389/fnbot.2017.00004

Ohara, S., Gianatti, M., Itou, K., Berndtsson, C. H., Doan, T. P., Kitanishi, T., Mizuseki, K., Iijima, T., Tsutsui, K. I., & Witter, M. P. (2019). Entorhinal Layer II Calbindin-Expressing Neurons Originate Widespread Telencephalic and Intrinsic Projections. *Frontiers in Systems Neuroscience*, *13*, 1–14. https://doi.org/10.3389/fnsys.2019.00054

Olsen, G. M., Ohara, S., Iijima, T., & Witter, M. P. (2017). Parahippocampal and retrosplenial connections of rat posterior parietal cortex. *In Hippocampus* (Vol. 27, Issue 4, pp. 335–358). https://doi.org/10.1002/hipo.22701

Palomero-Gallagher, N., Vogt, B. A., Schleicher, A., Mayberg, H. S., & Zilles, K. (2009). Receptor architecture of human cingulate cortex: evaluation of the four-region neurobiologial model. *Human Brain Mappin, 30*(8), 2336–2355. https://doi.org/10.1002/hbm.20667

Parker, D. a S., Ong, J., Marino, V., & Kerr, D. I. B. (2004). Gabapentin activates presynaptic GABAB geteroreceptors in rat cortical slices. *European Journalof Pharmacology, 495*(2-3), 137-143. https://doi.org/10.1016/j.ejphar.2004.05.029

Petreanu, L., Huber, D., Sobczyk, A., & Svoboda, K. (2007). Channelrhodopsin-2-assisted circuit mapping of long-range callosal projections. *Nature Nuerosciencie, 10*(5), 663-668. https://doi.org/10.1038/nn1891

Pinard, A., Seddik, R., & Bettler, B. (n.d.). GABA B receptors: physiological functions and mechanisms of diversity. In *GABAb Receptor Pharmacology: A Tribute to Norman*

Bowery (First, Vol. 58, Issue 10). Elsevier Inc. https://doi.org/10.1016/S1054-3589(10)58010-4

Pinto, D. J., Patrick, S. L., Huang, W. C., & Connors, B. W. (2005). Initiation, propagation, and termination of epileptiform activity in rodent neocortex in vitro involve distinc mechanisms. The Journal of Neuroscience: *The Official Journal of the Society for Neuroscience, 25*(36), 8131-8140. https://doi.org/10.1523/JNEUROSCI.2278-05.2005

Powell, A. L., Vann, S. D., Olarte-Sánchez, C. M., Kinnavane, L., Davies, M., Amin, E., Aggleton, J. P., & Nelson, A. J. D. (2017). The retrosplenial cortex and object recency memory in the rat. *European Journal of Neuroscience*, *45*(11), 1451–1464. https://doi.org/10.1111/ejn.13577

Puelles, L., Harrinson, M., Paxinos, G., & Watson, C. (2013). A developmental ontology foro the mammalian brain based on the prosomeric model. *Trends in Neurosciences*, *36*(10), 570–578. https://doi.org/10.1016/j.tins.2013.06.004

Rakic, P. (1972). Mose oof cell migration to the superficial layers oof fetal monkey neocortex. *The Journal of Comparative Neurology, 145*(1), 61–83. https://doi.org/10.1002/cne.901450105

Rakic, P. (2010). Evoluioon of the neocortex: Perspective from developmental biology. Nature Reviews Nueroscience, *10*(10), 724–735. https://doi.org/10.1038/nrn2719.Evolution

Ramaswamy, S., & Markram, H. (2015). Anatomy and physiology of the thick-tufted layer 5 pyramidal neuron. *Frontiers in Cellular Neuroscience, 9*, 1–29. https://doi.org/10.3389/fncel.2015.00233

Raveh, A., Turecek, R., & Bettler, B. (2015). Mechanisms of fast desensitization of GABA(B) receptor-gated currents. *Advances in pharmacology,* 73. Elsevier Inc. https://doi.org/10.1016/bs.apha.2014.11.004

Regen, W., Kyle, S. D., Nissen, C., Feige, B., Baglioni, C., Henning, J., Riemann, D., & Spiegelhalder, K. (2016). Bjective sleep disturbances are associated with greater waking resting-state connectivity between the retrosplenial corotex/hippocampus and various nodes of the default mode network. *Journal of Psychiatry and Neuroscience, 41*(5), 295–303. https://doi.org/10.1503/jpn.140290

Reimann, M. W., Nolte, M., Scolamiero, M., Turner, K., Perin, R., Chindemi, G., Dlotko, P., Levi, R., Hess, K., & Markram, H. (2017). Cliques of neurons bound into cavities prvide a missing link between structure and function. *Frontiers in Computational Neuroscience, 11*. https://doi.org/10.3389/fncom.2017.00048

Robinson, S., Todd, T. P., Pasternak, A. R., Luikart, B. W., Skelton, P. D., Urban, D. J., & Bucci, D. J. (2014). Chemogenetic silencing of neurons in retrosplenial cortex disrupts sensory preconditioning. *The Journal of Neuroscience : The Official Journal of the Society for Neuroscience*, *34*(33), 10982–10988. https://doi.org/10.1523/JNEUROSCI.1349-14.2014

Robles, R. M., Domínguez-Sala, E., Martínez, S., & Geijo-Barrientos, E. (2020). Layer 2/3 pyramidal neurons of the mouse granular retrosplenial cortex and their innervation by cortico-cortical axons. *Frontiers in Neural Circuits*, *14*(November), 1–15. https://doi.org/10.3389/fncir.2020.576504

Rogawski, M. A. (2013). AMPA receptors as a molecular target in epilepsy therapy. *Acta Neurologica Scandinavica, 127*(197), 9-18. https://doi.org/10.1111/ane.12099

Rotarska-Jagiela, A., Oertel-Knoechel, V., DeMartino, F., van de Ven, V., Formisano, E., Roebroeck, A., Rami, A., Schoenmeyer, R., Haenschel, C., Hendler, T. Maurer, K., Vogeley, K., & Linden, D. E. J. (2009). Anatomical brain connectivity and positive sumptms of schizophrenia: a diffusion tensor imaging study. *Psychiatry Research-Neuroimaging, 174*(1), 9–16. https://doi.org/10.1016/j.pscychresns.2009.03.002

Rovira, V., & Geijo-Barrientos, E. (2016). Intra- and interhemispheric propagation oof electrophysiological synchronous activity and its modulation by serotonin in the cingulate cortex of juvenile mice. *PLoS ONE, 11*(3), 1–19. https://doi.org/10.1371/journal.pone.0150092

Sachser, R. M., Crestani, A. P., Quillfeldt, J. A., Souza, T. M. E., & De Oliveira Alvares, L. (2015). The cannabinoid system in the retrosplenial cortex modulates fear memoty consolidation and extinction. *Learning and Memory*, *22*(12), 584–588. https://doi.org/10.1101/lm.039891.115

Sakata, S., & Harris, K. D. (2009). Laminar structure of spontaneous and sensory-evoked population activity in auditory cortex. *Neuron, 64*(3), 404–418. https://doi.org/10.1016/j.neuron.2009.09.020

Salaj, M., Druga, R., Cerman, J., Kubová, H., & Barinka, F. (2015). Calretinin and parvalnumin immunoreactive interneurons in the retrosplenial cortex of the rat brain: qualitative and quantitative analyses. *Brain Research*, *1627*, 201–215. https://doi.org/10.1016/j.brainres.2015.09.031

Salgado-Pineda, P., Landin-Romero, R., Pomes, A., Spanlang, B., Sarró, S., Salvador, R., Slater, M., McKenna, P. J., & Pomarol-Clotet, E. (2017). Patterns of activation and de-activation associated with cue-guided spatial navigation: a whole-brain voxel-based study. *Neuroscience, 358,* 70-78. https://doi.org/10.1016/j.neuroscience.2017.06.029

Sawinski, J., Wallace, D. J., Greenberg, D. S., Grossmann, S., Denk, W., & Kerr, J. N. D. (2009). Visually evoked activity in cortical cells imaged in freely moving animals. Proceedings of the National Academy of Sciences of *the United States of America*, *106*(46), 19557–19562. https://doi.org/10.1073/pnas.0903680106

Schnepel, P., Kumar, A., Zohar, M., Aertsen, A., & Bucsein, C. (2015). Physiology and impact of horizontal connections in rat neocortex. *Cerebral Cortex*, *25*(10), 3818–3835. https://doi.org/10.1093/cercor/bhu265

Sebe, J. Y., Looke-Stewart, E., & Baraban, S. C. (2014). GABAB receptors in maintenance of neocortical circuit function. *Experimental Neurology*, *261*, 163–170. https://doi.org/10.1016/j.expneurol.2014.05.018

Sebe, J. Y., Looke-Stewart, E., Dinday, M. T., Alvarez-Buylla, A., & Baraban, S. C. (2014). Neocortical integration of transplanted GABA profenitoor cells from wild type and GABAB receptor knockout mouse donors. *Neuroscience Letters*, *561*, 52–57. https://doi.org/10.1016/j.neulet.2013.11.012

Sempere-Ferràndez, A. (2016). The callosal contribution to cortical microcircuits. *Doctoral tesis.*

Sempere-Ferràndez, A., Andrés-Bayón, B., & Geijo-Barrientos, E. (2018). Callosal responses in a retrosplenial column. *Brain Structure and Function*, *223*(3), 1051–1069. https://doi.org/10.1007/s00429-017-1529-5

Sempere-Ferràndez, A., Martínez, S., & Geijo-Barrientos, E. (2019). Synaptic mechanisms underlying the intense firing of neocortical layer 5B pyramidal neurons in response to cortico-cortical inputs. Brain Structure and Function, 224(4), 1403-1416. https://doi.org/10.1007/s00429-019-01842-8

Shao, Z., & Burkhalter, A. (1999). Role of GABA B receptor-mediated inhibition in reciprocal interareal pathways of rat visual cortex. *Journal of Neurophysiol, 81(3),* 1014–1024.

Shibata, H. (1998). Organization of projections of rat retrosplenial cortex to the anterior thalamic nuclei. *European Journal of Neuroscience, 10*(10), 3210-3219. https://doi.org/10.1046/j.1460-9568.1998.00328.x

Shibata, H. (2000). Organization of retrosplenial cortical projections to the laterodorsal thalamic nucleus in the rat. *Neuroscience Research*, *38*(3), 303–311. https://doi.org/10.1016/S0168-0102(00)00174-7

Shin, N. Y., Hong, J., Choi, J. Y., Lee, S. K., Lim, S. M., & Yoon, U. (2017). Retrosplenial cortical thinning as a possible major contributor for cognitive impairment in HIV

patients. In *European Radiology* (Vol. 27, Issue 11, pp. 4721–4729). https://doi.org/10.1007/s00330-017-4836-6

Shine, J. P., Valdés-Herrera, J. P., Hegarty, M., & Wolbers, T. (2016). The human retrosplenial cortex and thalamus code head direction in a global reference frame. *Journal of Neuroscience, 36*(24), 6371–6381. https://doi.org/10.1523/JNEUROSCI.1268-15.2016

Sigwald, E. L., Genoud, M. E., Giachero, M., de Olmos, S., Molina, V. A., & Lorenzo, A. (2016). Selective neuronal degeneration in the retrosplenial cortex impairs the recall of contextual fear memory. Brain Structure and Function, *221*(4), 1861–1875. https://doi.org/10.1007/s00429-015-1008-9

Spruston, N., (2008). Pyramidal neurons: dendritic structure and synaptic integration. ***Nature Reviews Neuroscience*** volume 9, pages206–221. https://doi.org/10.1038/nrn2286

Sugar, J., & Witter, M. P. (2016). Postnatal development of retrosplenial projections to the parahippocampal region of the rat. *ELife*, *5*(MARCH2016), 1–29. https://doi.org/10.7554/eLife.13925

Sulpizio, V., Committeri, G., Lambrey, S., Berthoz, A., & Galati, G. (2016). Role of the human retrosplenial cortex/parieto-occipital sulcus in perspective priming. *NeuroImage, 125,* 108-119.https://doi.org/10.1016/j.neuroimage.2015.10.040

Tamamaki, N., Yanagawa, Y., Tomioka, R., Miyazaki, J. I., Obata, K., & Kaneko, T. (2003). Green Fluorescent Protein Expression and Colocalization with Calretinin, Parvalbumin, and Somatostatin in the GAD67-GFP Knock-In Mouse. Journal of Comparative Neurology, 467(1), 60-79. https://doi.org/10.1002/cne.10905

Tanaka, K. Z., Pevzner, A., Hamidi, A. B., Nakazawa, Y., Graham, J., & Wiltgen, B. J. (2014). Cortical Representations Are Reinstated by the Hippocampus during Memory Retrieval. *Neuron*, *84*(2), 347–354. https://doi.org/10.1016/j.neuron.2014.09.037

Tendolkar, I., Wels, S., Guddat, O., Fernández, G., Brockhaus-Dumke, A., Specht, K., Klosterkötter, J., Reul, J., & Ruhrmann, S. (2004). Evidence for a dysfunctional retrosplenial cortex in patients with schizophrenia: a functional magnetic resonance imaging study with a semantic-perceptual contrast. *Neuroscience Letters, 369*(1), 4-8. https://doi.org/10.1016/j.neulet.2004.07.024

Todd, T. P., & Bucci, D. J. (2015). Retrosplenial cortex and long-term memory: molecules to behavior. *Neural Plasticity*. https://doi.org/10.1155/2015/414173

Todd, T. P., Huszár, R., DeAngeli, N. E., & Bucci, D. J. (2016). Higher-order conditioning and the retrosplenial cortex. *Neurobiology of Learning and Memory*, *133*, 257–264. https://doi.org/10.1016/j.nlm.2016.05.006

Todd, T. P., Mehlman, M. L., Keene, C. S., De Angeli, N. E., & Bucci, D. J. (2016). Retrosplenial cortex is required for the retrieval of remote memory for auditory cues. *Learning and Memory*, *23*(6), 278–288. https://doi.org/10.1101/lm.041822.116

Todd, T. P., Meyer, H. C., & Bucci, D. J. (2015). Contribution of retrosplenial cortex to temporal discrimination learning. *Hippocampus, 25*(2), 137–141. https://doi.org/10.1002/hipo.22385

Todd, T. P., Jiang, M. Y., DeAngeli, N. E., & Bucci, D. J. (2017). Intact renewal after extinction of conditioned suppression with lesions of either the retrosplenial cortex or dorsal hippocampus. *Behavioural Brain Research*, *320*, 143–153. https://doi.org/10.1016/j.bbr.2016.11.033

Toledo-Rodriguez, M., Goodman, P., Illic, M., Wu, C., & Markram, H. (2005). Neuropeptide and calcium-binding protein gene expression profiles predict neuronal anatomical type in the juvenile rat. *Journal of Physiology, 567*(2), 401-413. https://doi.org/10.1113/jphysiol.2005.089250

Torres-Escalante, J. L., Barral, J. a, Ibarra-Villa, M. D., Pérez-Burgos, A., Góngora-Alfaro, J. L., & Pineda, J. C. (2004). 5-HT1A, 5-HT2, GABAB receptors interact to modulate neurotransmitter release probability in layer 2/3 somatosnesory rat cortex as evaluated by the paired pulse protocol. *Journal of Neuroscience Research*, *78*(2), 268–278. https://doi.org/10.1002/jnr.20247

Turgeon, S. M., & Albin, R. L. (1994). Postnatal ontogeny of GABAB binding in rat brain. *Neuroscience, 62*(2), 601-613. https://doi.org/10.1016/0306-4522(94)90392-1

Tyler, W. A., Medalla, M., Guillamn-Vivancos, T., Luebke, J. I., & Haydar, T. F. (2015). Neural precursor lineages specify distinct neocortical pyramidal neuron types. *Journal of Neuroscience*, *35*(15), 6142–6152. https://doi.org/10.1523/JNEUROSCI.0335-15.2015

Unichenko, P., Dvorzhak, A., & Krischuk, S. (2013). Transporter-mediated replacement of extracellular glutamate for GABA in the developing murine neocortex. *The European Journal of Neuroscience*, *38*(11), 3580–3588. https://doi.org/10.1111/ejn.12380

Van Groen, T., & Wyss, J. M. (2003). Connections of the retrosplenial granular b cortex in the rat. *The Journal of Comparative Neurology*, *463*(3), 249-263. https://doi.org/10.1002/cne.10757

Van Groen, T., & Wyss, J. M. (1992). Connections of the retrosplenial dysgranylar cortex in the rat. *The Journal of Comparative Neurology, 315*(2), 200-216. https://doi.org/10.1002/cne.903150207

Vann, S. D., Aggleton, J. P., & Maguire, E. A. (2009). What does the retrosplenial cortex do? *Nature Reviews. Neuroscience, 10*(11), 792-802. https://doi.org/10.138/nrn2733

Vedder, L. C., Miller, A. M. P., Harrison, M. B., & Smith, D. M. (2017). Retrosplenial cortical neurons encode navifational cues, trajectories and reward locations during goal directed navigation. *Cerebral Cortex, 27*(7), 3713-3723. https:/doi.org/10.1093/cercor/bhw192

Vigot, R., Barbieri, S., Bräuner-osborne, H., Turecek, R., Fritschy, J., Vacher, C., Müller, M., Sansig, G., & Bettler, B. (2012). Differential compartimentalization and distinct functions og GABA B receptor variants. *Europe PMC Funders Group 50*(4), 589–601. https://doi.org/10.1016/j.neuron.2006.04.014.

Vogt, B. a, & Paxinos, G. (2014). Cytoarchitecture of mouse and rat cingulate cortex with human homologies. *Brain Structure & Function*, *219*(1), 185–192. https://doi.org/10.1007/s00429-012-0493-3

Walker, J., Storch, G., Quach-Wong, B., Sonnenfeld, J., & Aaron, G. (2012). Propagation of epileptiform events across the corpus callosum in a cingulate cortical slice preparation. *PloS One, 7*(2), e31415. https://doi.org/10.1371/journal.pone.0031415

Wang, J., Nie, B., Duan, S., Zhu, H., Liu, H., & Shan, B. (2016). Functionally brain network connected to the retrosplenial cortex of rats revealed by 7TfMRI. *PLoS ONE*, *11*(1), 1–8. https://doi.org/10.1371/journal.pone.0146535

Williams, S. R., & Stuart, G. J. (2002). Dependence of EPSP efficacy on synapse location in neocortical pyramidal neurons. *Science, 295*(5561), 1907–1910. https://doi.org/10.1126/science.1067903

Wixted, J. T. (2004). The psychology and neuroscience of forgetting. *Annual Review of Psychology*, *55*, 235–269. https://doi.org/10.1146/annurev.psych.55.090902.141555

Wyss, A. R., Norell, M. A., Flynn, J.J., Novacek, M. J., Charrier, R., Mckenna, M. C., Swisher, C. C., Frassinetti, D., Salinas, P., & Jin, M. (1990). A new early Tertiary mammal fauna froom central Chile: implications for Andean stratigraphy and tectonics. *Journal of Vertebrate Paleontology*, *10*(4), 518–522. https://doi.org/10.1080/02724634.1990.10011835

Xiao, Y., Huang, X. Y., Van Wert, S., Barreto, E., Wu, J. Young, Gluckman, B. J., & Schiff, S. J. (2012). The role of inhibition in oscillatory wave dynamics in the cortex.

European Juornal of Nueroscience, 36(2), 2201-2212. https://doi.org/10.1111/j.1460-9568.2012.08132.x

Yamawaki, N., Radulovic, J., & Shepherd, G. M. G. (2016). A corticocoortical circuit directly links retrosplenial cortex to secondary motor cortex in the mouse. *Journal of Neuroscience, 36*(36), 9365–9374. https://doi.org/10.1523/JNEUROSCI.1099-16.2016

Yamawaki, N., Li, X., Lambot, L., Ren, L. Y., Radulovic, J., & Shepherd G.M.G. (2019). Long-range inhibitory intersection of a retrosplenial thalamocortical circuit by apical tuft-targeting CA1 neurons. *Nat Neurosci. 22*(4): 618–626. https://doi:10.1038/s41593-019-0355-x

Yasuda, M., & Mayford, M.R. (2006). CaMKII activation in the Enthorhinal Cortex disrupts previously encoded spatial memory. Neuron, 50(2), 309-318. https://doi.org/10.1016/j.neuron.2006.03.035

Yasuno, F., Kazui, H., Yamamoto, A., Morita, N., Kajimoto, K., Ihara, M., Taguchi, A., Matsuoka, K., Kosaka, J., Tanaka, T., Kudo, T., Takeda, M., Nagatsuka, K., Iida, H., & Kishimoto, T. (2015). Resting-state synchrony between the retroosplenial cortex and anterior medial cortical structures relates to memory complaints in subjective cognitive impairment. *Neurobiology of Aging*, *36*(6), 2145–2152. https://doi.org/10.1016/j.neurobiolaging.2015.03.006

Yoshimura, Y., Dantzker, J. L. M., & Callaway, E. M. (2005). Excitatory cortical neurons form fine-scale functional netwoorks. *Nature, 433*(7028), 868-873. https://doi.org/10.1038/nature03252

Zgraggen, E., Boitard, M., Roman, I., Kanemitsu, M., Potter, G., Salmon, P., Vutskits, L., Dayer, A. G., & Kiss, J. Z. (2012). Early postnatal migration and development of layer II pyramidal neurons in the rodent cingulate/retrosplenial cortex. *Cerebral Cortex (New York, N.Y. : 1991)*, *22*(1), 144–157. https://doi.org/10.1093/cercor/bhr097

Zhang, P., Bannon, N. M., Ilin, V., Volgushev, M., & Chistiakova, M. (2015). Adenosine effects on inhibitory synaptic transmission and excitation-inhibition balance in the rat neocortex. *Journal of Physiology*, *593*(4), 825–841. https://doi.org/10.1113/jphysiol.2014.279901

Zhang, W., Xu, C., Tu, H., Wang, Y., Sun, Q., Hu, P., Hu, Y., Rondard, P., & Liu, J. (2015). GABAB receptor upregulated fragile X mental retardation protein expression in neurons. *Scientific Reports, 5,* 10468. https://doi.org/10.1038/srep10468

Zhou, Y., Shu, N., Liu, Y., Song, M., Haoo, Y., Liu, H., Yu, C., Liu, Z., & Jiang, T. (2008). Altered resting-state functional connectivity and anatomical connectivity of

hippocampus in schizophrenia. *Schizophrenia Research, 100* (1–3), 120–132. https://doi.org/10.1016/j.schres.2007.11.039

The end

Title of the Doctoral Thesis

LOCAL CIRCUITS OF THE MOUSE GRANULAR RETROSPLENIAL CORTEX

Doctoral Thesis presented by

Rita Mariana Robles Picó

Thesis Director: **Salvador Martínez Pérez**

Thesis Co-Director: **Emilio Carlos Geijo Barrientos**

PhD Program in Neuroscience

Neurosciences Institute

University Miguel Hernández of Elche

- 2021 -

INSTITUTO DE NEUROCIENCIAS

1999 - 2019

INSTITUTO DE NEUROCIENCIAS

EXCELENCIA SEVERO OCHOA